POLITECNICO DI MILANO

SCUOLA DI INGENGERIA INDUSTRIALE E DELL'INFORMAZIONE

Corso di Laurea Magistrale in Ingegneria Elettrica

POLITECNICO

MILANO 1863

Electric vehicle fast charging system powered from high speed railway lines

Relatore: Prof. Morris Brenna
Correlatore: Ing. Michela Longo

Tesi di Laurea Magistrale di:
Mauro Colombo
Matr. 817750

Anno Accademico 2014 - 2015

Contents

Abstract

This thesis is about fast charging electric cars in motorways service areas by using high speed lines to deliver the power necessary.

The need to reduce pollution, the relatively low cost of ownership and the new exhaust fumes scandal will probably lead to an increase in electric car sales. Electric cars also need a fast charging stations network to allow owners to quickly charge their batteries when they drive relatively long routes. This means building charging station in motorway service areas with the problem of finding a suitable electric power source. A possible solution is the high speed railway line, because it can power a high load and it can be relatively near the motorway itself.

The first step in solving the problem was modelling the 2 x 25 kV system used to feed the railway. The model is made using the Simpowersystems tool in MATLAB to simulate the railway itself. The same tool has been used to simulate the battery charger and the system as a whole in the two successive steps.

The results show the idea can work in a real situation, but if more than twenty 100 kW charging bays are required in each direction or the line topology is changed for whatever reason, it can not be guaranteed the railway system is able to provide the additional power requested.

Chapter 1

Introduction

People realised in the 1950s and 1960s trains could compete with commercial flights if the travelling time by train is shorter than by plane. Two things have to be remembered when comparing trains and planes: where airports and train stations are and the boarding procedures. Most airports are on the outskirts of the city and an additional trip by public transport or taxi is required to get to the city centre, while railway stations are already there. Boarding procedures are very different between trains and aeroplanes: usually the boarding procedure for trains requires getting to the station in time to catch the train and the passport control, while flying requires getting to the airport at least one hour before the flight departure for national flights (two hours when flying internationally) to embark the luggage and pass the security check and passport control. Flying requires time after landing especially for the luggage claim which is not needed for train travel. This means train travelling can be much faster than flying for short distance travel. An example of this is the Tokaido Shinkansen line between Tokyo and Osaka. Built in 1964, today it carries daily more than four hundred thousand passengers on average, with 330 thousand available seats on limited-stop trains compared to 30 thousand seats of airlines capacity. This is also due to the fact trains can carry far more passengers than any airliner, making trains more energy efficient.

This led other developed countries to establish their own high speed service and to build a high speed network. Because of the high power demands of high speed trains, it became clear that traditional electrifications schemes where not very good at delivering that much power, so the 2 x 25 kV autotransformer system was used for new lines and new electrifications. This system allows to have a relatively low number of substations while delivering a lot of power to the train with the advantage of minimising energy losses and voltage drops.

The issue of climate change and greenhouse effect led Governments and Regulating Agencies to enforce stricter emission limits on traditional internal combustion engines. This led to the rediscovery of the electric car. Invented in the 1830 the electric car became a research topic when it was clear that internal com-

bustion engines were the the best solution available. The recent developments in battery technology, especially the lithium ion batteries, and in electronics led to the modern electric car which is comparable with traditional cars performance wise. Despite the technological developments, the long charging times mean that electric vehicles are mostly used in cities and towns.

The increase in popularity of electric cars require the construction of a suitable fast charging infrastructure to allow driving over longer distances. Usually high speed lines are built (or designed to be built) near existing motorways. Since the best place to install fast charging facilities is motorways service areas because the necessary services are already there, it is interesting studying the possibility to connect these charging facility to the neighbouring high speed line rather than the high voltage transmission grid.

Chapter 2

The electric car

The invention of the electric car is not as recent as people may think. It actually dates back to the 1830s, pre-dating the petrol powered cars. Still in the early 1900s, the electric car was seen as superior to the petrol powered ones because of their ease of use and their reliability [39].In particular electric cars did not need frequent maintenance (especially fluids changes) and a clutch and gearbox system because the electric motor mechanical characteristic allows a simple gear reducer to be used instead. These advantages came with a huge problem: batteries capacity. At the time batteries could hold about 0.1 MJ of energy for each kilogram of mass against 47 MJ for each kilogram of petrol, that meant hundreds of kilograms of batteries were needed to achieve the same range as petrol powered cars even considering the two system's different efficiencies.

Figure 2.1: Lady driving an electric car in the early 1900s

Nevertheless, ladies favoured the electric car because of their ease of use and cleanness: no oil changes, no greasing, no noise, no burning oil smell [31]. By

the time of car mass production, though, the internal combustion engines (based either on the Otto or the Diesel cycle) were reliable enough to be the obvious power-train choice because of the high range while using only a few gallons of fuel. The unavoidable heat of these engines could be cheaply used for the heating system, so that the electric car has essentially been a research topic since then.

The electric car came back to the market in the WWII occupied France, when Peugeot technicians produced a small series of electric cars named VLV (Voiture Légère de Ville, i.e light town car) to overcome fuel rationing. The 350kg city-car with a 1.5 PS electric motor had a maximum speed of 30 km/h and the batteries granted a range of 70 km. Less than four hundred VLV were ever produced, but allowed the ones who could afford it to use the car anyway [31].

Figure 2.2: VLV electric car built in Paris during WWII

Electric cars disappeared from the market until 1990s, when some car manufacturers like GM, FIAT and others built some model that went beyond the prototyping phase like the GM EV-1 and the Fiat Panda Elettra among others.

The 1996 GM EV-1 car, for example, was the first car to have specifications similar to the fuel powered competitors: maximum speed of 130 km/h and a useful range up to 240 km. It used many up-to-date technical solutions to increase efficiency and get a longer range from her lead-acid batteries [39]. Some of those are:

- an aluminium frame,

- an extreme aerodynamic shape,

- an heat pump based heating system which is more efficient than traditional resistors in terms of power consumption.
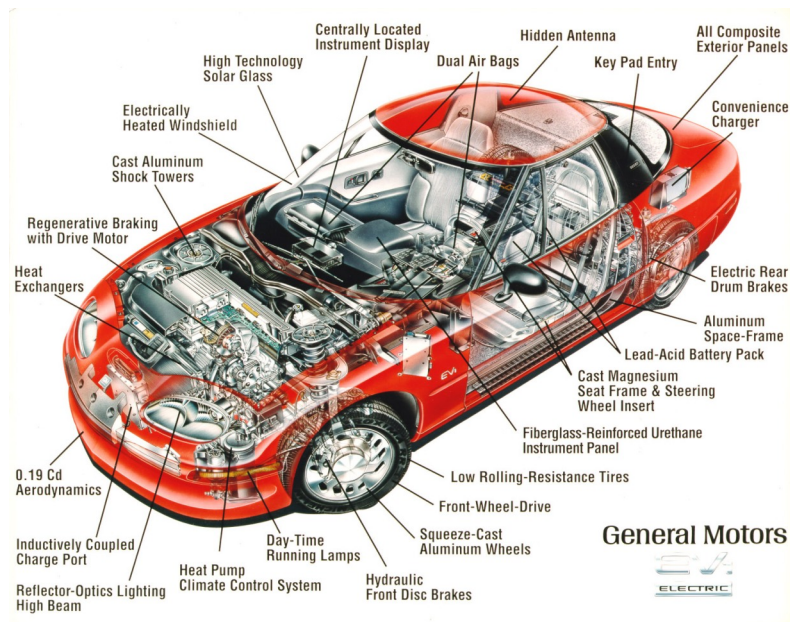
Figure 2.3: Inside components of the GM EV-1 electric car

The same model has been later refitted to use Ni-MH batteries: these allowed to double the amount energy per mass unit but revealed very unreliable. The EV-1 was leased for a brief period of time in California and Arizona to selected buyers only, when retired it was not available for sale (GM decided to recycle them with the exception of the ones that were disabled and donated to museums or universities) causing protests from the environmentalists.

In the meanwhile FIAT built the Panda Elettra, and the Seicento Elettra, both were conversion of the standard car.
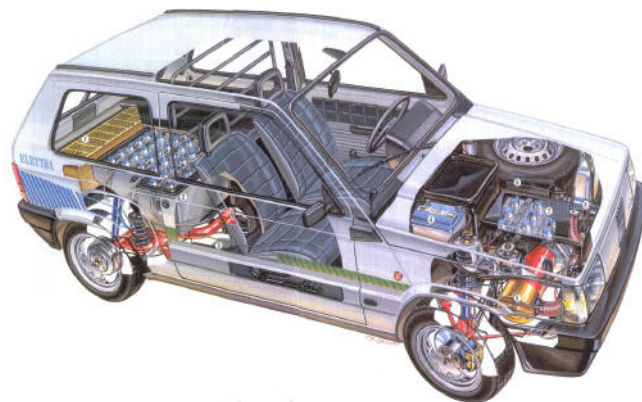

Figure 2.4: Cutaway view of the 1990 FIAT Panda Elettra

The 1990 Panda Elettra was a conversion of the entry level petrol based Panda car but with only the two front seats because the traction batteries were located

in the boot and in place of the rear seats. It had a 14 kW electric motor and a four speed gearbox, the lead acid batteries allowed ranges up to 100 km between two consecutive charges. Despite the good critical acclaim, the high price tag (ITL 25 million) made it a sales failure [32].

In 1996 FIAT proposed the Seicento Elettra, a conversion to the electric technology of the FIAT Seicento. This time Fiat redesigned the frame entirely to avoid the loss of the rear seats. This was achieved by putting the batteries in the bonnet, under the centre console and the rear seats. The power-train was made of a three-phase induction motor with a power rating of 15 kW controlled by a vector controlled inverter with no gearbox (direct drive). It is to be noted that Li-ion batteries were available as an optional [22].

Figure 2.5: Cutaway view of the FIAT Seicento Elettra

The high weigh and cost of the batteries combined with the low range and the relatively low fuel prices meant that the electric car was not competitive with the traditional oil powered vehicle. The turning point that made the battery powered car feasible did not come from the automotive industry, though. The need to power increasingly smaller and energy hungrier electronic devices has lead to the development of the lithium-ion battery, which power density is about six time bigger that of the lead-acid one. It means that the car industry can use a proven technology that has to be adapted to the new use-case. The concerns are especially on the lifespan of the battery itself and its price. This, nevertheless, allowed the introduction of the electric car in the market: today some of the most famous electric cars are the Tesla Roadster and the Nissan Leaf, both pure electric vehicles powered with Li-ion batteries.

Despite being more expensive, electric cars (e-car) have seen a steady raise in market share both in Europe and in the US. This trend is probably going to be affected by the recent emission scandal, as even more people may switch from the diesel to electric car. As of 2012 electric vehicles and charging station are spread in the world as shown in figure 2.6 [21].

At the moment the European market sees an increase in the number of e-cars sold and this is particularly evident in Norway and in the Netherlands [16]. In this countries the market share of electric vehicles is above 4% despite the higher price tag. The buyers statistically fall in at least one of two categories: they are
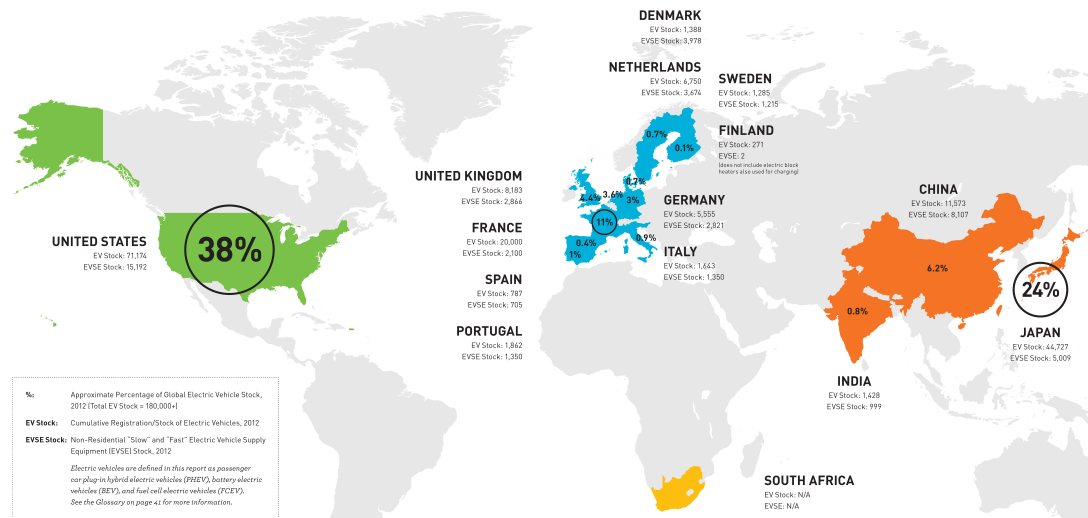
Figure 2.6: Distribution of electric vehicles stock in the world (2012) [21]

environmentally concerned or looking to save money but, in both cases, the potential buyers are usually high income and highly educated people. Nevertheless there are other form of incentive to make e-cars attractive, for example: preferential parking permits in big cities, tax exceptions (in Norway e-cars do not pay VAT, tolls, circulation and registration taxes) and usage of reserved lanes allowed [16].

The US States where most e-cars are sold are California, Washington, Georgia, Maryland, and DC where there is a system of tax cuts to people that buy an e-car. This has been achieved though tax discounts and appropriate laws to make this type of vehicle competitive with traditional petrol cars. It is interesting that the Californian law (ZEV law) mandates every car manufacturer to build and sell a certain percentage of electric cars [36]. FIAT, for instance, sells the 500e to comply with Californian regulation.

Even China is worrying for the poor air quality and the pollution, so much that the communist party is pushing to increase e-cars sales because the country's 2015 target has not been met yet. In addition to that, the Party is going to propose a speed up in charging points building and other measures to increase the e-car market share; among others subsidies to towns converting to new energy buses and increased research and development on battery technology [35].

In Japan, on the other hand, the sale of electric vehicles is still relatively low, despite the higher number of fast charger installed. This may be the consequence of the decision from Toyota and Honda to focus on hybrids and fuel-cell powered vehicles [47].

Forecasting the future trend on e-car sales is not an easy task because it has to take into account many factors, like the development potential of the current technology, oil prices and battery prices. According to statistical data, battery
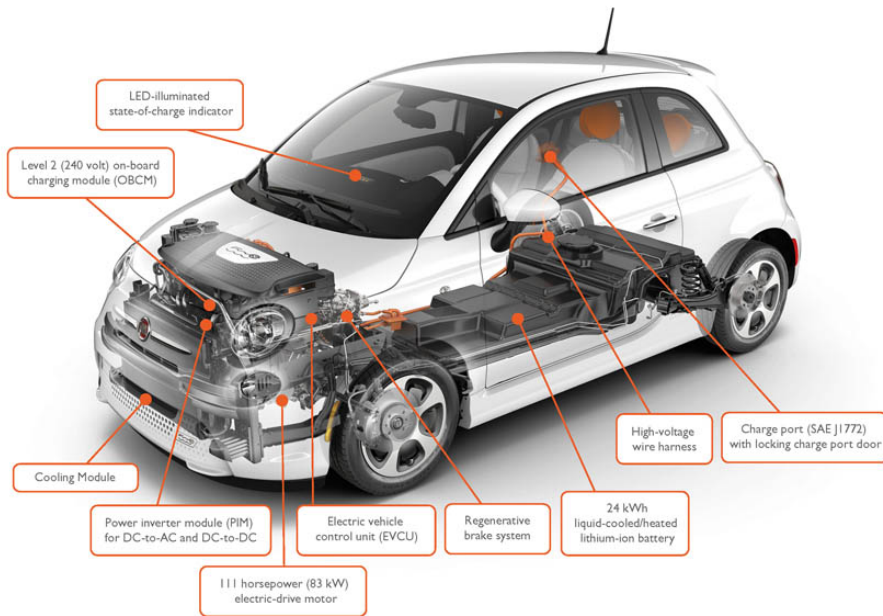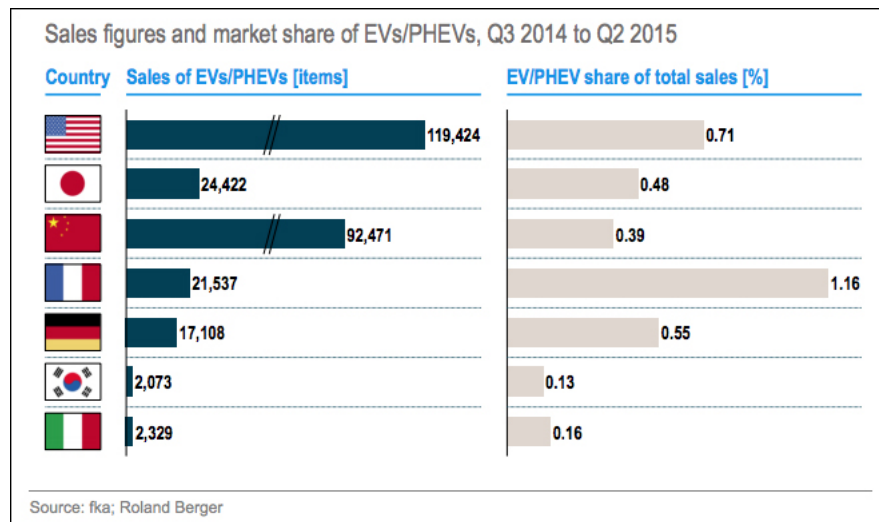
Figure 2.7: Cutaway view of the FIAT 500e

Figure 2.8: sales and market share of EVs, Q3 2014 to Q2 2015

prices will continue falling thanks to more advanced technologies and higher scale

economy, while several investment banks forecast increased oil prices in the range of 70 to 90 US dollars a barrel. Therefore it is to be expected, according to the
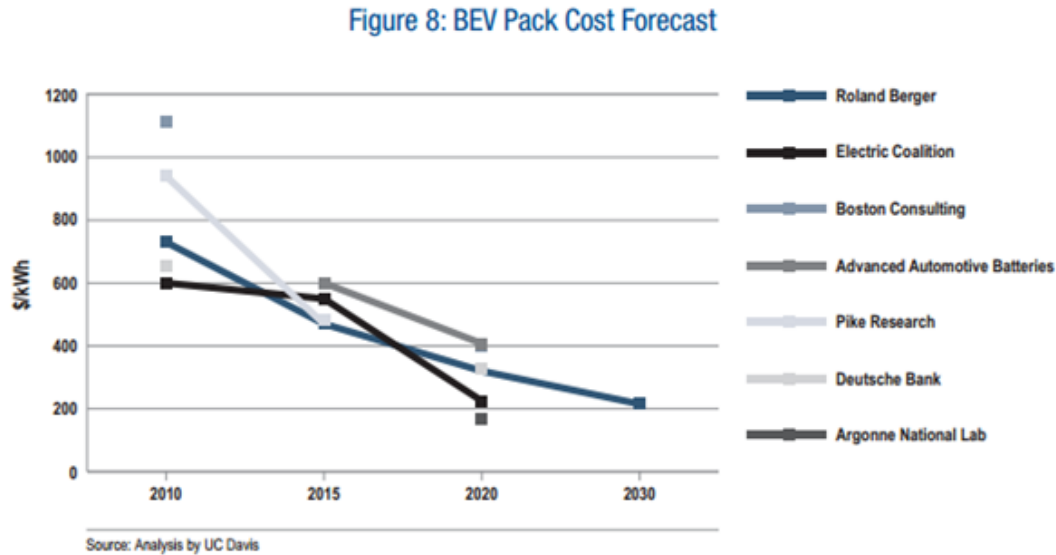

Figure 2.9: battery prices forecast [18]

data provided by UC Davis, that the batteries will be competitive with regular fuel by 2020 considering a crude price of $ 70 a barrel [18] (figures 2.10 and 2.9). This can also be sped up by laws, for example it is estimated that, because of the ZEV law, 15 % of cars sold on California by 2025 is going to be electric or fuel cell powered [36].

The EVI (Electric Vehicles Initiative) released a outlook in 2012 about the future of electric cars [21]. According to their forecast, it is necessary that, by 2050, three quarters of the vehicle sales in the world have to be electric (of some kind) to meet the 2°C average global temperature increase goal. Some countries set Electric Vehicles (EV) sales and/or stock targets, to signal their commitment to electrification. These are by no means determinant for a successful EV deployment, but give an idea of the ambition of the policy makers. Together the targets add up to 5.9 million EV in sales and 20 million in stock by 2020. Figures 2.11 and 2.12 show the national targets for sales and stock respectively. It is clear that targets are not actual forecasts, but allow to keep track of the progress made. The deployment of e-cars has to be accompanied by the right infrastructure, especially charging points. There is no right way of doing it, but the strategy has to be adapted for each country market and necessities: Japan, for example, has based his infrastructure strategy on fast chargers, while the US has emphasised slow chargers because of the predominance of the Plug-in Hybrid Electric Vehicles and the Netherlands has a mix of both. Another factor to be taken into account is the number of models available, because the market share appears to be directly
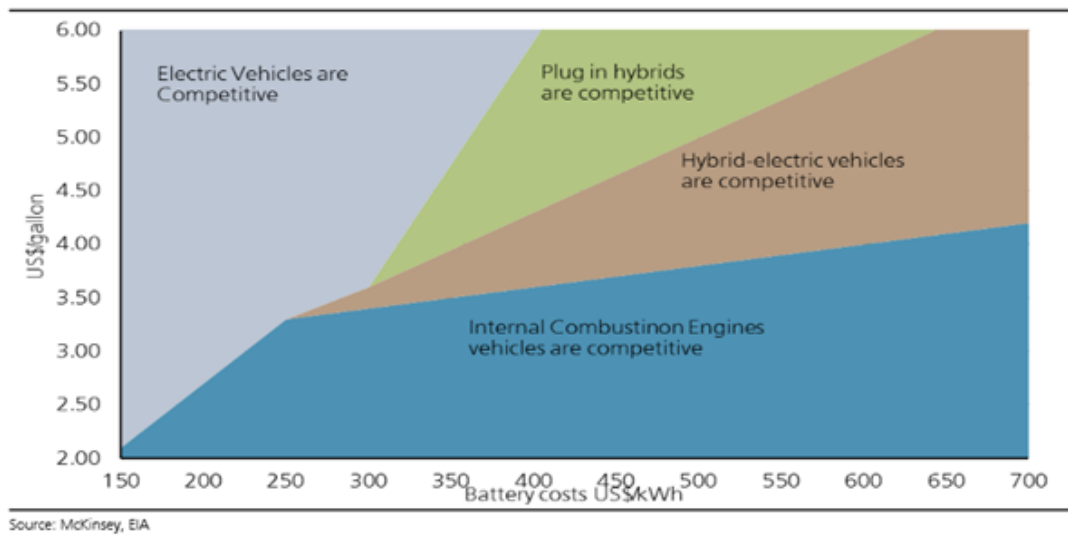
Figure 2.10: price competitiveness of EV and traditional vehicles basted on battery pack cost and oil prices [18]

linked to the number of models available on the market[21].

Figure 2. EV Sales Targets [select EVI members]

Source: EVI. Note: A 20% compound annual growth rate is assumed for countries without a specific sales target (i.e., only a stock target) or with targets that end before 2020.
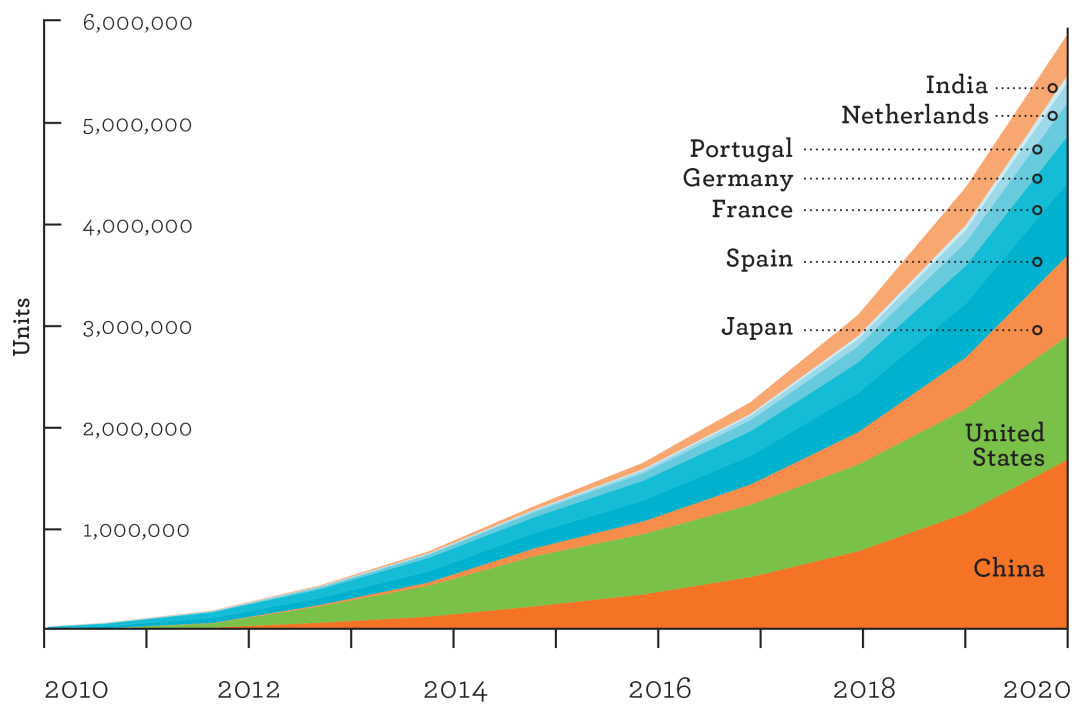

Figure 2.11: EV sales targets [21]

Figure 3. EV Stock Targets [select EVI members]

Source: EVI. Note: A 20% compound annual growth rate is assumed for countries without a specific stock target (i.e., only a sales target) or with targets that end before 2020.
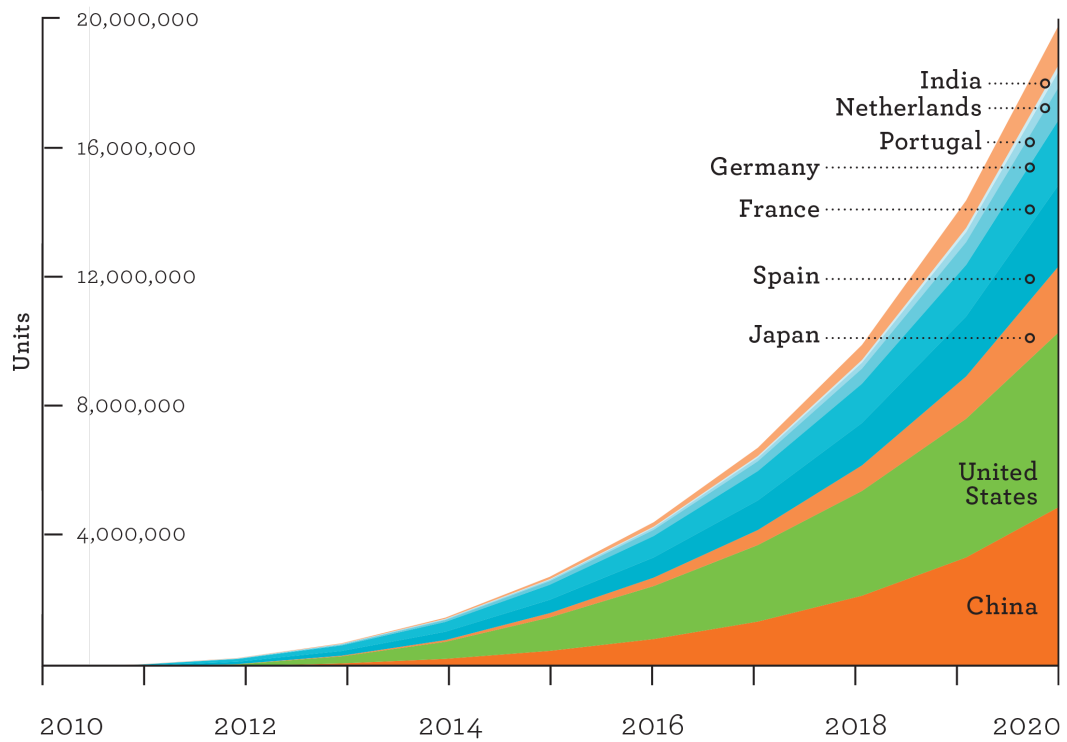

Figure 2.12: EV stock targets [21]

Chapter 3

Electric Vehicle charging

Electric vehicles need to have their batteries recharged to gain extra range just like a traditional petrol car needs to have its tank filled up at a petrol station. There are three ways to get the batteries charged [16]:

- Battery swapping consist in swapping the depleted batteries with fully charged ones. In practice almost no current electric car (except Tesla's) allows it and has lost much of it's appeal when a service provider went bankrupt in 2013.

- Wired charging brings electricity to the vehicle using cables and plugs. It is the most widely used technology.

- Induction charging transmits electricity though high frequency variable magnetic fields. It is still in development and it is only used in a few pilot locations.

The CENELEC EN 61851-1 standard on wired charging requires that the EV shall be connected to the EVSE (Electric Vehicle Supply Equipment) so that in normal conditions of use, the conductive energy transfer function operates safely.

In particular the standard defines four charging modes but they are not all legal in every country. The four charging modes are:

- Mode 1,
- Mode 2,
- Mode 3,
- Mode 4,

Mode 1 charging requires to connect the EV to the a.c. supply network (mains) utilizing standardized socket-outlets not exceeding 16 A and not exceeding 250 V single-phase or 480 V three-phase, at the supply side, and utilizing the power and protective earth conductors.

Mode 2 charging requires a connection of the EV to the a.c. supply network (mains) not exceeding 32 A and not exceeding 250 V single-phase or 480 V three-phase utilizing standardized single-phase or three-phase socket-outlets, and utilizing the power and protective earth conductors together with a control pilot function and system of personnel protection against electric shock (RCD) between the EV and the plug or as a part of the in-cable control box. The in-line control box shall be located within 0.3 m of the plug or the EVSE or in the plug.

Mode 3 charging requires to connect the EV to the a.c. supply network (mains) utilising dedicated EVSE where the control pilot function extends to control equipment in the EVSE, permanently connected to the a.c. supply network (mains).

Mode 4 charging needs a connection of the EV to the a.c. supply network (mains) utilising an off-board charger where the control pilot function extends to equipment permanently connected to the a.c. supply.

It possible to classify the four charging modes according to the charging speed: mode 1 and 2 are generally used for slow charging from the household plug, while mod 4 is usually used for fast DC charging at a charging station. Mode 3, on the other end, can be used both for slow charging and for fairly quick charging depending on the capability of the car and the infrastructure. The existence and the difference between modes 1, 2 and 3 is due to different positions: the consumer representatives want something cheap and feel that the stock household plugs are ok for home charging, while the industry feels a purpose built solution to be batter thanks to higher safety and reliability [13]. There are three connectors standardized for AC charging: the US, Japan, and other countries that have a predominantly single phase distribution network use the type 1 (or SAE) connector (shown in figure 3.1); Europe has settled on the Mennekes type 2 (fig. 3.2) connector which supports both single and three-phase power supply up to 40 kW and China uses its own standard.

Figure 3.1: SAE J1772 connector and docking port

Figure 3.2: Mennekes type 2 connector and docking port

DC fast charging (mode 4) sees a different situation, because there are four standards available on the market and the question has not been fully settled yet. The available standards are:

- Tesla's Supercharger,

- the Chinese GB/T,

- the CCS,

- the CHAdeMO.

3.1   Tesla's Supercharger

Tesla has it's own fast charging standard: the Supercharger. It is patented and proprietary but Tesla has already said it is willing to share the infrastructure and the underlying patents under certain conditions [44] [53], namely:

- the cars have to be able to use the full power of the supercharger,

- the service has to remain "free" for the customers,

- the cost of the infrastructure has to be fairly shared between the manufacturers proportionally to the number of vehicles that can use the facilities.
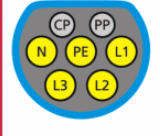
The Supercharger infrastructure has some differences between the American and the European market. These appear to be in the connector and in the power rating. The American connector is made for single phase and DC power and has therefore five pins (fig. 3.3).

Figure 3.3: Tesla Model S charging port on USA car

It is able to charge at 120 V and 240 V up to 11 kW per on-board charger and up to 135 kW for DC power at the Supercharger stations. The typical Supercharger is powered by a three-phase 12.5 kV line from the utility and it steps the voltage down to 480 V. Each charge-point-pair is supplied by twelve rectifiers rated 10 kW each. The 120 kW total is then shared between the two vehicles proportionally to the State Of Charge of each battery, i.e. the car with less battery charge will get the most power [38]. The European connector is based on the Mennekes type two, with the modifications needed to allow supercharging. The choice is due to the necessity of working with three-phase power, but it is not exactly the one produced by Mennekes (fig. 3.4) because it has to withstand the high power of supercharging [27].

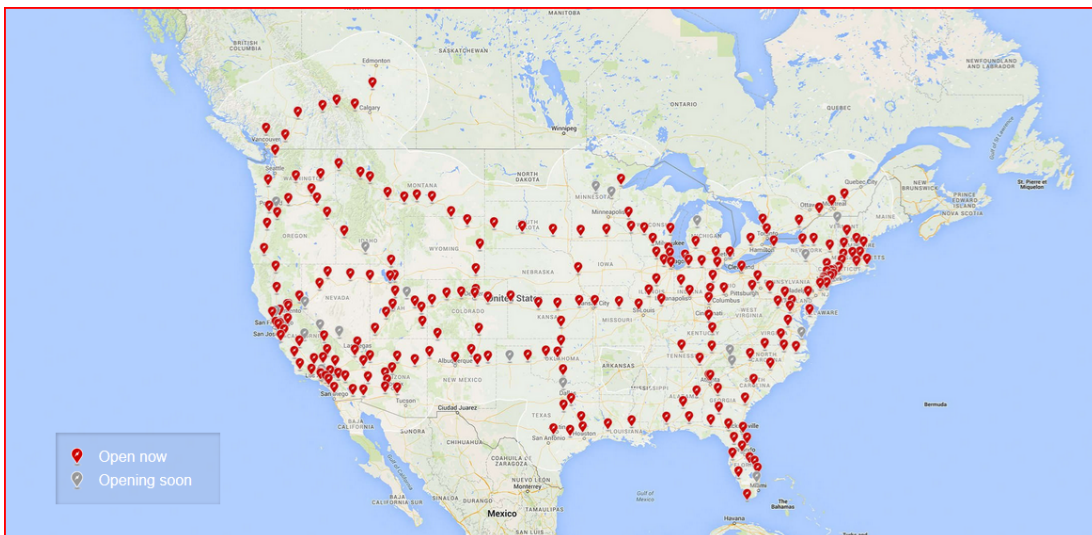Figure 3.4: Mennekes type 2 connector ratings

Figure 3.5: Distribution of Tesla's Superchargers in the US [9]

As of October 2015, maps in figures 3.5 and 3.6 represent the location where Superchargers can be found in the US and in Europe respectively.
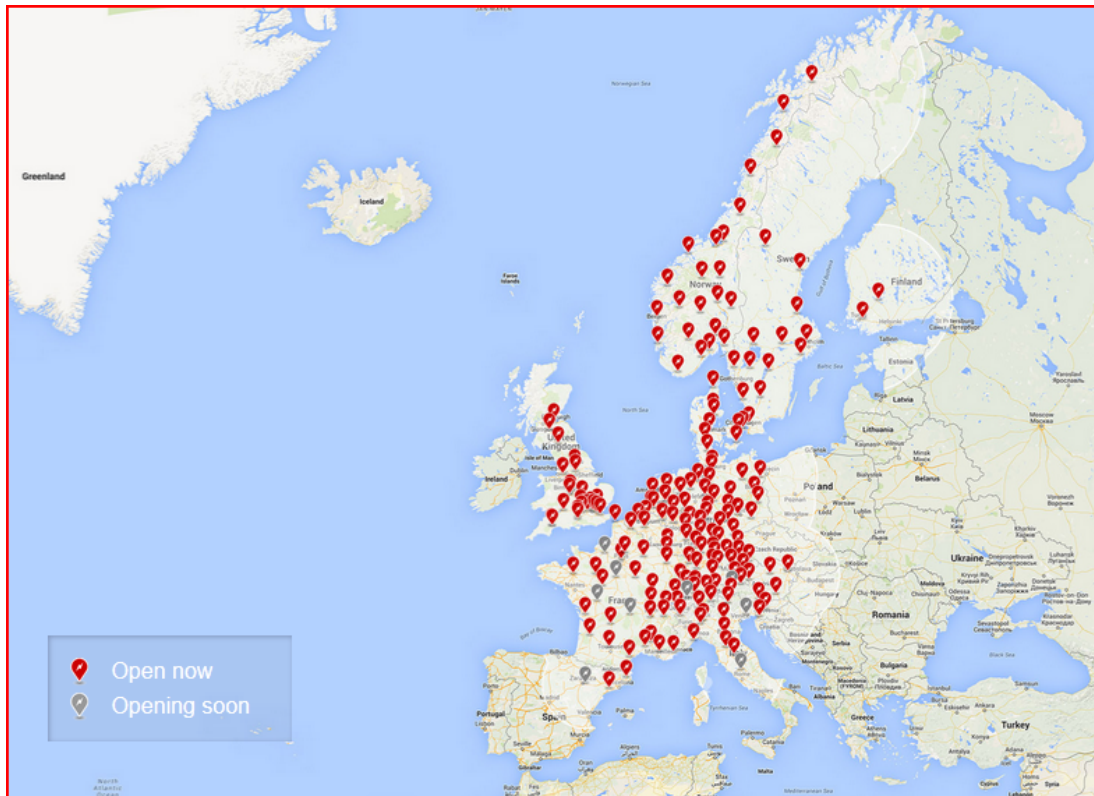
Figure 3.6: Distribution of Tesla's Superchargers in Europe [9]

Tesla's official website also has information on Supercharger installations projected in year 2016 as shown in figures 3.7 and 3.8.
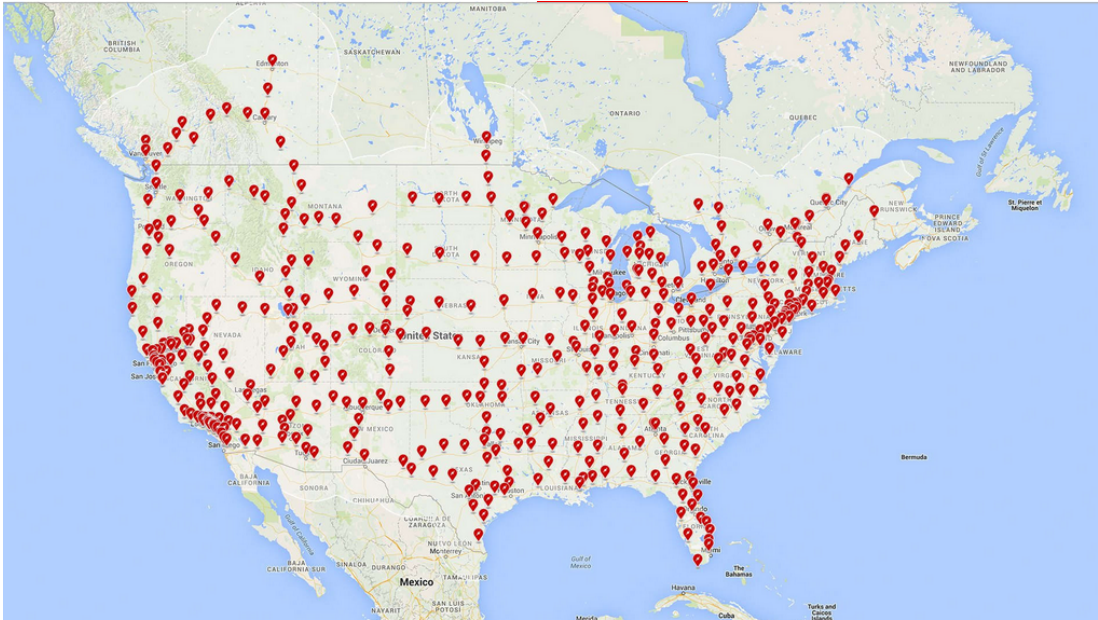
Figure 3.7: Supercharger stations available in the US by 2016 [9]
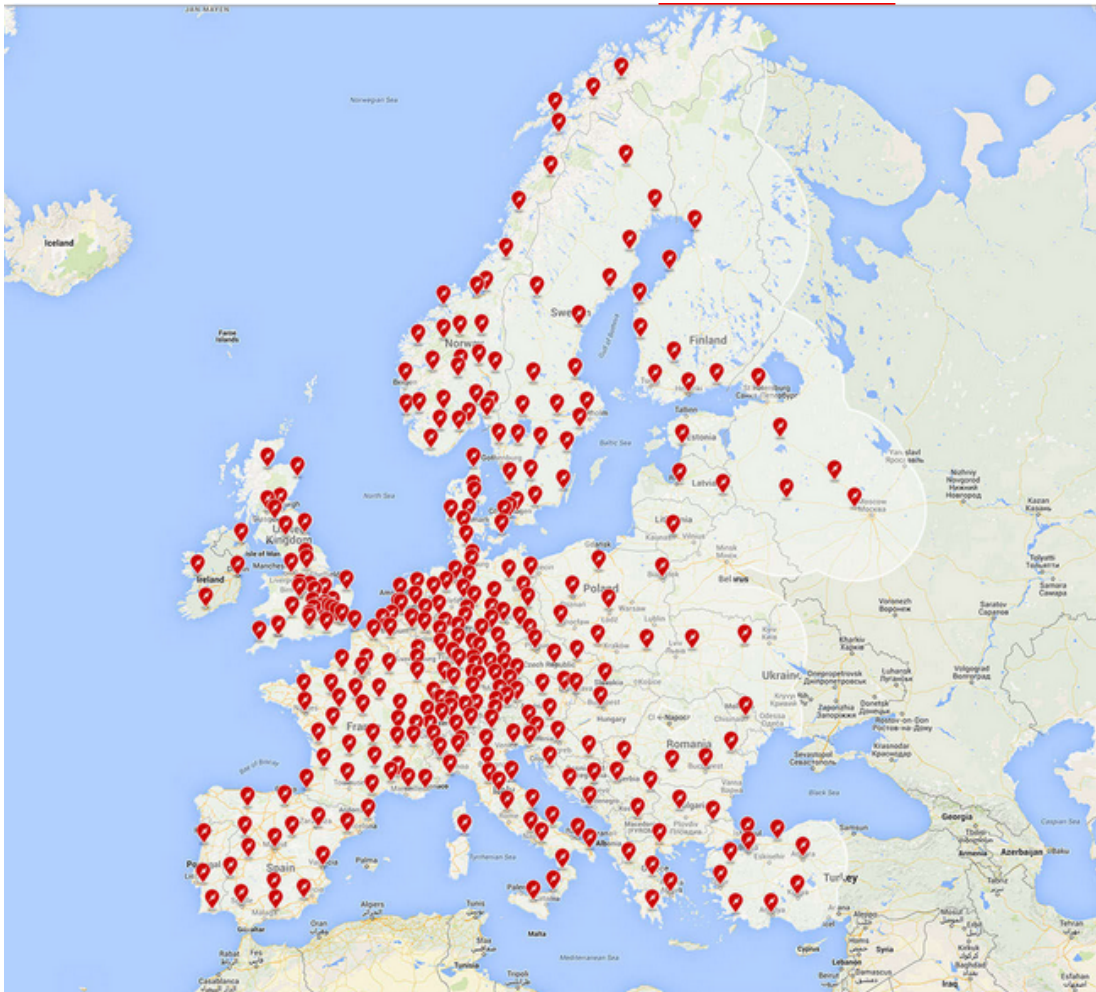
Figure 3.8: Supercharger stations available in Europe by 2016 [9]

3.2 The Chinese GB/T standard

The Chinese connector is called GB/T from the standard in which it is described: the GB/T 20234. This is a recommended standard from the Standardisation Administration of China whose standards begin with the GB acronym (Guo Biao, i.e. National Standard). The GB/T 20234 standard describes both the AC connector and the DC connector we are interested in (fig. 3.9).

Figure 3.9: DC connector and plug described standard GB/T 20234.3

The DC GB/T connector is designed to be used for both light vehicles (cars) and buses. It is able to deliver up to 170 kW of power as it can withstand up to 750 V and 250 A of DC current[37]. The communication system is based on CAN bus and protocol. The IEC adopted the GB/T 20234 standard including it in the IEC 62196-3 standard[23].

3.3 The Combined Charging System (CCS)

The CCS has been developed by American and German car manufactures, namely General Motors, Chrysler, Ford, Volkswagen, Daimler, BMW, Audi and Porsche to reduce the EV charging times from hours to about half an hour. Being an extension of the AC charging standard, the CCS exists in two variants: the type 1 for the US and Canada (fig. 3.10) and the type 2 for Europe (fig. 3.11) [41]. Despite the differences in plug and receptacles, this standard is identical between the two markets. The CCS is an international standard as described by the IEC 61851 and others[28] and has been chosen to be the quick charging standard in the European Economic Area [15].

Figure 3.10: CCS type 1 plug and connector

Figure 3.11: CCS type 2 plug and connector

This standard can deliver up to 200 A at 850 V (160 kW) and has growth potential. The communication system uses the same PLC based system of AC

charging with the addition of the DC specific data[28]. This standard can be used to charge both buses and electric cars and it is already being deployed in the UK, the US and other countries and the cars that can use this standard are the BMW i3 and the VW e-Golf [51]. According to [1], the availability of CCS quick-charging infrastructure is shown in figures 3.12 and 3.13 in the US and Europe respectively.
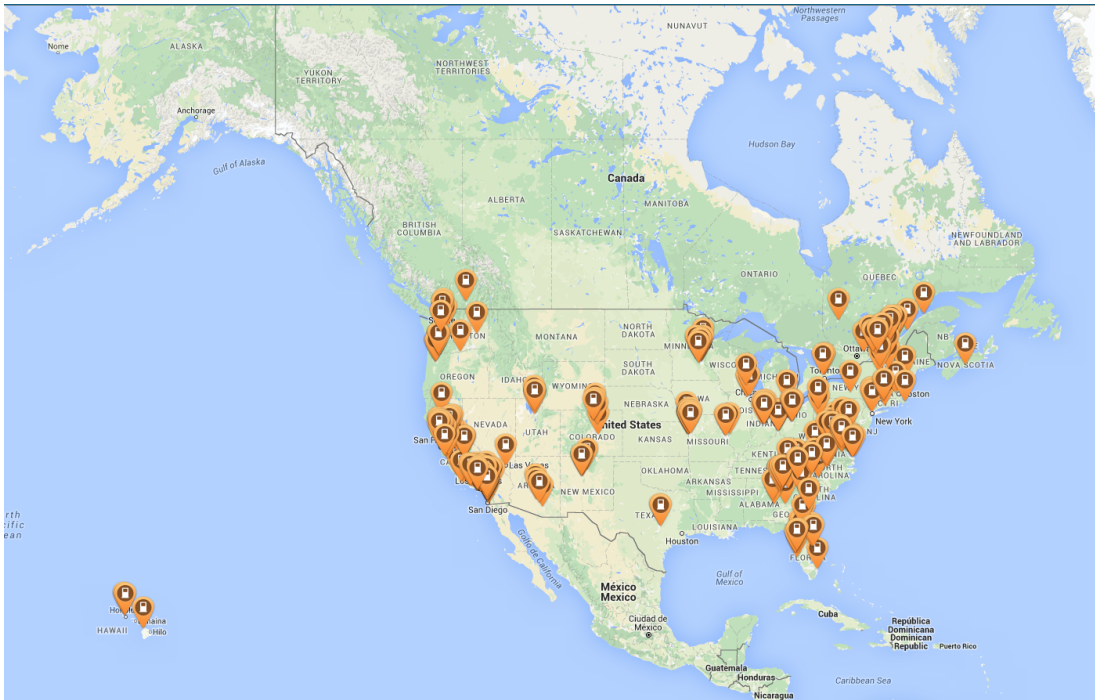

Figure 3.12: Distribution of CCS quick-charger in the USA [1]

The different CCS features are not set in a single standard, each feature has its own. The plug is standardised in the IEC 62196-3 as configuration EE for the American variant and configuration FF for the European one. Among other things, the IEC 62196-3 defines compatibility between the various plugs and sockets in table 3.1, while socket dimensions and electrical ratings are referred respectively to IEC 62196-2 and IEC 62196-1. The 2014 version of the IEC 62196-1 standard indicates a maximum voltage and current allowed on each contact according to table 3.2.

On the other hand, the charging procedure is described in the IEC 61851-23 standard. It describes, among other things, the process of energy supply in the following tables and images: figure 3.14 and table 3.3 describe the normal start-up procedure while figure 3.15 and table 3.4 describe the normal shut down procedure.

Figure 3.13: Distribution of CCS quick-chargers in Europe [1]

Table 3.1: plugs and sockets compatibility [26]

		Vehicle connector								
		Type 1	Type 2	Type 3	Configuration AA	Configuration BB	Configuration EE	Configuration FF	Universal, high power a.c.	Universal, high power d.c.
Vehicle inlet	Type 1	Yes	-	-	-	-	-	-	-	-
	Type 2	-	Yes	-	-	-	-	-	-	-
	Type 3	-	-	Yes	-	-	-	-	-	-
	Configuration AA	-	-	-	Yes	-	-	-	-	-
	Configuration BB	-	-	-	-	Yes	-	-	-	-
	Configuration EE	Yes	-	-	-	-	Yes	-	-	-
	Configuration FF	-	Yes	-	-	-	-	Yes	-	-
	Universal, high power a.c.	-	-	-	-	-	-	-	Yes	-
	Universal, high power d.c.	-	-	-	-	-	-	-	-	Yes

NOTE 1   For Type 1, Type 2 and Type 3 refer to the corresponding standard sheets in IEC 62196-2:2011.

NOTE 2   For Configurations AA, BB, EE, and FF, refer to the corresponding standards sheets.

NOTE 3   For Universal high power a.c. and Universal high power d.c., refer to IEC 62196-1:2014.

Table 3.2: Overview of the combined a.c./d.c. vehicle interface [26]

Position number [a]	Configuration								Symbol	Function
	Group 1 (under consideration)				Group 2					
	CC		DD		EE		FF			
	U_{max} V	I_{max} A	U_{max} V	I_{max} A	U_{max} V	I_{max} A	U_{max} V	I_{max} A		
1	Under consideration		Under consideration		600	200	1 000	200	D.C. +	d.c. +
2					600	200	1 000	200	D.C. −	d.c. −
3					--[b]	--[b]	--	--		d.c. −
4					--	--	--[b]	--[b]		d.c. −
5					--	--	--[b]	--[b]		d.c. +
6					--[b]	--[b]	--	--		d.c. +
7					600 [c]	--	1 000 [c]	--	PE	Protective earth
8					30 [c]	2 [c]	30 [c]	2 [c]	CP	Control Pilot
9					30 [c]	2 [c]	30 [c]	2 [c]	PP or CS	Proximity detection or connection switch

[a] Position number does not refer to the location and/or identification of the contact in the accessory.

[b] This contact is only available in Configuration EE and FF Inlets, may be used as portion of basic interface, see IEC 62196-2:2011, Standard Sheets 2-I, and 2-II.

[c] May be used as basic interface, requirements for basic interface see IEC 62196-2:2011, Standard Sheets 2-I and 2-II.

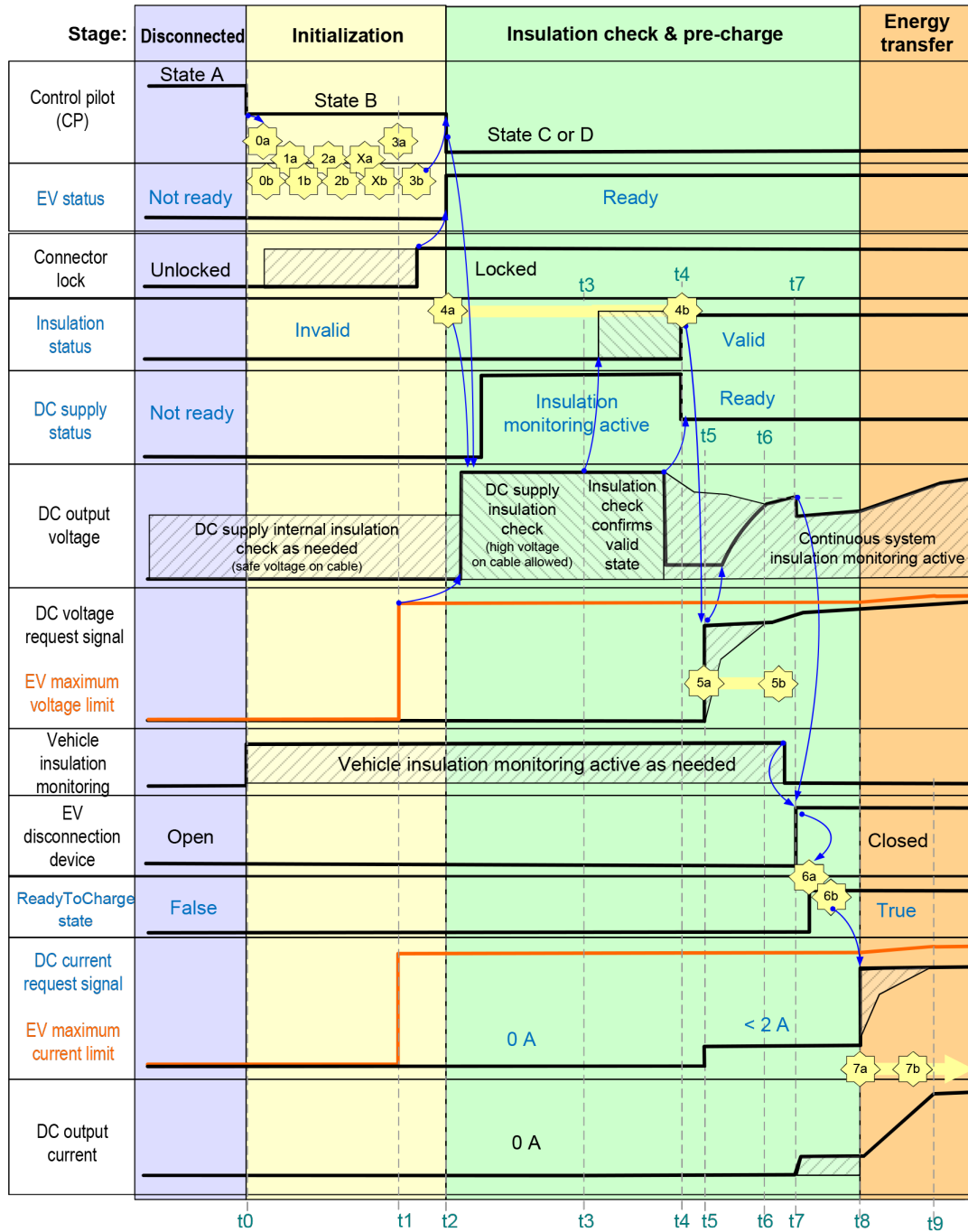NOTE   For combined a.c./d.c. vehicle interface, see IEC 62196-3.

Figure 3.14: sequence diagram for the normal start up procedure [25]

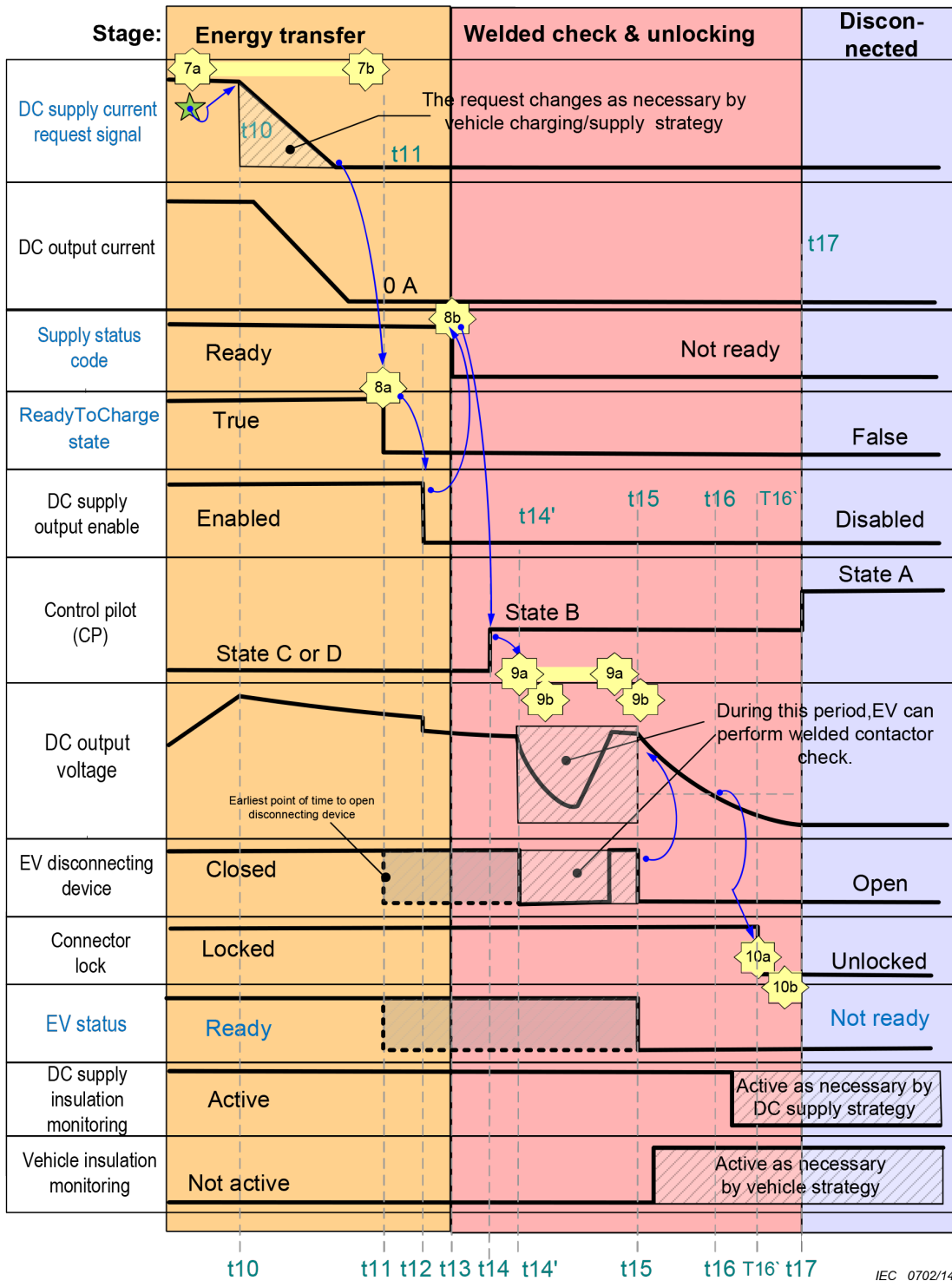|	Description
(t0)	− Vehicle connector is plugged into vehicle inlet which changes CP state from A to B.
(t0 → t1)	− High level communication (PLC) starts and handshaking with exchange of charging parameters takes place. − DC supply checks if d.c. output voltage is less than 60 V and terminates supply session if 60 V is exceeded.
(t1)	− EV sends its maximum limits (amongst other parameters) for d.c. supply output current and voltage with <3a>.
(t1 → t2)	− EV locks vehicle connector in its inlet. − Maximum values of the d.c. supply are responded to the EV with <3b>. − DC supply can check internal insulation as long as no voltage is applied to the connector. − If EV and d.c. supply are not compatible, then the vehicle will not go to Ready, and will transition to step t16 in the normal shutdown sequence.
(t2)	− EV changes CP state from B to C/D by closing S2 and sets EV status "Ready", which ends initialization phase.
(t2→t3)	− EV requests cable and insulation check by <4a> after connector lock has been confirmed. − DC supply starts checking HV system insulation and continuously reports insulation state by <4b>.
(t3)	− DC supply determines that insulation resistance of system is above 100 kΩ (cf. CC.4.1).
(t3→t4)	− After having successfully finished the insulation check, d.c. supply indicates status "Valid" with subsequent message <4b>
(t4)	− DC supply status changes to "Ready" with Cable Check Response <4b>
(t5)	− Start of pre-charge phase with EV sending Pre-Charge Request <5a>, which contains both requested DC current <2A (maximum inrush current according to CC.5.2) and requested d.c. voltage.
(t5→t6)	− DC supply adapts d.c. output voltage to requested value in <5a> while limiting current to maximum value of 2 A (maximum inrush current according to CC.6.1)
(t6)	− DC output voltage reaches requested voltage within tolerances given in 101.2.1.2.
(t6→t7)	− EV stops vehicle internal insulation monitoring, if any and necessary. − If necessary EV adapts requested d.c. voltage with cyclic messages <5a> in order to limit deviation of d.c. output voltage from EV battery voltage to less than 20 V (cf. Note in CC.5.1).
(t7)	− EV closes its disconnecting device after deviation of d.c. output voltage from EV battery voltage is less than 20 V.
(t7→t8)	− EV sends Power Delivery Request <6a> with ReadyToChargeState "True" to enable d.c. power supply output. − After disabling pre-charge circuit, if any, and switching on its power supply output, d.c. Supply gives feedback <6b> that it is ready for energy transfer.
(t8)	− EV sets d.c. current request with <7a> to start energy transfer phase.
(t8→t9)	− DC supply adapts its output current and voltage to the requested values. − DC supply reports its present output current and output voltage, its present current limit and voltage limit, and its present status back to the EV in message <7b>. NOTE EV may change its voltage request and current request even if output current has not reached the previous request.
(t9)	− DC output current reaches d.c. current request within delay time T_d defined in 101.2.1.3. (time span t9 − t8 = T_d, if one request has been made, bold line shows this situation)
(t9→)	− EV adapts d.c. current request and d.c. voltage request according to its charging/supply strategy with cyclic message <7a>.

Table 3.3: sequence description for normal start up [25]

Figure 3.15: sequence diagram for the normal shut down procedure [25]

	Description
(t10)	The EV reduces the current request to complete the energy transfer. Reduction is done on EV charging/supply strategy.
(t10→t11)	DC supply shall follow current request with a time delay acc. to 101.2.1.3 and it shall reduce the output current to less than 1 A before disabling its output.
(t11)	The EV requests the DC supply to disable its output by sending message <8a> power delivery request with ReadyToChargeState set to False.
(t11→t12)	EV may open its disconnection device after current is below 1 A.
(t12)	– DC supply disables its output and opens contactors, if any – DC supply shall enable its circuit to actively discharge any internal capacitance on its output after receiving message <8a> with "ReadToChargeState" set to false. – DC supply shall not cause any current flow on EV input during discharge.
(t13)	DC supply reports status code "Not Ready" with message <8b> to indicate it has disabled its output within 2 s.
(t14)	EV changes CP state to B after receiving message <8b> or after timeout to ensure that DC.. supply has discharged its output at latest by t14 (in case message <8a> was lost)
(t14')	EV can optionally perform its welded contactor check and indicate this to the d.c. supply with message <9a>.
(t14'→t15)	The vehicle may send multiple <9a> requests in order to read the d.c. supply output voltage measured by the d.c. supply in the response message <9b>
(t15)	Latest point in time for EV going into "Not Ready" status and opening its disconnecting device
(t15→t16)	EV can start EV isolation monitoring, if any.
(t16)	EV unlocks the connector after d.c. output has dropped below 60 V.
(t16→t16')	DC supply continues insulation monitoring dependant on d.c. supply strategy.
(t16')	– SessionStopRequest with message <10a> terminates digital communication (PLC). – DC supply shall maintain state B2 (5 %) until 2 s to5 s after SessionStopRequest was received and then change to B1 (100 %). NOTE If the EV wants to restart supply again, it locks the connector, asserts "EV Ready", after which it initialization phase starts from t1. The communications session may have to re-start from t0 if the modems have shutdown.
(t17)	Disconnecting of vehicle connector changes CP state from B to A.

Table 3.4: sequence description for normal shut down [25]

The IEC 61851-24 standard describes the communication protocol for the CCS charging system through a redirection to standards DIN 70121, ISO/IEC 15118-1, ISO/IEC 15118-2:—, ISO/IEC 15118-3:— and states that SAE J2836/2[TM], SAE J2847/2, SAE J2931/1 and SAE J2931/4 standards can be used for information too.

3.4 The Japanese CHArge de MOve (CHAdeMO)

The CHAdeMO standard is developed by the CHAdeMO association which includes, among others, car manufacturers Daihatsu, Mazda, Mitsubishi, Nissan, Subaru, electronics industries NEC, Panasonic, utilities as TEPCO [2] and is international standard[48]. This standard is particularly known because of its usage on the Nissan Leaf electric car and Mitsubishi iMiev and is, consequently, particularly wide spread: according to the official CHAdeMO website there are over nine thousand stations worldwide; figures 3.16, 3.17 and 3.18 show the distribution of CHAdeMO chargers in Japan, the US and Europe respectively. In addition to the native CHAdeMO compatible cars, Tesla released an adapter for its Model S[3]: this optional allows Model S owners to charge at CHAdeMO stations even if it is slower than the Supercharger.

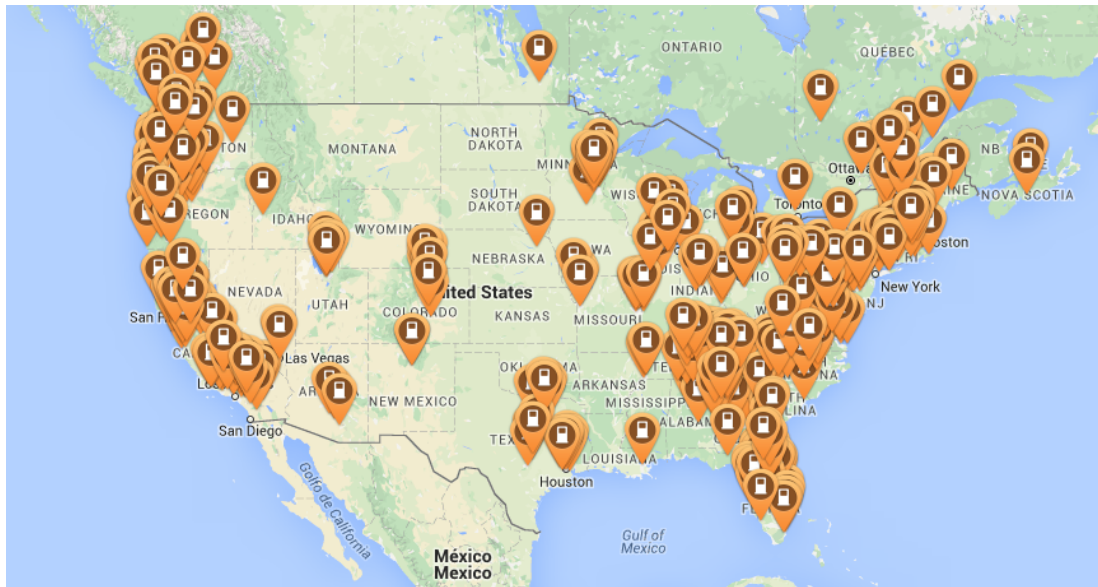Figure 3.16: distribution of CHAdeMO charger in Japan [4]

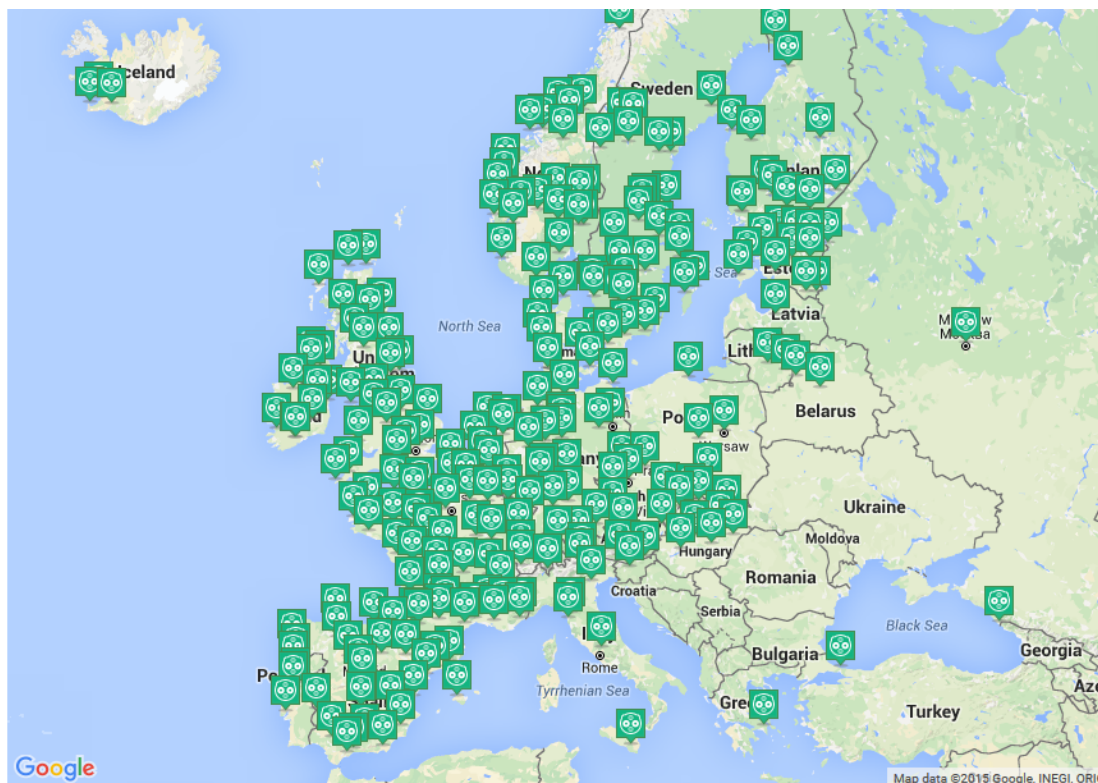Figure 3.17: Distribution of CHAdeMO chargers in the US [4]

Figure 3.18: Distribution of CHAdeMO chargers in Europe [4]

At the moment CHAdeMO can supply up to 500 V and 125 A (62.5 kW)[28], but most of the station are able to supply up to 50 kW. The conductor geometry
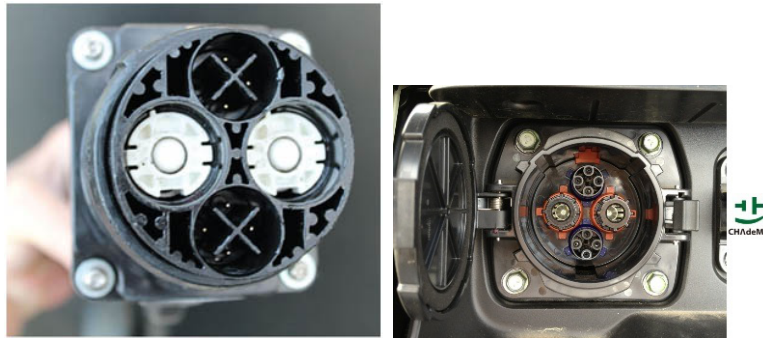
Figure 3.19: CHAdeMO connector and inlet

of CHAdeMO connector is designed to allow for 200 A, which means it can almost double its power level to adapt to the market environment as necessary[7]. The communication between vehicle and charger uses a CAN bus with the necessary redundancy features to allow a safe charging. Other characteristics allowing safe charging are[5]:

- no voltage when the coupler is disconnected,

- pre-charge automatic insulation test,

- vehicle coupler electrically and mechanically locked during charging,

- isolation transformer on the AC side and leakage monitoring device on the DC side,

- power cut-off if earthing and pilot wires are disconnected

An overview of the internal connection between the CHAdeMO charger and the vehicle is shown in figure 3.20.

Other CHAdeMO characteristics are:

- user friendly connector,

- future proof flexibility,

- smart grid compatibility.

The connector and the inlet have been designed to ensure the optimal balance between ergonomics performance, simplicity, and charging capability: despite the bulky appearance (70 mm in diameter), the DC inlet design allows CHAdeMO to keep the weight of coupler comfortably light for customers' everyday easy use. The use of different connector is a common practice in the electrical equipment industry when dealing with different types of supply and it allows the two charging inlets to be independently placed on the vehicle. The specification is also future
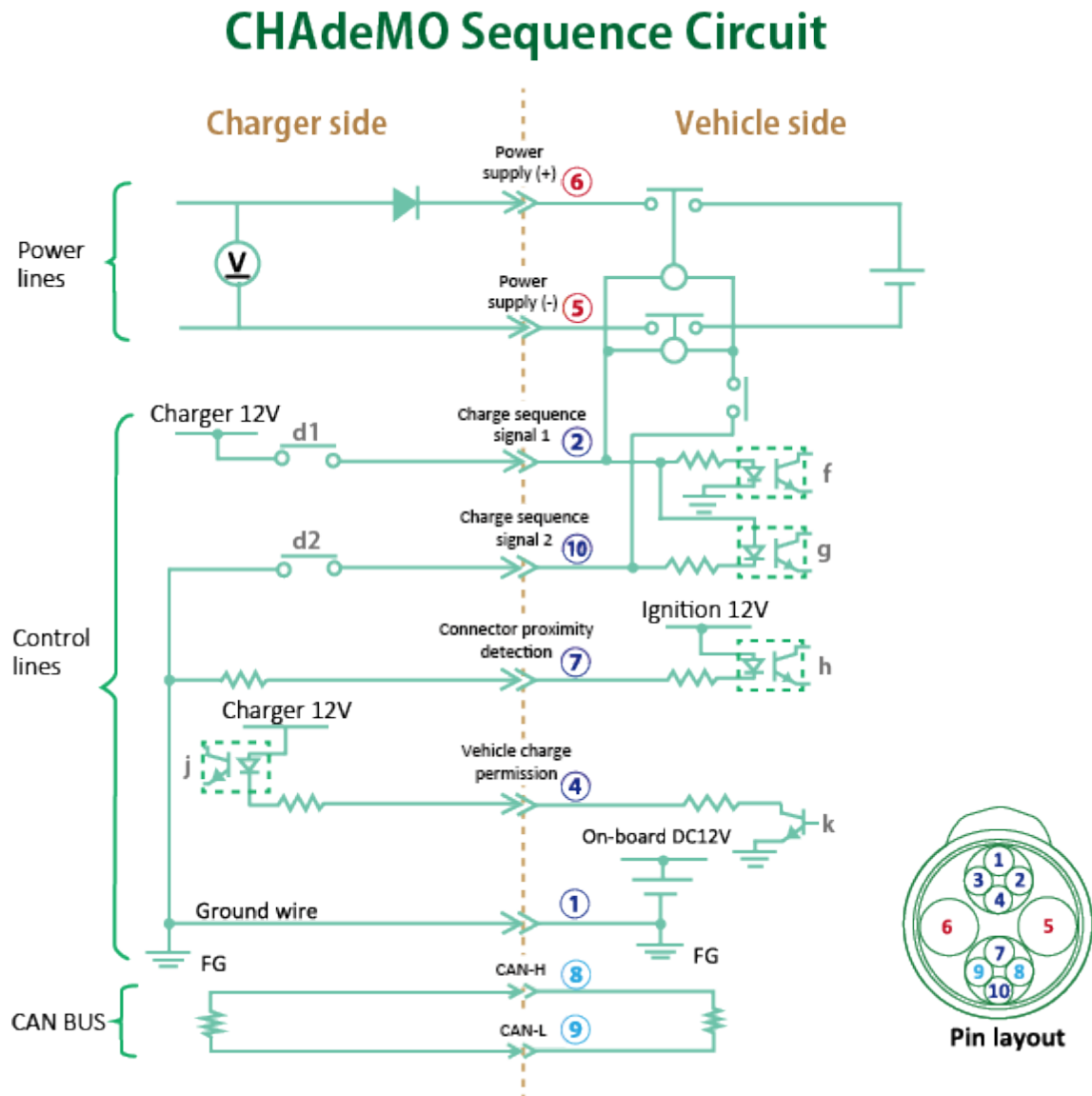
CHAdeMO Sequence Circuit

Figure 3.20: CHAdeMO Sequence Circuit [5]

proof, as the protocol only specifies the charging process between charger and EV, while leaving everything else to the provider's choice allowing it to meet the local requirements and to adopt payment method that suits them the most. The added bonus is that technologies and devices already in use on conventional vehicles are compatible with CHAdeMO charging because they are unaffected. The smart grid compatibility is achieved through the charger's ability to communicate with the vehicle and the grid. Being the connection ring between the two worlds, the charging point is able to adapt it's charging rate to the grid needs, i.e. without going beyond the grid capacity, and to use the car's advanced battery in a vehicle to home configuration: that means using the vehicle battery as a storage point

for the renewable energy source like a roof-top photovoltaic panel[6].

As said, the CHAdeMO specification is part of the IEC 61851-23, IEC 61851-24 and IEC 62196-3 according to the graph in figure 3.21 [48]. It is to be noted that the CHAdeMO official specifications and the IEC standards do not give the same amount of detail, because the IEC standards talk about essences and principle for ensuring electrical safety, power quality and design consistency while the CHAdeMO specifications include detailed technical information for charger and vehicle manufacture as they can timely reflect market needs [48].
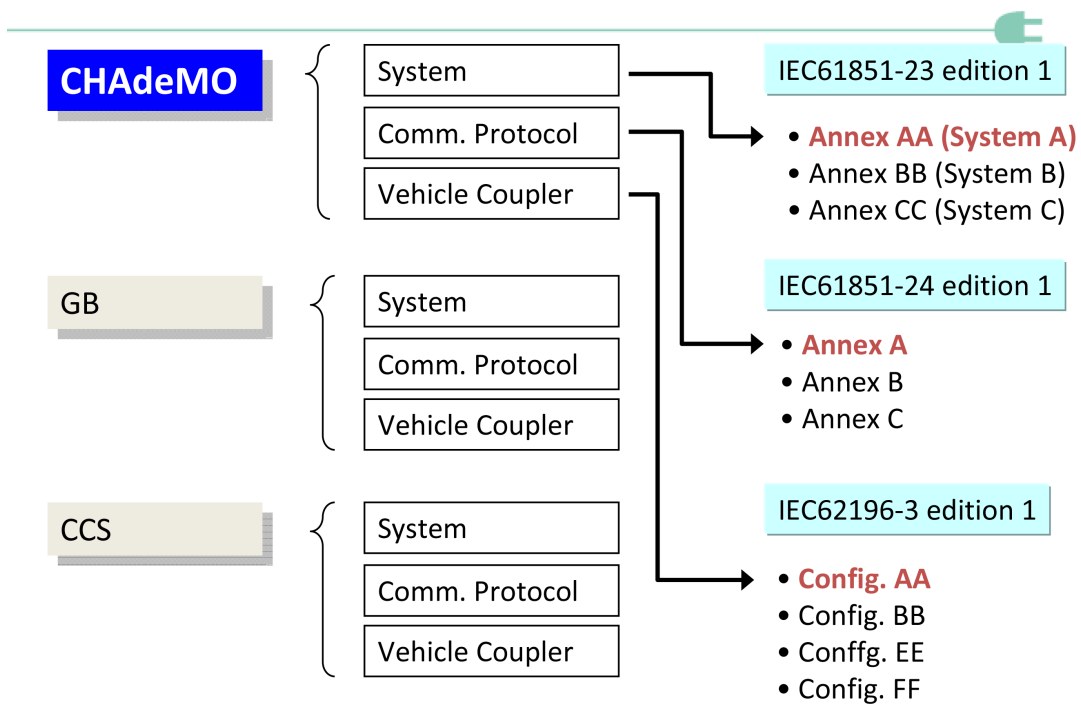
Figure 3.21: Integration of CHAdeMO into IEC standards [48]

3.5 Induction charging

Induction charging means replacing hard wired connections with other obtained through magnetic coupling of two (or more) coils to charge the battery of en electric vehicle. Using the magnetic field to transfer power between two circuits is nothing new: transformers and induction motors are based on this principle, but most of the magnetic circuit is made of magnetic steel or ferrite depending on the operating frequency. Induction charging a vehicle, despite how similar it may look, involves having a big air gap between the two circuits with the challenges associated.

The induction charging is being developed for a couple of reasons:

- inherent safety from electrocution (no need to touch parts potentially under dangerous voltage),

- no need to stand in a particular place to get the battery recharged,

- galvanic isolation of on-board electronics,

but the main disadvantage is the need of good inductive coupling to minimise losses and maximise energy transfer rate and efficiency and the presence of potentially dangerous high frequency electromagnetic fields.

There are different technologies for induction charging and wireless charging in general [33], some of them are:

- Inductive Wireless Power Transfer,

- Capacitive Wireless Power Transfer,

- Low Frequency Permanent Magnet Coupling Power Transfer,

- Resonant Inductive Power Transfer,

- Roadway/on-Line Power Transfer,

- Resonant Antennae Power Transfer.

Inductive Power Transfer (IPT) has already been used to charge a vehicle: the GM EV 1 featured a receptacle for the inductive charger shown in figure 3.22. The major benefit of this system is the ability to place the magnetic core in the charger, thereby minimizing the sensitivity of on-board EV components to flux density and frequency. Moreover it can be implemented as a single loop, which can function over a wide range of frequencies and can be adapted to meet a variety of power requirements. The main problem is the presence of a non linear flux distribution over the magnetic core that effects eddy current losses and electromagnetic interference[33].

Figure 3.22: Small paddle inductive station (Left), and the paddle (Right)

Capacitive power transfer is based on coupling capacitors, and it performs better than induction coupling for low power applications such as tooth brushes and mobile phones because the magnetic coupling does not scale down in power as desired. High power applications such as electric vehicles are, however, better suited for magnetic coupling [33].

Low frequency permanent magnet coupling power transfer combines known elements from magnetic gears and synchronous-permanent-magnet-electric-machine technology and it is made of two components: transmitter and receiver. The transmitter is made of a permanently magnetised cylindrical rotor that rotates though an external drive or through static windings separated by an air gap. The receiver has a similar rotor that is parallel to the utility side installation with a maximum distance of 150 mm and that is magnetically coupled so that its speed is the same of the transmitter's rotor (magnetic gear effect). This rotor is placed inside a generator to generate electricity. The apparatus is shown in figure 3.23. The main problem of this are the rotating parts that have to be maintained, cause noise and vibration; the apparatus has a low efficiency quoted as about 80% [33].

Resonant inductive power transfer (RIPT) is the most common wireless power transfer technology. It uses at least two tuned resonant tanks (combinations of inductances and capacitances) which resonate at the same frequency [33]. The primary functions of the resonant circuits include:

- Maximizing the transferred power,

- Optimizing the transmission efficiency,

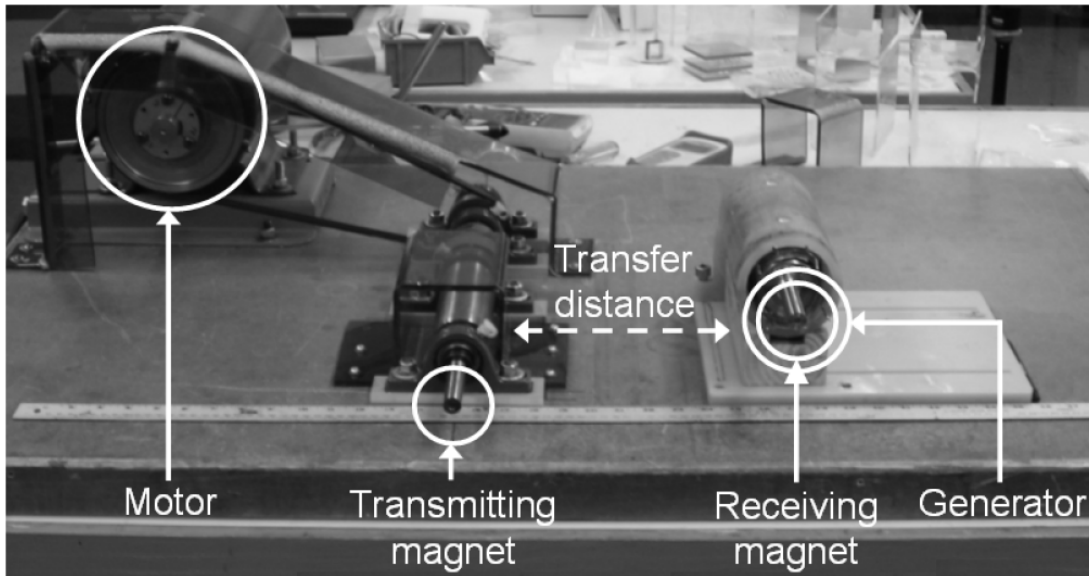- Controlling the transmitted power by frequency variation,

Figure 3.23: Photograph of a kW scale low frequency permanent magnet coupling power transfer prototype

- Creating a certain source characteristic (current or voltage source),

- Compensating variation of the magnetic coupling,

- Compensating the magnetizing current in the transmitter coil to reduce generator losses,

- Matching the transmitter coil impedance to the generator,

- Suppressing higher harmonics from the generator.

The advantages of RIPT over IPT include higher effective range (up to 40 cm), reduced electromagnetic interference, higher frequency operation, resonant switching of inverter and rectifier and higher efficiency. This system operates in the kilohertz range which is feasible with the current state of the art technology. A laboratory prototype has been built and has transmitted about 4 kW of power with a 92% efficiency, but it is expected that the overall efficiency is going to be about 85% due to the power factor correction and power supply efficiencies [33].

An on-line wireless power is similar to RIPT, however a lower resonant frequency is used and the technology has been reported for application higher power. Technologically, the primary coil is spread out over an area on the roadway and the power transfer happens at multiple locations within this area. Typically, the combination of the input side of the resonant converter along with the distributed primary windings is called the track and the secondary is called as the pick-up coil. Considering both the short range of EVs and the associated cost of

infrastructure, the feasibility of these charging systems might be unfavourable. However, one benefit is that due to frequent and convenient charging, vehicles can be built with a minimal battery capacity (about 20% compared to that of the conventional battery-powered electric vehicles), which can consequently minimise the weight and the price of the vehicle [33].

Resonant antennae power transfer is based on two or more aerials tuned at the same frequency. Capacitances and inductances are integrated into the aerials and allow acceptably efficient power transfer at distances up to 10 m. The working principle is similar to RIPT, but the impedance match frequencies are in the MHz range. This poses problems because of electromagnetic interference and compatibility concerns and limits for human exposure to radio frequency radiation are exceeded because the device is difficult to shield without hampering on performance and range. In addition to that, it is very difficult to generate high frequency power signal in the MHz range with the current power electronics technology [33].

One example of wireless charging technology is the Korean OLEV (On-Line Electric Vehicles). Developed by the Korean Advanced Institute of Science and Technology (KAIST), the OLEV technology is used for charging buses both in a city environment and in amusement parks, but can potentially be used in airports. OLEV uses Shaped Magnetic Field In Resonance to transmit power from the

Figure 3.24: OLEV based train in an amusement park

road surface to the vehicle, even if it is moving. At the moment this system can

transmit up to 100 kW of power up to 85% efficiency [14]. The transmitter is based on 5 m long segments that can be laid one after the other to get to the wanted length; this has the advantage that the control electronics can be shared and only the segments under the pick-ups will be turned on. Each receiver has a maximum power rating of 20 kW and weights about 400 lb (200 kg)[43]; that means it is feasible for heavy vehicles such as buses. Even though five pick-ups are
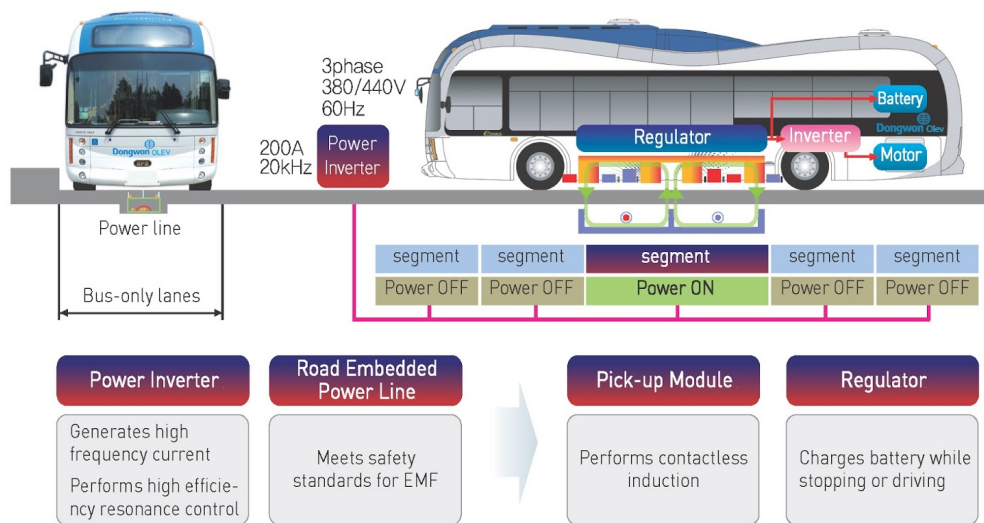

Figure 3.25: components of and OLEV system

needed to get 100 kW the reduced weight of batteries and the highly reduced need for high capacity recharging facilities make the OLEV system very competitive. One of the said application is public transit buses: in this scenario the OLEV system requires that only 10 to 15 percent of the line to be covered with the charging pads, but allows to reduce the battery size to one fifth of the capacity of a comparable vehicle. The system is very safe: despite the high operating frequency of 20 kHz the magnetic field emission is very low and well under the requirements of national and international standards.

Figure 3.26: OLEV based bus in service

Chapter 4

The 25 kV railway electrification system

The 25 kV AC single phase is the most common electrification system for new high speed lines in the variant 2 x 25 kV autotransformer feed. This electrification system is commonly used with the industrial frequency (50 or 60 Hz) but it may be used for the railway frequency as well [20].

The 25 kV electrification schemes are single phase electrification systems that are powered from the three phase industrial grid. This poses some problems due to the unbalance that a high power single phase load creates on the grid's voltage. The degree of unbalance on the grid is limited to reduce the possibility of damage to generators and electric motors and it is measured though the unbalance coefficient which is defined as follows [54]:

$$K = \frac{U_i}{U_d} \tag{4.1}$$

where U_i is the negative sequence voltage and U_d is the positive sequence voltage. In practice the unbalance coefficient is measured through the following approximated formula:

$$K = \frac{P_m}{P_{cc}} \tag{4.2}$$

where P_m is the power of the single phase load and P_{cc} is the three phase short circuit power of in the connection node. The international standards and the transmission system operators set the maximum degree of unbalance between 1 and 2 %, that means the load has to be connected to a high voltage node with sufficiently high short-circuit-power: this is no problem where a high power grid is available, but can be difficult in islands with a less powerful grid such as Sardinia [17]. The railway line is powered by several substations which are connected to a different phase pairs to further reduce load unbalance on the industrial grid. Each substation is build with redundant apparatuses such as two transformers and two connections to the industrial grid to prevent the line grinding to a halt in
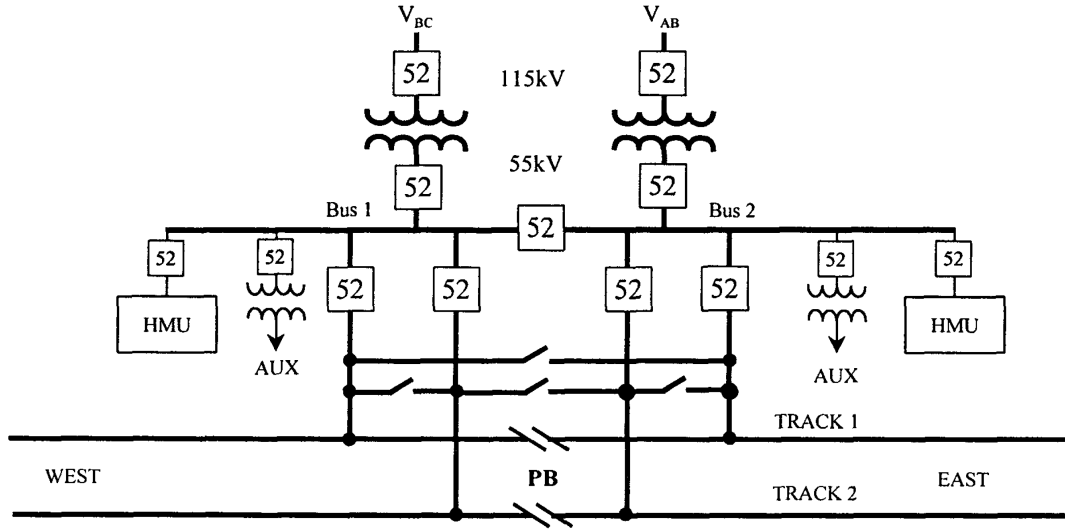
Figure 4.1: Simplified Single-Line Diagram of a Supply Station.
The boxes with the number 52 indicate circuit breakers

case of failure of any of these components. The connection between two different
phase-couples of two successive ESS implies that a neutral section has to be built
when the power supply switches from one ESS to the next because of the voltage
difference between two out-of-phase circuits; usually neutral sections are placed
at the substations and halfway through them. Each neutral section is signalled to
the engine driver to allow him to disconnect all the train loads (traction motors
included) before entering the neutral section itself. The neutral sections can be
energised form either end when needed. International standards set the tolerance
of the voltage in the system once the nominal value is chosen. The tolerances
and the maximum duration allowed for a nominal voltage of 25 kV are reported
in table 4.1.

U_{min2}	: lowest non permanent voltage (max. 10 min.)	17.5 kV
U_{min1}	: lowest permanent voltage	19 kV
U_n	: nominal voltage	25 kV
U_{max1}	: highest permanent voltage	27.5 kV
U_{max2}	: highest non permanent voltage (max. 5 min.)	29 kV

Table 4.1: 25 kV system operating voltages [52]

Low traffic lines are usually fed directly from the transformer through the
over-head line and the rail as return conductor. High traffic lines and high speed
lines are usually fed with an autotransformer system because it allows building the
feeding stations further apart and, consequently, to contain the costs of building
high voltage lines to connect substations to the grid.

The system was developed in the States by a specialists team comprising, among others, professor Scott for the New York, New Haven & Hartford Railroad in 1914 to reduce electromagnetic interference on neighbouring telephone and telegraph circuits due to the railway lines; the results were largely removed disturbance in the adjacent lines and higher energy transmission efficiency [11]. The first modern lines using the autotransformer system are the San Yo line (1972) and the Paris-Lyon High Speed Line (1981).

The system is called autotransformer system (or in our case 2 x 25 kV) because autotransformers allow to transmit energy to the train at higher voltage (50 kV), but the train is powered at 25 kV thus maintaining compatibility with existing rolling stock. Each electrical substation has two power transformers which supply the system from the high voltage industrial network. The distance between substations is usually between 40 to 60 km. Autotransformers are installed regularly every 10 to 15 km between two consecutive substations[34]. An hypothetical section of the line is represented in figure 4.2.
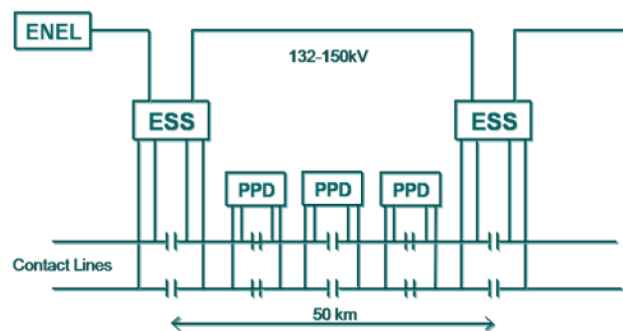
Figure 4.2: Position of the power supply equipment along a section of railway line [34]

The power circuit consists of the overhead line, a feeder and the running rail. The secondary winding of the transformer is centre tapped with the two poles connected to the overhead line and the feeder and the centre tap connected to rail earth. The voltage between the rails and the feeder and between rails and the overhead line is 25 kV; usually the rail-overhead-line voltage is chosen as phase reference and the feeder-rail voltage is therefore indicated as -25 kV because its phase is shifted by 180 degrees. The ESS provides power to the system trough the feeder and the overhead line and, ideally, the autotransformer steps down the voltage to the one used by the train, it means the autotransformer splits the current due to the power the train uses to the feeder and the overhead line as shown in figure 4.3. It also shows that the train gets power from the two nearest autotransformers, the one in front and the one behind the train, so the current is split between the two.

Professor Zaninelli studied the behaviour of the real 2 x 25 kV system as
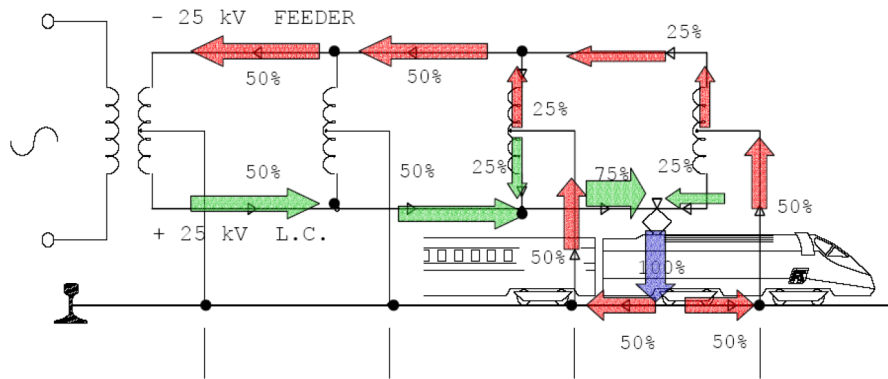
Figure 4.3: Power flow in an ideal 2 x 25 kV autotransformer system [34]

implemented by the Italian State Railways. According to his study, the real autotransformer system behaves very much like the ideal one with a very small part of the total current flowing in the rails in an empty cell thanks to the low short circuit impedance of the autotransformers [54].

The system is built differently depending on the number of tracks available. Each track has a complete set of wires if the rail is double tracked (figure 4.4(a)), four track railways can be built in two different configurations: it is possible to feed the fast tracks separately, thus requiring two autoransformers at each AT site or feed all the tracks together that means only two feeders and one autotransformer are needed (figure 4.4(b)) [52].

(a) Two track railway line

(b) Four track railway line

Figure 4.4: Autotransformer fed railway lines

The railway traction supply system has to be protected against faults so circuit breakers and switches are vital to isolate the faulted section and keep the system running. The hart of the protection system is a distance protection relay whose characteristic's shape can vary depending on the manufacturer and it is programmed to allow heavy loads without causing a trip. The same relay

has an integrated overcurrent protection to clear close-in faults as fast as possible and a close-onto-fault protection. The protection schematic is shown in figure 4.5 [45]. The distance protection relay monitors catenary voltage and the sum of
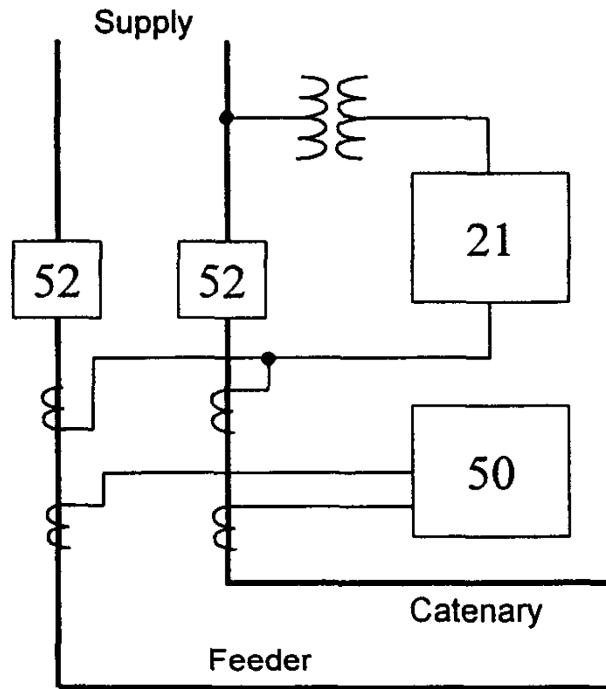
Figure 4.5: Protection scheme for catenary and feeder line.
The boxes with the number 52 indicate circuit breakers [45]

catenary and feeder currents. In the event of a phase-to-ground fault the relay measures the correct fault distance, but in the event of a catenary-to-feeder fault the calculated distance will be half of the real one and that is fine because the tripping decision will be correct. An automatic recloser is installed to reclose the circuit breaker after a specified dead time to energise the system again after the fault. If the fault is still present, the protection system trips again. All trains and autotrasformers have circuit breakers connected to under-voltage relays which disconnect them if the line isn't energised. This ensures that the reclose happens in a no load condition and allows to easily determine where the fault is because the current will flow only through the fault itself. If current flows on in the catenary, there is a catenary-to-ground fault. If the current flows only through the feeder, there is a feeder-to-ground fault. If the current flows through both catenary and feeder, there is a catenary-to-feeder fault. This information is gathered through an overcurrent relay which is not used to trip the circuit breaker, but sends it's signal to a PLC unit. Note that the overcurrent data gatherer relay can be set to a current less than the nominal of the system because of the no load condition (the

train has been disconnected and has not been powered yet). The PLC unit can then isolate the faulted Elementary Electrified Section (which the line is divided in) through SCADA-controlled motor-operated disconnectors and restore power to remainder of the line sections. Overvoltage relays with time-delayed pick-up (59 TDPU) automatically reconnect the autotransformers to the line once the voltage has stabilised [45].

The power transformers in the supply station and the autotrasformers are protected with transformer differential relays. The schematic of a paralleling station with autotransformer is shown in figure 4.6.
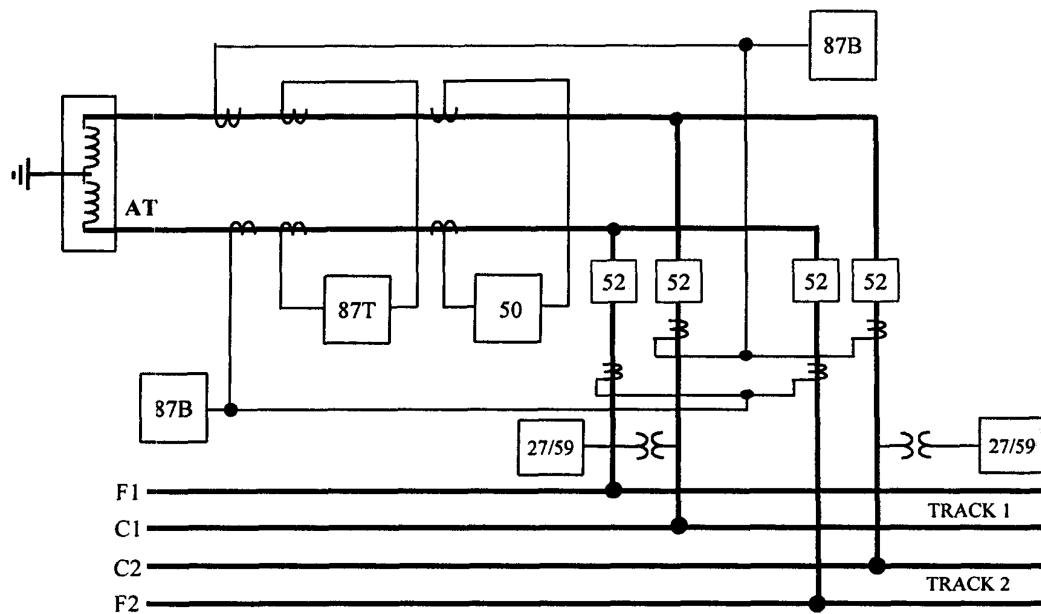
Figure 4.6: Protection scheme for a paralleling station.
The boxes with the number 52 indicate circuit breakers [45]

The transformer protection can be very sensitive because the current in the two ends of the autotransformers is always equal. An instantaneous overcurrent protection relay (ANSI 50) is used as a backup. In addition to these, an under/overvoltage relay (ANSI 27/59) disconnect the autotransformers in the event of voltage loss and reconnect it after voltage restoration and high impedance bus protection relays (ANSI 87B) protect the catenary and feeder buses. All relays report their trip events to the overcurrent relay which keeps a centralised event log. All clocks are synchronised through a time-pulse signal [45]. Although this describes how Amtrak implemented the protection system on its line, it is safe to assume other railway administrations have similar implementations.

At the moment some of the autotransformer-feeding-system users are the following:

- some French lines [42],

- most Japanese AC electrified lines [29],

- the Italian high speed network [8],

- parts of the North East Corridor in the US [12],

- parts of the British rail network including HS1 [52],

- the Chinese high speed railway network [24],

and it is proposed for the electrification of the new California high speed network [10] and for the Metrolink system in Ontario (Canada) [12].

In essence the 2x25 autotransformer system is preferred for new electrifications because of this advantages [52]:

- larger distance between feed station and, consequently, less high voltage gear to be used,

- reduced electromagnetic interference with telecommunication networks,

- reduced losses in the distribution system and reduced voltage drops in the overhead line allowing higher traction loads,

- compatible with existing rolling stock;

despite [52]:

- the need to provide autotransformers every five to ten kilometres,

- the increased clearances and insulation,

- the increased complexity and number of circuit breakers required,

- the complexity to interface the the classic 25 kV system.

4.1 Voltage drop model of the 2 x 25 kV system

E. Pilo, L. Rouco and A. Fernández have developed se following model in [40]. All currents, voltages and impedances are computed using a unitary scale (p.u.). The model consider loads (trains) as ideal current sources to simplify the analysis; the assumption does not imply any loss of generality. The basic assumptions are the following:

1. voltage drop along a cell in the positive and in the negative side have the same value but different sign.

2. if autotransformers can be supposed ideal, it can be assumed current flows only in the autotransformers that are immediately adjacent to the considered load.

It should be noted that current flows in the ground conductors of the transmission cells have not been assumed to be zero, but they will take the value that fulfils the condition of voltage drops equal to zero.

In the transmission cells (i.e. the cells with no load in them), the first assumption can be expressed as:

$$
\begin{bmatrix} \mathbf{v}_{cell,trans} \\ -\mathbf{v}_{cell,trans} \end{bmatrix} = \mathbf{L}_{cell} \cdot [\tilde{\mathbf{z}}_{cell}] \cdot [\mathbf{i}_{trans}] = \mathbf{L}_{cell} \cdot \begin{bmatrix} \tilde{\mathbf{z}}_{pp} & \tilde{\mathbf{z}}_{pn} \\ \tilde{\mathbf{z}}_{np} & \tilde{\mathbf{z}}_{nn} \end{bmatrix} \cdot \begin{bmatrix} \mathbf{i}_{p,trans} \\ \mathbf{i}_{n,trans} \end{bmatrix} \qquad (4.3)
$$

where the sub-indexes p and n represent the positive and the negative conductors respectively and the symbol $\tilde{\mathbf{z}}$ means that the impedance z is expressed per length unit. It is possible to obtain $\mathbf{i}_{p,trans}$ as

$$
\mathbf{i}_{p,trans} = \mathbf{c}_{pn,trans} \cdot \mathbf{i}_{n,trans} \qquad (4.4)
$$

where

$$
\mathbf{c}_{pn,trans} = -\frac{\tilde{\mathbf{z}}_{nn} + \tilde{\mathbf{z}}_{pn}}{\tilde{\mathbf{z}}_{np} + \tilde{\mathbf{z}}_{pp}} \qquad (4.5)
$$

In the load's cell the first assumption can be expressed as:

$$
\begin{bmatrix} \mathbf{v}_{cell,load} \\ -\mathbf{v}_{cell,load} \end{bmatrix} = x \cdot \mathbf{L}_{cell} \cdot [\tilde{\mathbf{z}}_{cell}] \cdot \begin{bmatrix} \mathbf{i}_{p,cell} \\ -\mathbf{i}_{n,cell} \end{bmatrix} + (1-x) \cdot \mathbf{L}_{cell} \cdot [\tilde{\mathbf{z}}_{cell}] \cdot \begin{bmatrix} -\mathbf{i}_{n,cell} \\ -\mathbf{i}_{n,cell} \end{bmatrix} \quad (4.6)
$$

where x is the relative position of the load in its cell. Eliminating $\mathbf{v}_{cell,load}$ from the previous equation it can be obtained:

$$
\mathbf{i}_{p,load} = \mathbf{c}_{pn,load} \cdot \mathbf{i}_{n,load} \qquad (4.7)
$$

where

$$
\mathbf{c}_{pn,trans} = -\frac{(1-x) \cdot (\tilde{\mathbf{z}}_{np} + \tilde{\mathbf{z}}_{pp}) + (\tilde{\mathbf{z}}_{nn} + \tilde{\mathbf{z}}_{pn})}{x \cdot (\tilde{\mathbf{z}}_{np} + \tilde{\mathbf{z}}_{pp})} \qquad (4.8)
$$

Furthermore, currents $\mathbf{i}_{p,load}$ and $\mathbf{i}_{n,load}$ can be calculated from the current $\mathbf{i}_{load}$ drawn by the load because:

$$\mathbf{i}_{p,load} + \mathbf{i}_{n,load} = \mathbf{i}_{load} \tag{4.9}$$

From expressions 4.8 and 4.9, it can be obtained

$$\mathbf{i}_{p,load} = \mathbf{c}_{p,load} \cdot \mathbf{i}_{load} \tag{4.10}$$

$$\mathbf{i}_{n,load} = \mathbf{c}_{n,load} \cdot \mathbf{i}_{load} \tag{4.11}$$

where

$$\mathbf{c}_{p,load} = (1 - x) \cdot \frac{\tilde{\mathbf{z}}_{pp} + \tilde{\mathbf{z}}_{np}}{\tilde{\mathbf{z}}_{pp} + \tilde{\mathbf{z}}_{pn} + \tilde{\mathbf{z}}_{np} + \tilde{\mathbf{z}}_{nn}} \tag{4.12}$$

$$\mathbf{c}_{n,load} = x \cdot \frac{\tilde{\mathbf{z}}_{pp} + \tilde{\mathbf{z}}_{np}}{\tilde{\mathbf{z}}_{pp} + \tilde{\mathbf{z}}_{pn} + \tilde{\mathbf{z}}_{np} + \tilde{\mathbf{z}}_{nn}} \tag{4.13}$$

From 4.9, 4.10 and 4.11 it can also be established that

$$\mathbf{c}_{p,load} + \mathbf{c}_{n,load} = 1 \tag{4.14}$$

By applying Kirchhoff law for currents to buses A and B (see figure):

$$\mathbf{i}_{p,load} - \mathbf{i}_{AT1} = \mathbf{i}_{p,trans} \tag{4.15}$$

$$-\mathbf{i}_{n,load} - \mathbf{i}_{AT1} = \mathbf{i}_{n,trans} \tag{4.16}$$

Eliminating $\mathbf{i}_{AT1}$ form 4.15 and 4.16, and expressing and $\mathbf{i}_{p,load}$ and $\mathbf{i}_{n,load}$ as a function of $\mathbf{i}_{load}$:

$$\mathbf{i}_{p,trans} = \mathbf{c}_{p,trans} \cdot \mathbf{i}_{load} \tag{4.17}$$

$$\mathbf{i}_{n,trans} = \mathbf{c}_{n,load} \cdot \mathbf{i}_{load} \tag{4.18}$$

where

$$\mathbf{c}_{p,trans} = \frac{\tilde{\mathbf{z}}_{nn} + \tilde{\mathbf{z}}_{pn}}{\tilde{\mathbf{z}}_{pp} + \tilde{\mathbf{z}}_{pn} + \tilde{\mathbf{z}}_{np} + \tilde{\mathbf{z}}_{nn}} \tag{4.19}$$

$$\mathbf{c}_{n,trans} = -\frac{\tilde{\mathbf{z}}_{np} + \tilde{\mathbf{z}}_{pp}}{\tilde{\mathbf{z}}_{pp} + \tilde{\mathbf{z}}_{pn} + \tilde{\mathbf{z}}_{np} + \tilde{\mathbf{z}}_{nn}} \tag{4.20}$$

From 4.19 and 4.20, it can be established that

$$\mathbf{c}_{p,trans} - \mathbf{c}_{n,trans} = 1 \tag{4.21}$$

The bus voltages are affected by the voltage drops in the traction substation and in the cells (both transmission and load cells).

Voltage drops in the substation are due to the impedances $\mathbf{z}_{HV,ss}$, $\mathbf{z}_{p,ss}$ and $\mathbf{z}_{n,ss}$ which can be expressed as:

$$\mathbf{v}_{HV,ss} = \mathbf{z}_{HV,ss} \cdot \mathbf{i}_{load} \tag{4.22}$$

$$\mathbf{v}_{p,ss} = \mathbf{z}_{eqv,p,ss} \cdot \mathbf{i}_{load} = (\mathbf{z}_{p,ss} \cdot c_{p,trans}) \cdot \mathbf{i}_{load} \tag{4.23}$$

$$\mathbf{v}_{n,ss} = \mathbf{z}_{eqv,n,ss} \cdot \mathbf{i}_{load} = (\mathbf{z}_{n,ss} \cdot c_{n,trans}) \cdot \mathbf{i}_{load} \tag{4.24}$$

The expressions of the voltage drops along the positive and negative conductors of the transmission cells can respectively be obtained from 4.3:

$$\mathbf{v}_{p,trans} = \tilde{\mathbf{z}}_{eqv,cat} \cdot X \cdot \mathbf{i}_{load} \tag{4.25}$$

$$\mathbf{v}_{n,trans} = -\mathbf{v}_{p,trans} \tag{4.26}$$

with:

$$\tilde{\mathbf{z}}_{eqv,cat} = \tilde{\mathbf{z}}_{pp} \cdot \mathbf{c}_{p,trans} + \tilde{\mathbf{z}}_{pn} \cdot \mathbf{c}_{n,trans} \tag{4.27}$$

where X is the distance between the considered position of the catenary and the substation.

The equivalent impedance $\tilde{\mathbf{z}}_{eqv,cat}$ can be written as:

$$\tilde{\mathbf{z}}_{eqv,cat} = \frac{\tilde{\mathbf{z}}_{pp} \cdot \tilde{\mathbf{z}}_{nn} - \tilde{\mathbf{z}}_{pn} \cdot \tilde{\mathbf{z}}_{np}}{\tilde{\mathbf{z}}_{pp} + \tilde{\mathbf{z}}_{nn} + \tilde{\mathbf{z}}_{pn} + \tilde{\mathbf{z}}_{np}} \tag{4.28}$$

In the cell of the load, voltage between the first autotransformer and the load itself corresponds to the first part of expression 4.6:

$$\mathbf{v}_{p,AT1} - \mathbf{v}_{p,load} = x \cdot L_{cell} \cdot (\tilde{\mathbf{z}}_{pp} \cdot \mathbf{i}_{p,cell} - \tilde{\mathbf{z}}_{pn} \cdot \mathbf{i}_{n,cell}) \tag{4.29}$$

$$\mathbf{v}_{n,AT1} - \mathbf{v}_{n,load} = x \cdot L_{cell} \cdot (\tilde{\mathbf{z}}_{np} \cdot \mathbf{i}_{p,cell} - \tilde{\mathbf{z}}_{nn} \cdot \mathbf{i}_{n,cell}) \tag{4.30}$$

The voltage drop $\mathbf{v}_{p,AT1} - \mathbf{v}_{p,load}$ can be expressed as a function of $\mathbf{i}_{load}$ and grouped in two terms:

1. the voltage drop with the same expression that has been used for transmission cells

2. the deviation between the real voltage drop and the first term:

$$\mathbf{v}_{p,AT1} - \mathbf{v}_{p,load} = (x \cdot L_{cell} \cdot \tilde{\mathbf{z}}_{eqv,cat} + z_{gap}) \cdot \mathbf{i}_{train} \tag{4.31}$$

with

$$z_{gap} = L_{cell} \cdot x \cdot (1 - x) \cdot \frac{\tilde{\mathbf{z}}_{pp}^2 + \tilde{\mathbf{z}}_{pp}\tilde{\mathbf{z}}_{np} + \tilde{\mathbf{z}}_{pn}\tilde{\mathbf{z}}_{pp} + \tilde{\mathbf{z}}_{pn}\tilde{\mathbf{z}}_{np}}{\tilde{\mathbf{z}}_{pp} + \tilde{\mathbf{z}}_{pn} + \tilde{\mathbf{z}}_{np} + \tilde{\mathbf{z}}_{nn}} \tag{4.32}$$

It can be proven by differentiating expression 4.32 with respect to x and calculating the derivative's root that the maximum deviation occurs when the train is in the middle of the sector ($x = \frac{1}{2}$). This can be used to calculate the upper bound of the voltage deviation:

$$\mathbf{v}_{dev,max} = \frac{1}{4} \cdot L_{cell} \cdot \frac{\tilde{\mathbf{z}}_{pp}^2 + \tilde{\mathbf{z}}_{pp}\tilde{\mathbf{z}}_{np} + \tilde{\mathbf{z}}_{pn}\tilde{\mathbf{z}}_{pp} + \tilde{\mathbf{z}}_{pn}\tilde{\mathbf{z}}_{np}}{\tilde{\mathbf{z}}_{pp} + \tilde{\mathbf{z}}_{pn} + \tilde{\mathbf{z}}_{np} + \tilde{\mathbf{z}}_{nn}} \qquad (4.33)$$

The voltage drop between the first and second autotransformer of the load's cell corresponds to equation 4.6. If the current $\mathbf{i}_{p,load}$ and $\mathbf{i}_{n,load}$ are expressed as function of $\mathbf{i}_{load}$, the voltage drop can be expressed as:

$$\mathbf{v}_{p,AT1} - \mathbf{v}_{p,AT2} = \frac{\tilde{\mathbf{z}}_{pp}\tilde{\mathbf{z}}_{nn} - \tilde{\mathbf{z}}_{pn}\tilde{\mathbf{z}}_{np}}{\tilde{\mathbf{z}}_{pp} + \tilde{\mathbf{z}}_{nn} + \tilde{\mathbf{z}}_{pn} + \tilde{\mathbf{z}}_{np}} \cdot x \cdot \mathbf{i}_{load} = \tilde{\mathbf{z}}_{eqv,cat} \cdot x \cdot \mathbf{i}_{load} \qquad (4.34)$$

$$\mathbf{v}_{p,AT1} - \mathbf{v}_{p,AT2} = -(\mathbf{v}_{n,AT1} - \mathbf{v}_{n,AT2}) \qquad (4.35)$$

Expression 4.34 and 4.35 correspond exactly to the voltage drop along the catenary between the cell's first autotransformer and the load if the transmission cell's model is used. That means that the voltage deviation is completely recovered by the effect of the second autotransformer of this cell and there are no additional voltage drops in the downward cells.

4.2 MATLAB simulation of the 2 x 25 KV system

U. J. Shenoy and others [46] proposed a new model for the 25 kV electrification system built with MATLAB and SIMULINK to simulate the effects of a high load or a short circuit on the system itself. A model of the 2 x 25 kV system has been developed by Sisi Li in her Master of Science thesis [30].

I used these models as a starting point to develop a 2 x 25 kV autotransformer-fed-system SIMULINK model to evaluate the effects of high power train loads leaving it open to eventually evaluate the effects of a second load between feeder and earth.

The model represents a 25 km long section of an Italian High speed railway line as built for Rete Ferroviaria Italiana (RFI) on an embankment (fig. 4.7).

Figure 4.7: Italian High Speed Line section

Each High Speed line is fed with a 2 x 25 kv autotransformer system capable of delivering 2 MW of power of each kilometre of line: this allows "the simultaneous presence of 12 MW trains travelling at 300 km/h (180 mph) 5 minutes apart with no limits but with margin". This has been achieved through two 60 MVA feeding transformers in each electrical substation which are located 50 km (30 miles) apart; during normal operation each transformer feeds a section 25 km long. The substations are fed through a dedicated power-line at the nominal voltage of 132 kV (in northern Italy) or 150 kV (in southern Italy) capable of delivering 200 MW that connects all the substation of the railway line. Both ends of the power-line are connected to the national grid in very high voltage (400 kV) nodes though two 250 MVA autotransformers. This allows to feed the railway line from a single very high voltage substation when needed. Paralleling posts are located every 12.5 km on average and are equipped with two 15 MVA

autotransformers; they allow to put the two tracks in electrically parallel and connect them to the autotransformers. During normal operation only one of the two autotransformers is in use, except when a phase break is present in which case they are both energised one for each phase. This normally happens half-way between two substations.

The railway line is made of seven conductors of each track at three different voltage levels: contact wire and messenger wire are fed at +25 kV, the feeder is connected to the -25 kV bus, the two rails, the overhead earth wire and the buried earth wire are connected to earth, i.e. they have zero volts potential.

The model of a two track line is made of the following four elements:

- wires and rails,

- inductive couplers,

- the feeder transformer,

- autotransformers.

The hypothesis the model is based on are that the current flowing through the soil and the buried earth conductor is negligible, so it is possible to simulate the line as if all current flows through the rails themselves or the the overhead earth wire. Electrical lines are usually modelled with series resistances and inductances and with capacitances and conductances in parallel. In most cases a loaded line can be modelled excluding the parallel capacitances and conductances as their effect is negligible. In the case of the high speed railway line, the power-line is not symmetric on each track even if the two track are built symmetrically so inductance and resistance are represented by a big matrix that in our case has dimensions twelve by twelve. The big advantage that the symmetry between the two track brings us is that the matrices are symmetric themselves, potentially reducing the amount of calculation needed. The reason why such big matrices are needed is that the distance between the two track centrelines is 5 meters, so the tracks can not be considered independent in terms of magnetic coupling. Such hypothesis would mean the two track are very far apart, which is not viable in both terms of environmental impact and economics.

If it is hypothesised that all conductors are parallel and the messenger wire has a constant hight; then self and mutual inductances of each conductor can be computed using Neumann formulas which are [49]:

$$L_{ij} = \frac{\mu_0}{2\pi} ln \frac{2 \cdot l}{D \cdot e} \qquad (4.36)$$

$$L_{ii} = \frac{\mu_0}{2\pi} ln \frac{2 \cdot l}{K \cdot r_0 \cdot e} \qquad (4.37)$$

where D is the distance between the wires, l is the wire length, r_0 is the wire radius and K is a coefficient used to represent how the current is distributed inside the wire. These equations can be simplified if the sum of the currents is taken into account, in this case the sum of all currents is zero for each track, which means the inductance equations can be written as following:

$$L_{ij} = \frac{\mu_0}{2\pi} ln\frac{l}{D} \tag{4.38}$$

$$L_{ii} = \frac{\mu_0}{2\pi} ln\frac{l}{K \cdot r_0} \tag{4.39}$$

If l is equal to 1 and all units are SI, the result is the inductance per length unit in henry per meter. Exceptions to these formulas are the rails themselves: since steel is a magnetic material and the cross section is high and not entirely used, the preceding formula can not be used, but the value for the self-inductance is available in the literature either measured or computed through finite elements simulation. In this case the value 0.359 mH/km has been used [55].

In opposition to the inductances, only the self-resistances of each conductor are meaningful, so the resistances matrix is diagonal. Another great feature of this matrix is due to how the line is built: as the each track uses the same type of wires, the values can be computed for only one track, because the other track values are the same. The line resistances of each wire are computed with the usual formula

$$R = \rho \cdot \frac{l}{S} \tag{4.40}$$

where ρ is the resistivity of the material, l is the wire length and S is the useful cross section of the wire itself. The rail resistances is again taken from the literature for the same reason it is not possible to compute the self-inductances easily: the value used is 0.116 Ω/km [55].

All the calculation are done using MATLAB for an Italian high speed rail line built on an embankment. The wires and rail positions in table 4.2 are given with coordinates on a plain whose origin is placed in the middle between the two tracks on rail level [56].

The resulting inductance and resistance per length unit values are shown in tables 4.3 and 4.4 .

Table 4.2: Wires and rail positions on a Italian High Speed line built on an embankment [56]

	Wire	X coordinate [m]	Y coordinate [m]
track 1	Contact wire	-2.5	5.3
	Messenger wire	-2.5	6.55
	Earth wire	-6.1	5.5
	Rail 1	-3.22	0
	Rail 2	-1.78	0
	Feeder	-6.60	8
track 2	Contact wire	2.5	5.3
	Messenger wire	2.5	6.55
	Earth wire	6.1	5.5
	Rail 1	1.78	0
	Rail 2	3.22	0
	Feeder	6.6	8

Table 4.3: Resistances per length unit in mΩ/m

Contact wire	0.1173
Messenger wire	0.1467
Earth wire	0.1880
Rail 1	0.1160
Rail 2	0.1160
Feeder	0.1065

The line model itself has been built in SIMULINK using inductances and resistances from tables 4.3 and 4.3 as shown in figure 4.8. The blocks used to make the line model are mutual inductances, resistors and inductors. Each block represents a base line section 1.5 km long; the distance has been chosen because inductive couplers are installed every 1.5 km.

The inductive couplers are inductors installed every 1.5 km that connect the two running rails of each track together to allow the traction current to flow in the earth wire without short-circuiting the rails themselves. The inductance is 1.2 mH [56] which is low enough lo let the 50 Hz traction current through and high enough to block the audio-frequency current and allow track circuits to function properly. The inductor is centre-tapped and as been modelled as two separate inductors in series to have the same total inductance and the tap to connect to the earth wire. The installation requires the centre tap to be connected to the earth wire and the two edges to be connected to each rail. The model details are shown in figure 4.9.

The feeding substation is fed through a high voltage power-line connecting the various substations, so each substation has an incoming power-line connected

Table 4.4: self and mutual inductances per length unit in nH/m

		Track 1					
		Contact wire	Messenger wire	Earth wire	Rail 1	Rail 2	Feeder
Track 1	Contact wire	1030.84	-44.63	-256.49	-335.37	-335.37	-318.22
	Messenger wire	-44.63	1030.84	-264.35	-377.09	-377.09	-293.98
	Earth wire	-256.49	-264.35	1007.29	-365.18	-389.00	-187.18
	Rail 1	-335.37	-377.09	-365.18	359.00	-72.93	-432.31
	Rail 2	-335.37	-377.09	-389.00	-72.93	359.00	-446.86
	Feeder	-318.22	-293.98	-187.18	-432.31	-446.86	777.27
Track 2	Contact wire	-321.89	-327.95	-430.41	-410.77	-383.75	-450.09
	Messenger wire	-327.95	-321.89	-431.83	-432.57	-411.45	-444.16
	Earth wire	-430.41	-431.83	-500.29	-476.31	-452.55	-512.12
	Rail 1	-383.75	-411.45	-452.55	-321.89	-253.95	-489.95
	Rail 2	-410.77	-432.57	-476.31	-372.51	-321.89	-507.79
	Feeder	-450.09	-444.16	-512.12	-507.79	-489.95	-516.04

		Track 2					
		Contact wire	Messenger wire	Earth wire	Rail 1	Rail 2	Feeder
Track 1	Contact wire	-321.89	-327.95	-430.41	-383.75	-410.77	-450.09
	Messenger wire	-327.95	-321.89	-431.83	-411.45	-432.57	-444.16
	Earth wire	-430.41	-431.83	-500.29	-452.55	-476.31	-512.12
	Rail 1	-410.77	-432.57	-476.31	-321.89	-372.51	-507.79
	Rail 2	-383.75	-411.45	-452.55	-253.95	-321.89	-489.95
	Feeder	-450.09	-444.16	-512.12	-489.95	-507.79	-516.04
Track 2	Contact wire	1030.84	-44.63	-256.49	-335.37	-335.37	-318.22
	Messenger wire	-44.63	1030.84	-264.35	-377.09	-377.09	-293.98
	Earth wire	-256.49	-264.35	1007.29	-389.00	-365.18	-187.18
	Rail 1	-335.37	-377.09	-389.00	359.00	-72.93	-446.86
	Rail 2	-335.37	-377.09	-365.18	-72.93	359.00	-432.31
	Feeder	-318.22	-293.98	-187.18	-446.86	-432.31	777.27

to the substation high voltage three-phase bus-bars and an outgoing one from the same bus-bars so that in practice the various power-lines can be seen as sections of a single power-line. Since I don't feel the need to represent more than the section fed with a single transformer, I replaced the power-lines with a three-phase generator with the nominal voltage, frequency and short-circuit power similar to that of the high voltage bus-bars. It is also possible to replace the three-phase generator with an AC ideal voltage source with the right voltage and frequency. There may be the need to represent a longer section of the high speed line fed with multiple substation, in that case it is possible to add a more detailed representation of the power-lines and the feeding 400 KV node. An appropriate power-line model can be made with the "distributed parameters line" simulink block, the autotransformer can be replaced by an equivalent transformer and a suitable three-phase voltage source. It is also possible skip the 400/132 kV autotransformers as long as the three-phase voltage source has the correct short-circuit power.

The feeder transformer is single phase with a centre tap on the secondary
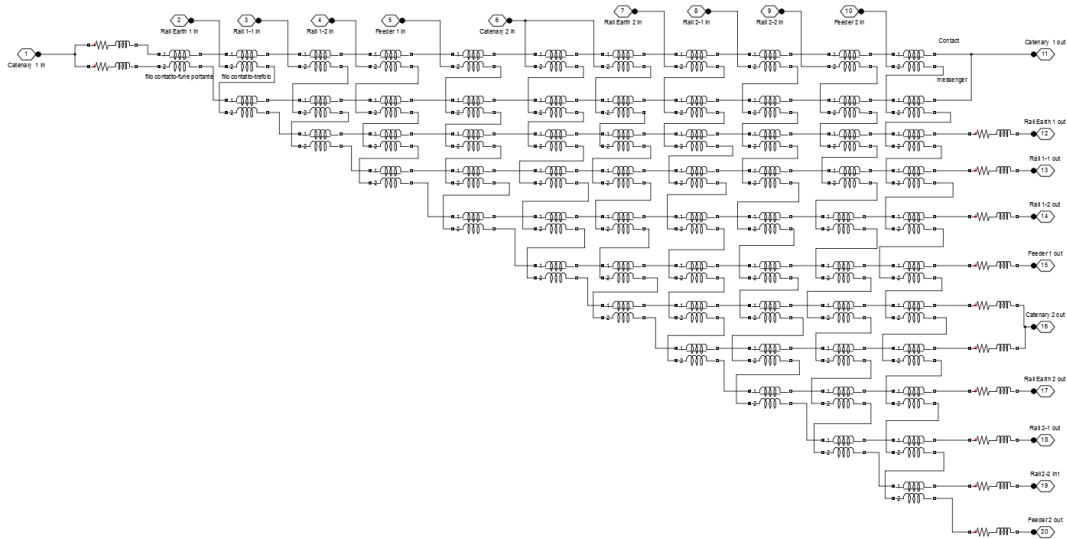
Figure 4.8: SIMULINK model of an elementary section of railway line
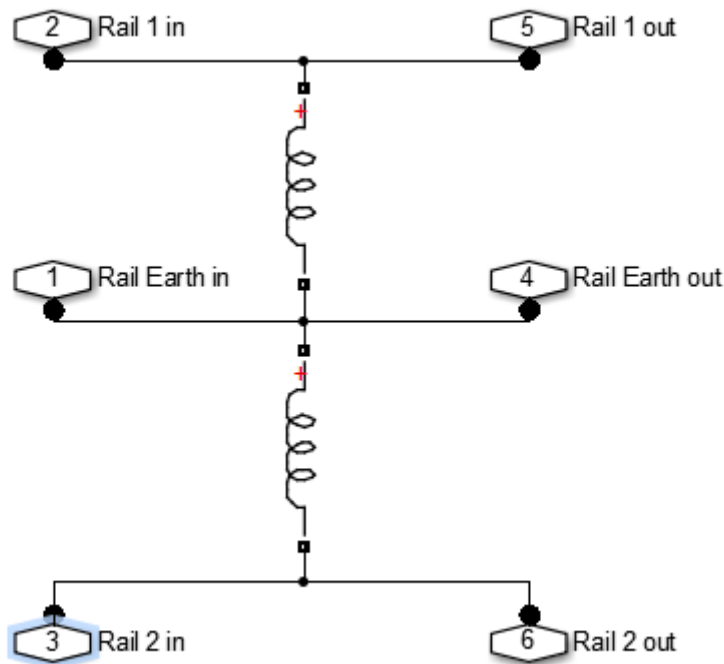
Figure 4.9: SIMULINK model of the coupling inductance

winding and it is modelled as a three-winding transformer whose low voltage windings are connected in series. The transformer nameplate data shown in table 4.5 are used inside the SIMULINK block.

Figure 4.10 shows the SIMULINK model of the transformer and the supplying

Table 4.5: Feeder transformer nameplate data [56]

	High voltage winding	Low voltage windings
Nominal power [MVA]	60	2 x 30
Nominal Voltages [kV]	132 +4 x 1.25% -12 x 1.25%	2 x 27.5
Short circuit voltage [%]	10	10

source.
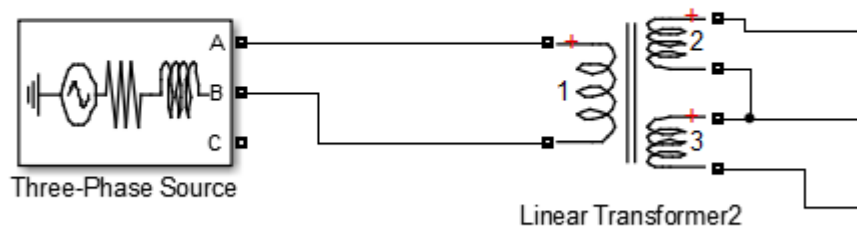
Figure 4.10: SIMULINK model of the feeder transformer and the high voltage line powering it

Other important component is the autotransformer which is necessary to connect the 50 kV catenary to feeder transmission line to the 25 kV train feeding system. The real machine is made of two windings wound on each column of the steel core connected together so that both windings share the same magnetic flux. As SIMULINK does not have an already-made autotransformer model, it is possible to replace the autotransformer with a transformer as long as the windings are connected appropriately as shown in figure 4.11.

The model parameters are taken form the real machine nameplate and are shown in table 4.6.

Table 4.6: Autotransformer nameplate data [56]

Nominal power[MVA]	15
Nominal Voltages [kV]	55/27.5
Short-circuit voltage [%]	1

The main load of the line are going to be trains. The train model varies depending on electronic converter used to rectify the AC current to DC. Old trains
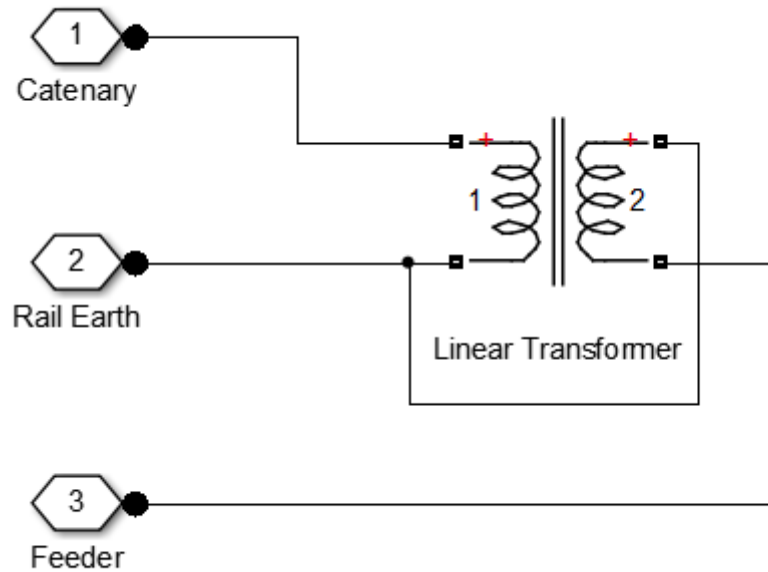
Figure 4.11: SIMULINK model of the paralleling post autotransformer

used diode or thyristor bridges which make the train absorb highly distorted currents, i.e. the current absorbed is rich in low order harmonics especially the third, fifth, seventh. This means that the fastest way to model these trains is by using a rectifier bridge feeding an appropriate load. When the use of GTOs and later IGBTs became widespread, rectifier bridges were replaced by four quadrant converters in all newly constructed trains. This allows to convert AC to DC while absorbing a sinusoidal current in phase with the voltage (to be clear there are other harmonics, but their order is multiple of the switching frequency of the converter usually in the range of kilohertz). This means that, unless necessary, the load can be represented by a sinusoidal current injected through a current generator. This is achieved with a controlled generator; the control is very straightforward: the voltage is measured on site where the current will be injected and the signal is scaled with a gain block to the value of the current drown by the load itself. If an ETR 500 (Trenitalia Frecciarossa) is used as an example, the current drawn at the maximum power (8.8 MW) is 352 A at 25 KV; the gain block will scale the voltage to the current with the ratio 352/25000 so that the current is in phase with the voltage and the power drown is the nominal train power as shown in figure .

The model can be used either to calculate the voltage profile along the line or to calculate the waveforms of voltages and currents wherever it is needed. As the line is built with 1.5 km long elementary line pieces, it is possible to simulate the case in which everything works correctly as well as the case with one or more

faulty pieces of equipment.

Chapter 5

Charging facility

Fast charging electric vehicles requires a sufficiently powerful connection to the electrical grid which may require connecting directly to the high voltage transmission grid. It is quite expensive to connect it to the high voltage mains because of the switchgear and the space required to build a substation. There are service areas distributed every 30 km on average in the Italian motorway system and, according to my survey, each service area has 13 fuel pumps on average in each direction. The survey data come from Google Earth and Google Street View imaging service; I counted the number of refuelling bays in some service stations on A4 Milan-Turin, A1 Milan-Bologna and A1 Rome-Naples motorway and then I calculated an average. If the refuelling process lasts 5 minutes and all the available fuel pumps are being used, it is possible to refuel 78 cars in half an hour, that means 78 charging bays are needed to recharge the same amount of vehicles in the same half an hour. This means each direction needs 7.8 MW of power to recharge each vehicle 100 kW rating. The Italian high speed rail network has been built near the motorways, when possible, and is able to deliver high power at a relatively low voltage, so it makes sense studying the effects of such solution on the 2 x 25 kV railway supply system to evaluate the possibility to connect the motorway charging points to the nearby railway. This solution can be particularly advantageous in the countryside where the high voltage network node is relatively far away and the high speed line is pretty near the service station because it avoids the construction of high voltage lines. It is important to note that the railway infrastructure owner has the right to disconnect the motorway car charging facility in case that power is needed to maintain a set quality of service on the railway line itself.

The hypothesis of simultaneous use of all the refuelling bays is not quite true, as usually only some are actually used simultaneously in real life. This can be expressed through a coefficient that indicates the percentage of bays used. This is actually very useful, because it allows three options: reducing the number of available charging bays or share the total 100 kW power rating between two bays or both. If the power sharing option is chosen, It would be better to share the

power dynamically between the two cars on order to give more power to the car with the lower state of charge rather than sharing the power fifty-fifty between the two users.

5.1 The load

Each charging bay is a variable load with 100 kW maximum power. The load model has to potentially include each main rectifier topology for harmonics injection in the network and reactive power consumption. The main topologies are Graetz bridges with both diodes and thyristors and the PWM controlled switched AC/DC converter: these are very different in both harmonics injected and reactive power consumption.

The Graetz bridge configuration is characterised by high harmonic currents at low frequency, i.e. bridge rectifiers inject high third, fifth and seventh harmonic order currents that normally have to be filtered out. On the other hand they are easy to maintain because each valve is turned on and off naturally, but the output voltage can not be regulated without an additional switching DC/DC converter. Thyristors bridges are more complicated indeed requiring a firing device, but they allow to regulate the output voltage. Voltage regulation is possible by changing the firing angle which causes the output voltage to drop; on the other hand the firing angle is directly linked to the reactive power absorbed, that means an appropriate power factor correction device is needed.

Switched AC/DC power converters are the most modern approach to rectification. Their main feature is they achieve unity power factor and limit low-order-harmonic-current injection trough their high switching frequency which, depending on the type of semiconductor used (MOSFETs, IGBTs, GTOs), varies form some kilohertz to over 20 kHz. Being directly linked to the switching frequency, the frequency of the current harmonics is high enough to make the current amplitude be naturally dumped by cables and transformers inductances resulting to low THD without the need of expensive filters. In addition to that, if converters are grouped and controlled with a technique called interlacing, the net result is that each group harmonic emissions are equivalent to those of a single converter operating at a frequency multiple of the converters number in each group and each converter's switching frequency.

Most simulations feature a switching AC/DC converter. The load itself is made of the battery, the converters and the interfacing transformer.

The battery has been modelled using the battery block available in Simpowersystems. It is able to simulate every kind of batteries form lead-acid to lithium-ion. The battery modelled in this case is the one available in the Nissan Leaf care for sale in the US and the battery data are taken form the Government's tests available from the US Department of Energy [50]. The battery main features are summed up in table 5.1.

Table 5.1: main characteristics of the Nissan Leaf battery

Nominal voltage [V]	364.8
Rated pack energy [kW h]	24
Rated pack capacity [A h]	66.2

The 4Q converter used to rectify the AC voltage uses IGBTs as semiconductors and is controlled through a PWM controller copied from the 240 V, 3500 W MATLAB PV example. The main modifications needed to make it run consisted in disabling the MPPT tracking system used to extract the maximum power available from the PV panel and adjusting the regulators parameters. This second step has been done through the trial and error process until I got a functioning device. Other aspect gone through revision is the value of the DC bus capacitor that has been changed to 40 mF to maintain the voltage ripple in a 5% band. The DC bus nominal voltage has been changed to 500 V from the previous value of 425 V. The new nominal value has been chosen because, at the moment, it is the maximum voltage that CHAdeMO and CCS charging systems allow as explained in chapter 1 in their own dedicated section. The converter and its control system are shown in figure 5.1.

It is necessary to install a DC/DC converter to adjust the current flow to the battery because of the difference between the battery voltage(about 400 V when fully charged) and the main DC bus (500 V). This converter is a two quadrant converter that allow the power to flow in both directions, i.e. from the battery to the grid or vice-versa. In this case the battery charging function is more interesting. The control is done through a PI controller to obtain a voltage reference able to drive the PWM signal generator. The controller is again tuned through a trial and error process. The current reference signal has been made variable so that the regulator is enabled with a current reference equal to zero. The reference signal grows linearly to the maximum value of 250 A in 2 seconds. Battery, converter and filters are shown in figure 5.2.

The connection between the low voltage system to which the power electronics is attached and the medium voltage from the railway line is achieved through a short cable and a power transformer rated at 150 kVA. I chose to maintain the original topology of a centre-tapped two windings transformer used for the 120 V distribution system in the US for a couple of reasons, the most important of those is safety. As both lines are live, but their potential to earth is only 120 V it is safer for people in case of an insulation failure. I hypothesised a cable about 200 m long with a cross section of $180\,\text{mm}^2$ and a resistance of $0.106\,\Omega\,\text{km}^{-1}$. The transformer and line model is shown in figure 5.3. The resistor Rg represents the Earth system resistance.
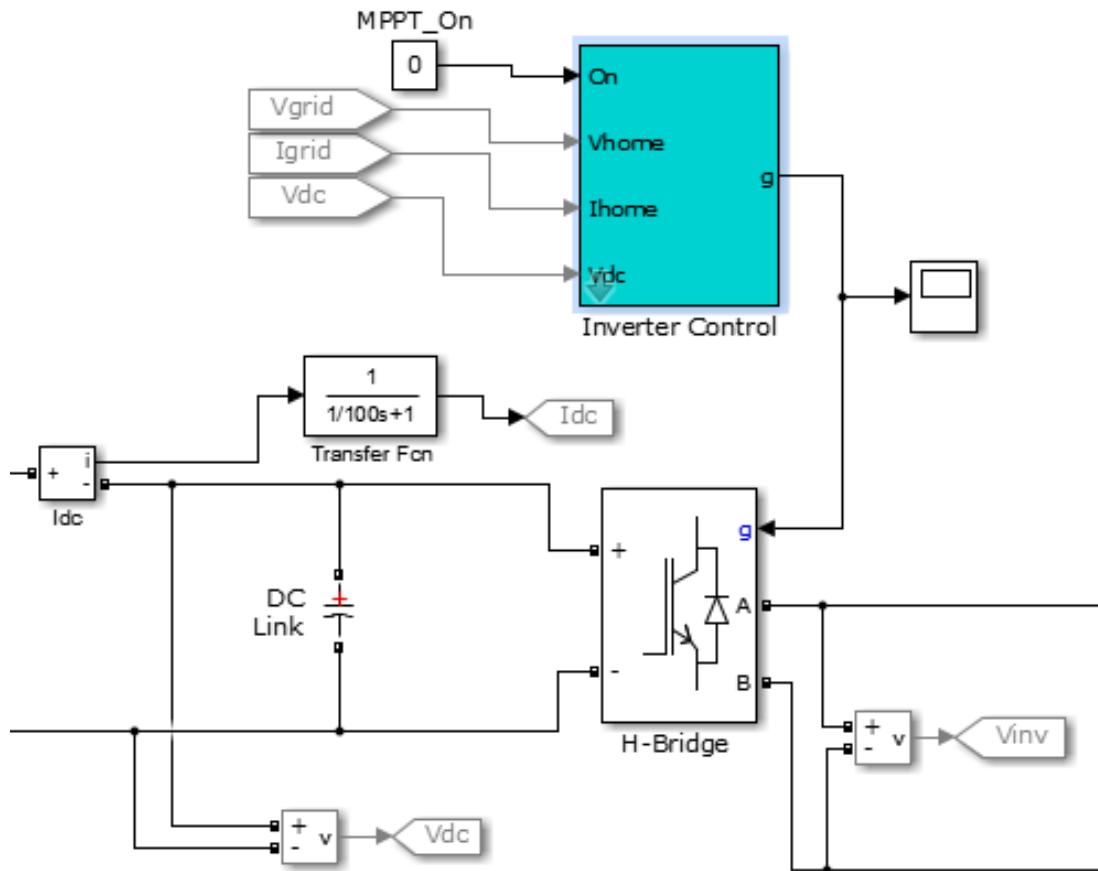
Figure 5.1: 4Q converter and its control system
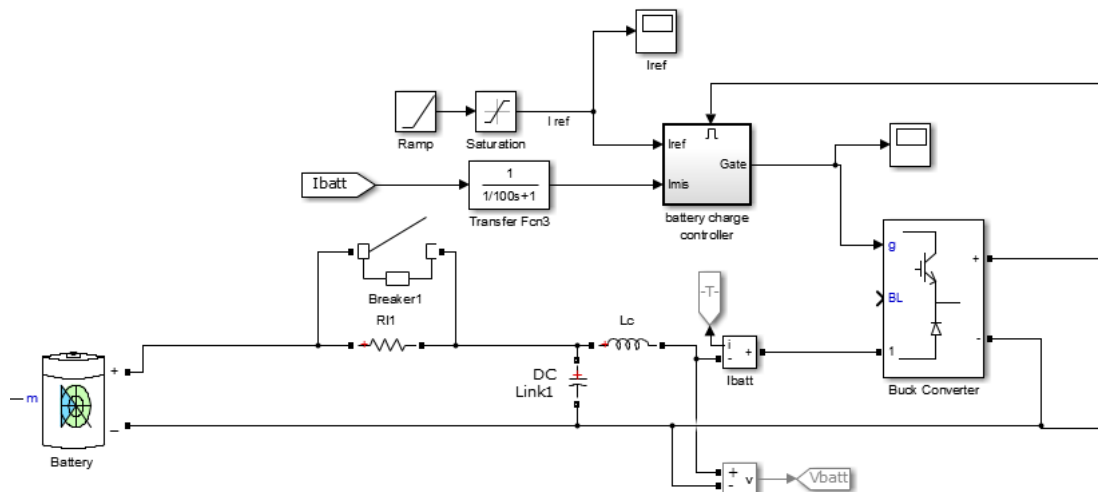
Figure 5.2: Model of the car battery and the converter
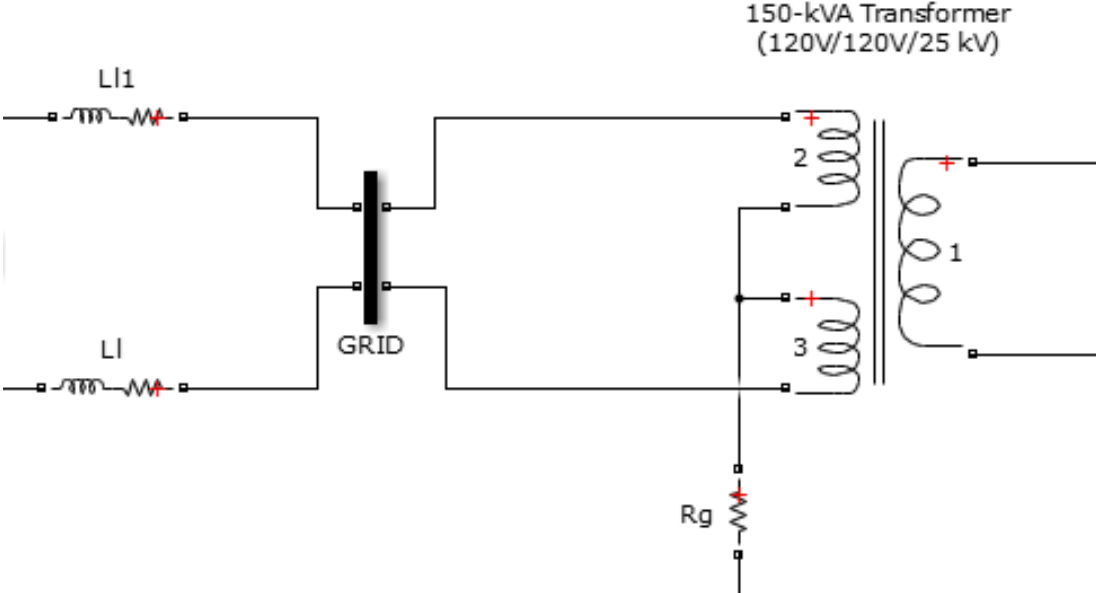
Figure 5.3: Model of the power transformer and the short low voltage line.

5.2   2 x 25 system

The 2 x 25 kV system is modelled as shown in chapter 3 section 2. Four cases
will be examined, these are: the absence of trains, the presence of one train and
the presence of two trains in the same or in different cells. This is particularly
important as the main load continues to be the train traffic and the system is
viable only if it is possible to power both the railway traffic and the charging
facility at the same time.

   One of the possible scenarios simulated is the presence of two trains in the
same cell to evaluate the voltage drop in the system. The considered trains
are: an ETR 500 and an ETR 400 with power consumption of 8.8 MW and
9.8 MW respectively. It is assumed the two trains absorb a sinusoidal current
and a unity power factor. As shown in figure 5.4 the system is capable to supply
both trains with no problem and maintains a voltage near the nominal value.
The currents measured on the transformer and autotransformer connections (fig-
ures 5.5 and 5.6) are in line with what is expected from the system.
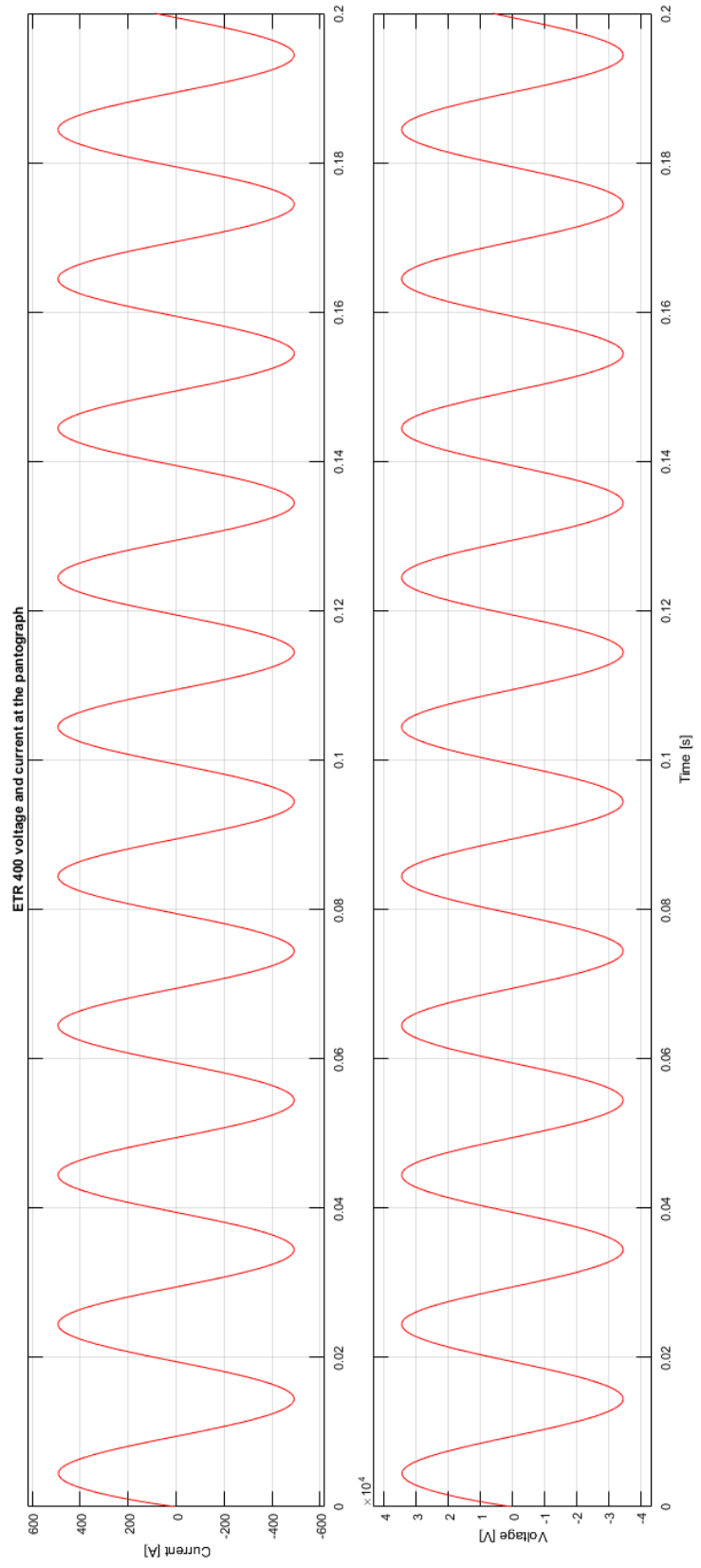
Figure 5.4: Voltage and current drown by an ETR 400 on a high speed line with no charging stations
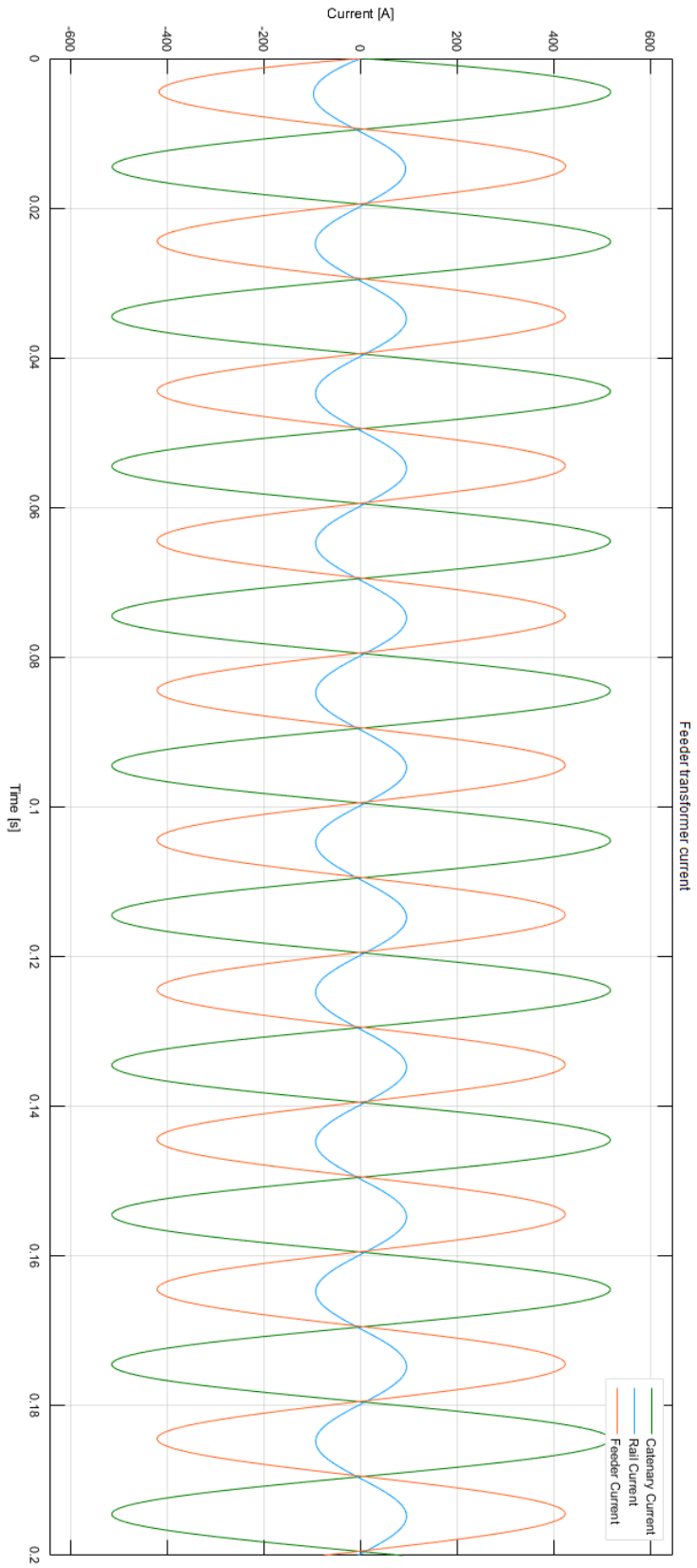
Figure 5.5: Currents measured on the feeding transformer connections with trains as the only load
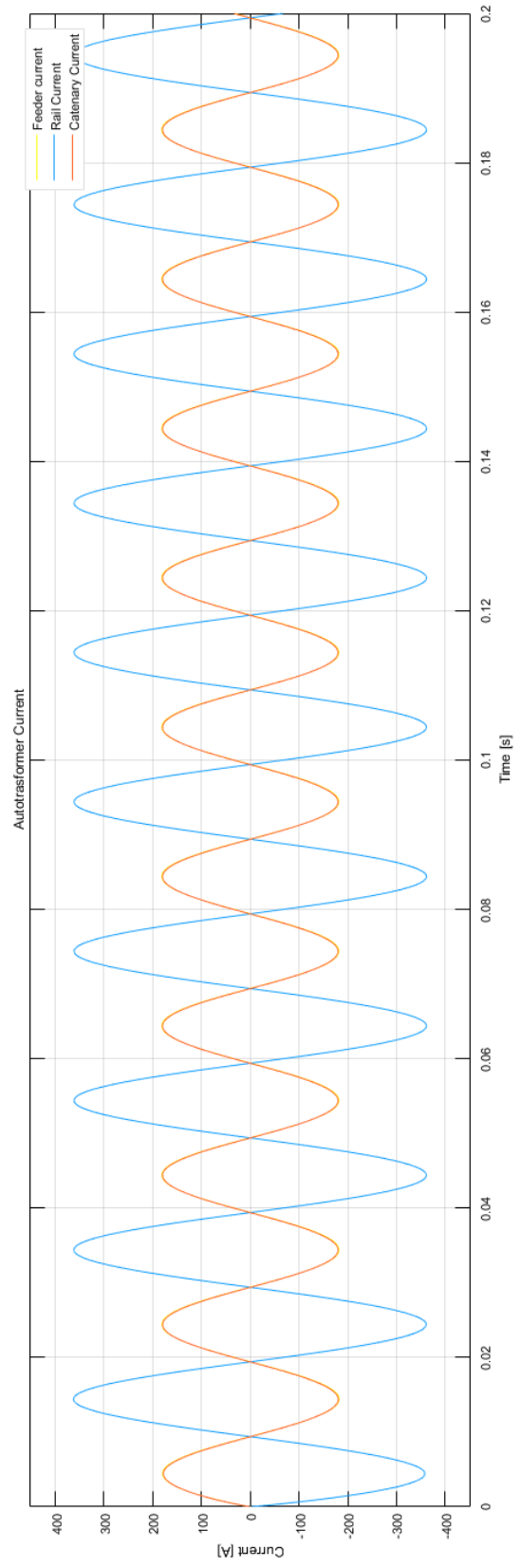
Figure 5.6: Currents measured on the autotransformer connections with trains as the only load

5.3   System simulation and results

There are two simulation steps: the first step is about making the charging system work by itself. This first step is very important because it allows to sort out the system problems before the two systems are made working together. When both system work as expected, it is possible to connect them together and have the complete simulation of all the effects.

The first simulation phase has given the following results: the model was working with the following regulator values: 3000 and 1000 as proportional and integrator coefficients for the voltage regulator and 500 and 1000 as proportional and integrator coefficients for the current regulator. The current absorbed was not constant when the device was on full load as the DC bus voltage was still floating as shown in figure 5.7.

The battery status is shown in figure 5.8, it can be seen that the battery is actually recharged from the initial state of charge set to 10%. The graph also shows current and voltage of the battery; current is represented with a negative value because it is charging. On the other end the battery current would be positive if the battery was discharging.

It is important to control harmonics emission on the AC side of the 4Q converter. Excluding sections where the waveform is not very clean, in general the current follows the voltage quite well as shown in figure 5.9. This result is confirmed by the Fourier transform which is used to calculate the spectrum of the signal itself as shown in figure 5.10.
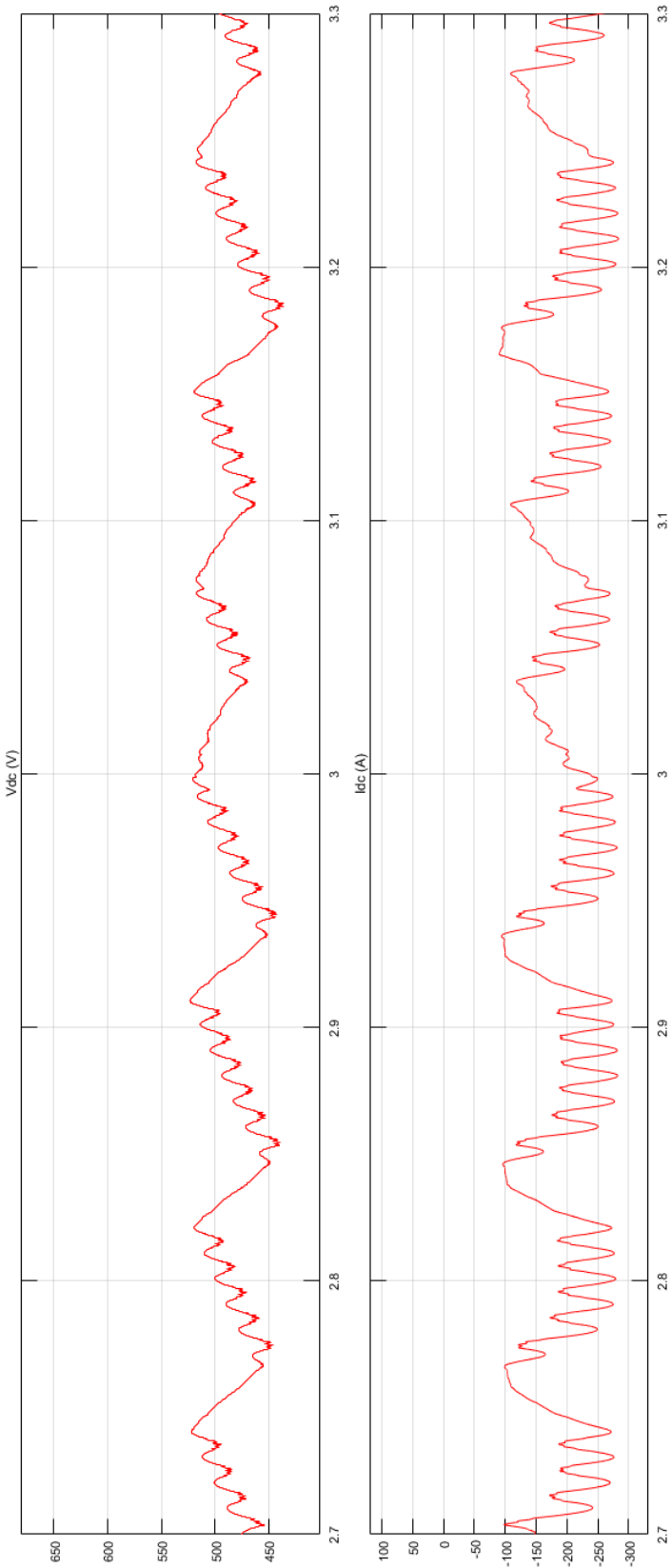
Figure 5.7: voltage and current on the 4Q converter DC bus
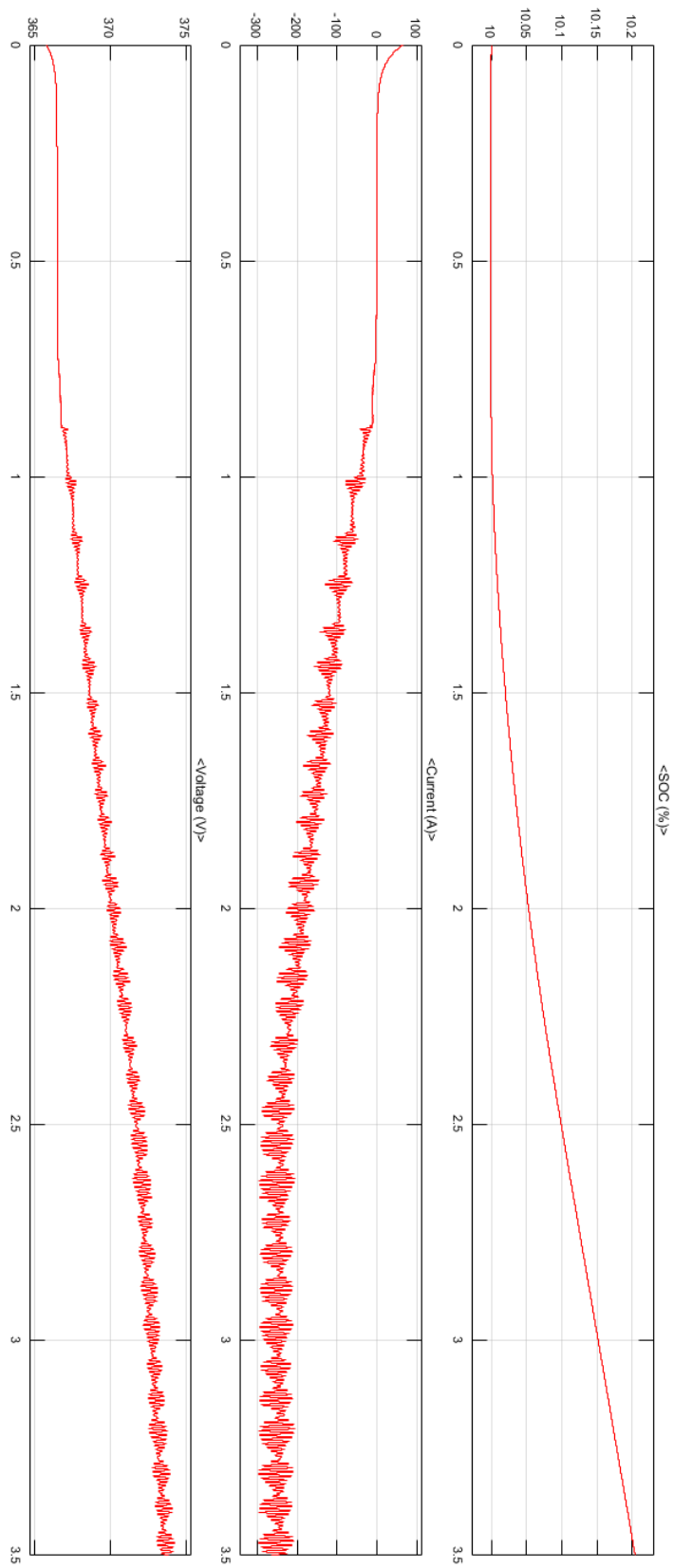
Figure 5.8: Battery state during the simulation: current, voltage and state of charge are shown
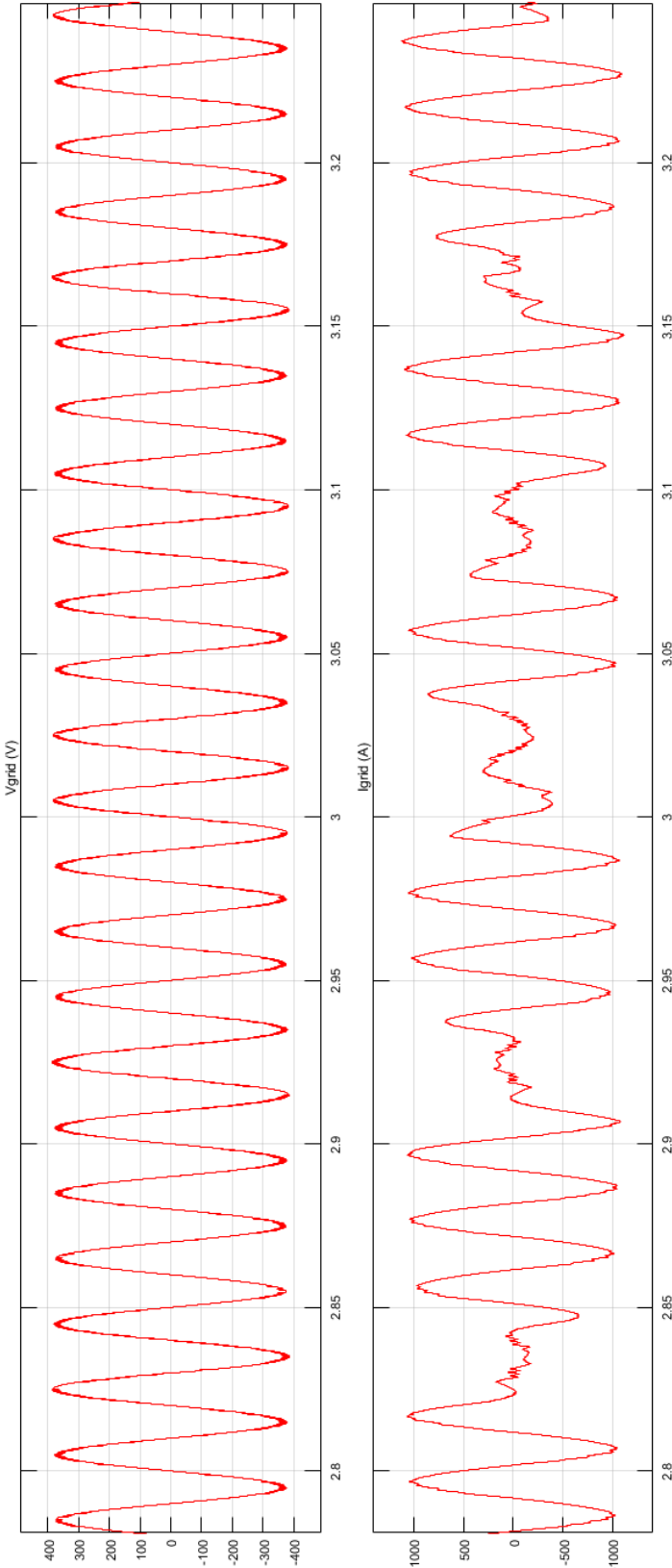
Figure 5.9: Voltage and current on the low voltage grid when the converter is working at full load
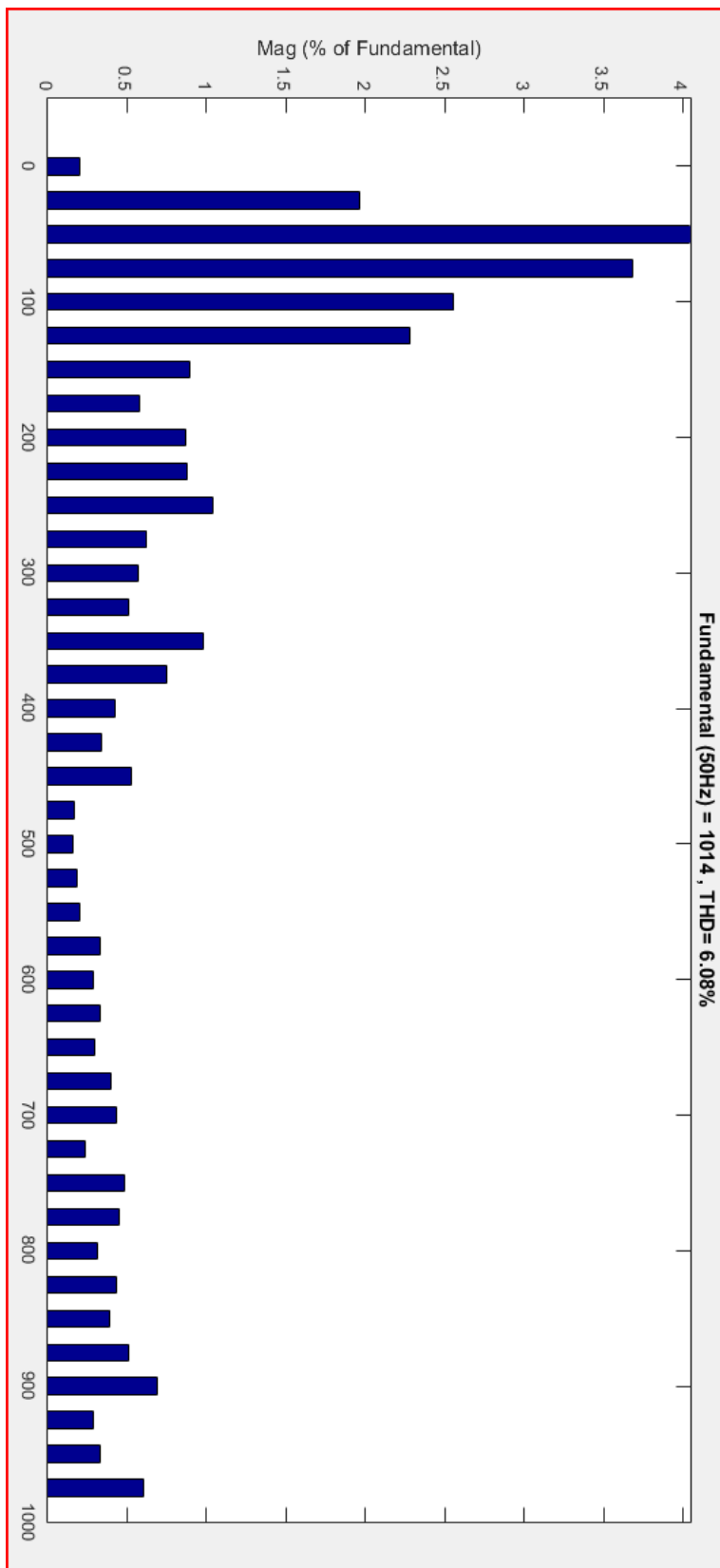
Figure 5.10: Spectrum of the 4Q converter AC current

The system is then tested on the 2 x 25 kV railway line. This time the model does not consider only one 100 kW charging spot, but twenty 100 kW charging bays for each direction. It is possible replace the single bay with double bays sharing the same amount of power, thus allowing more people to charge simultaneously even if at a lower rate. The charging area is modelled with one charging bay and a current generator. The idea is to model one charging bay to see the current shape it absorbs and, at the same time, inject in the railway system the same current multiplied for the remaining charging bays. The hypothesis is all charging bays are working at the same rate. The charging bays are connected from feeder to earth, rather than from catenary to earth as trains are (figure 5.11).
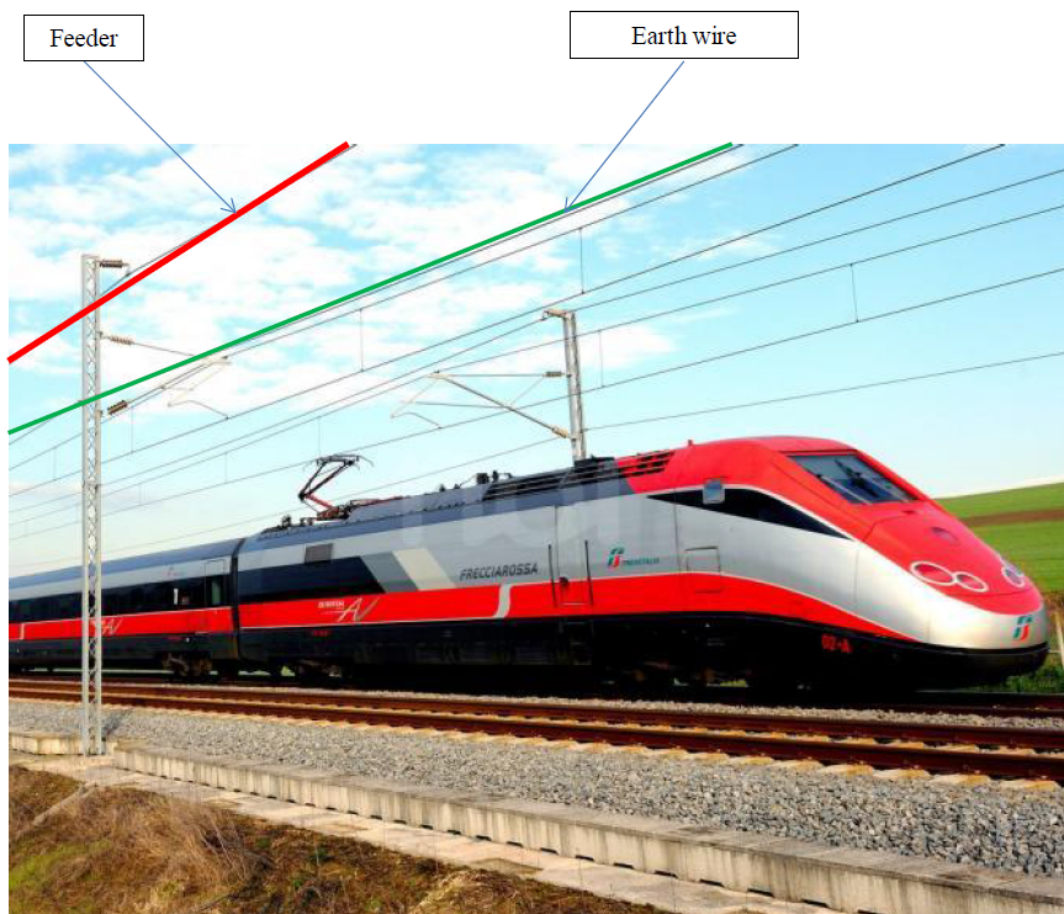
Figure 5.11: Section of a real AV line with indication of the feeder and earth wires

It has been chosen tu connect the charging facility between the two paralleling posts. The first scenario is simulated with no train on the line and the results show that the system works quite well. The simulated time lapse is 3.5 seconds,

but for graph clearness only a relatively small part if it is shown. I chose to show the results towards the end of the simulation because the charger is working at full load there. Figure 5.12 shows the voltage near the charging area is still inside the limits set for the system on both track, despite the current is not always sinusoidal. Despite the shape of the current, figure 5.13 shows that the autotransformers work as expected shifting the earth current to the feeder and catenary system. This means that the feeding transformers sees the most current coming from the feeder and the catenary with only a small current in the rail as figure5.14 shows.
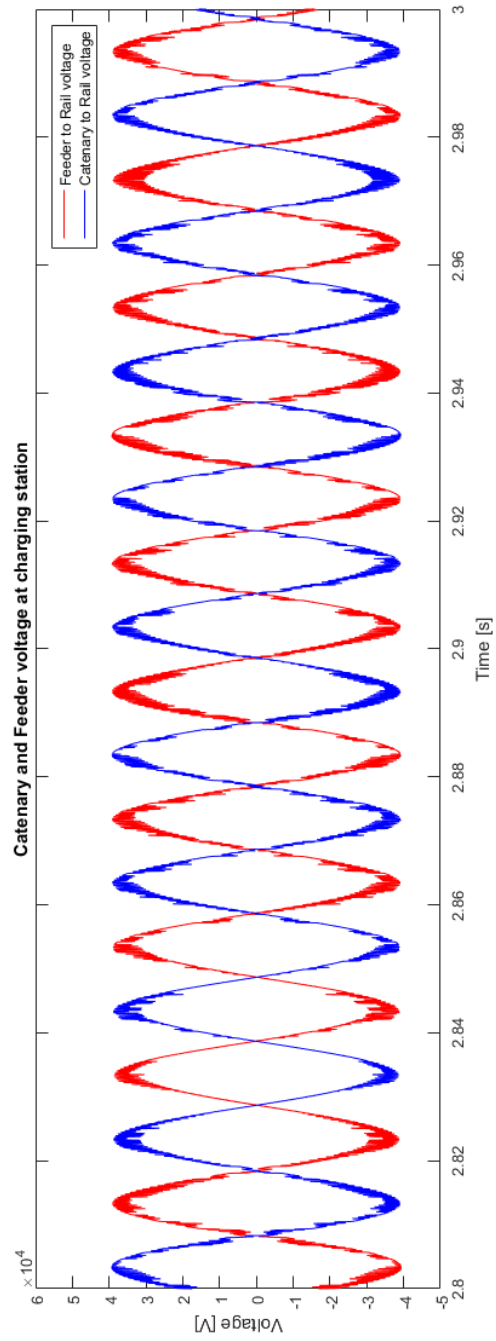
Figure 5.12: Feeder and catenary voltage due to the charging station presence
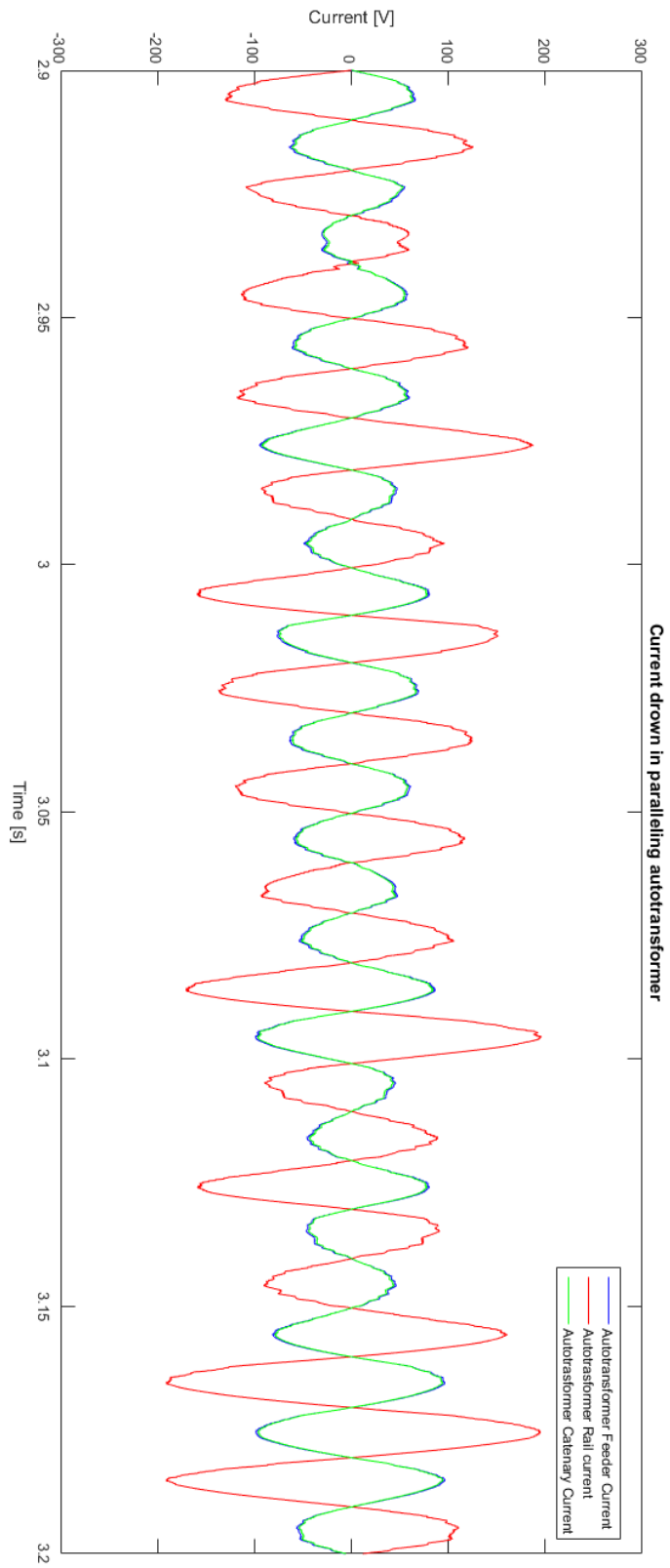
Figure 5.13: Current measured on the Autotransformers connections due to the charging stations
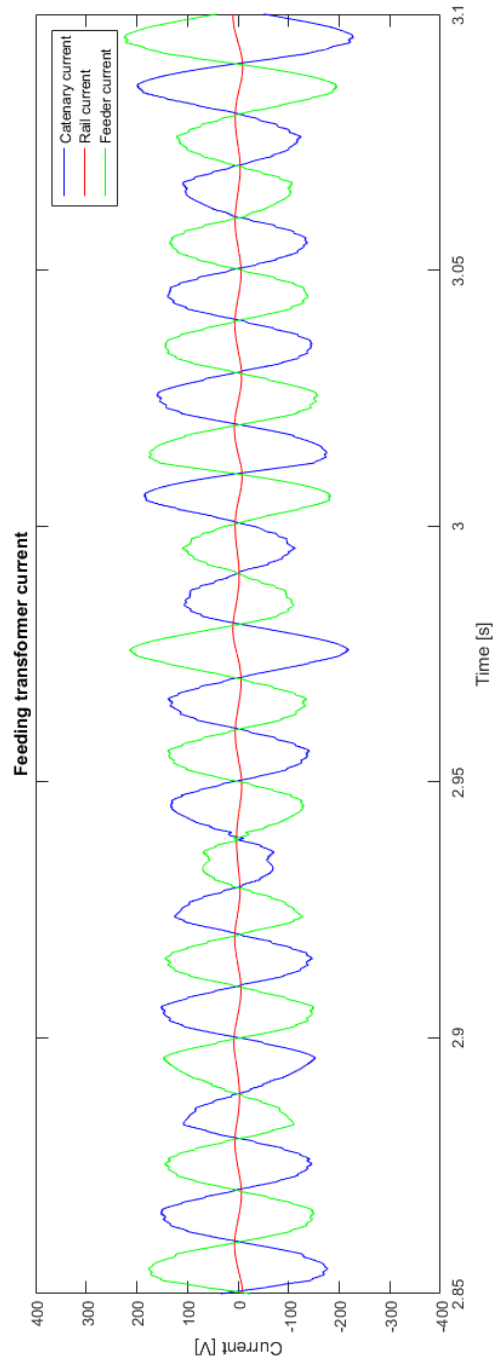
Figure 5.14: Current measured on the feeding transformer with the charging stations and no trains on the track

The fact that the system works with no trains does not imply it works while performing its main duty, i.e. powering high speed trains. In order to verify this, I have simulated the system when one or more trains are on the tracks. The simulation represents the worst case scenario with all the loads fed from the two autotransformers. The first simulation involves the presence of one train on the line. The modelled train is an ETR 400 (known as Frecciarossa 1000) high speed train with a maximum power of 9.8 MW [19] located 3 km away from the charging stations. I have computed that in the 3.5 seconds the train travels less than 500 m so I modelled the train as being still. The total power of the three loads is about 14 MW, so it is expected that the system is able to power all the loads without an excessive voltage drop. The simulation results show exactly that the three loads can coexist. Figures 5.15 and 5.16 show that the voltage measured near the loads and the train is within the limits set by international standards with voltage value being around 23 kV.

There are some differences between this and the preceding scenario in particular the currents have a different shape because of the sinusoidal train current superposed to the charger current. Figures 5.17 and 5.18 show the currents flowing in the autotransformers and in the main transformer.
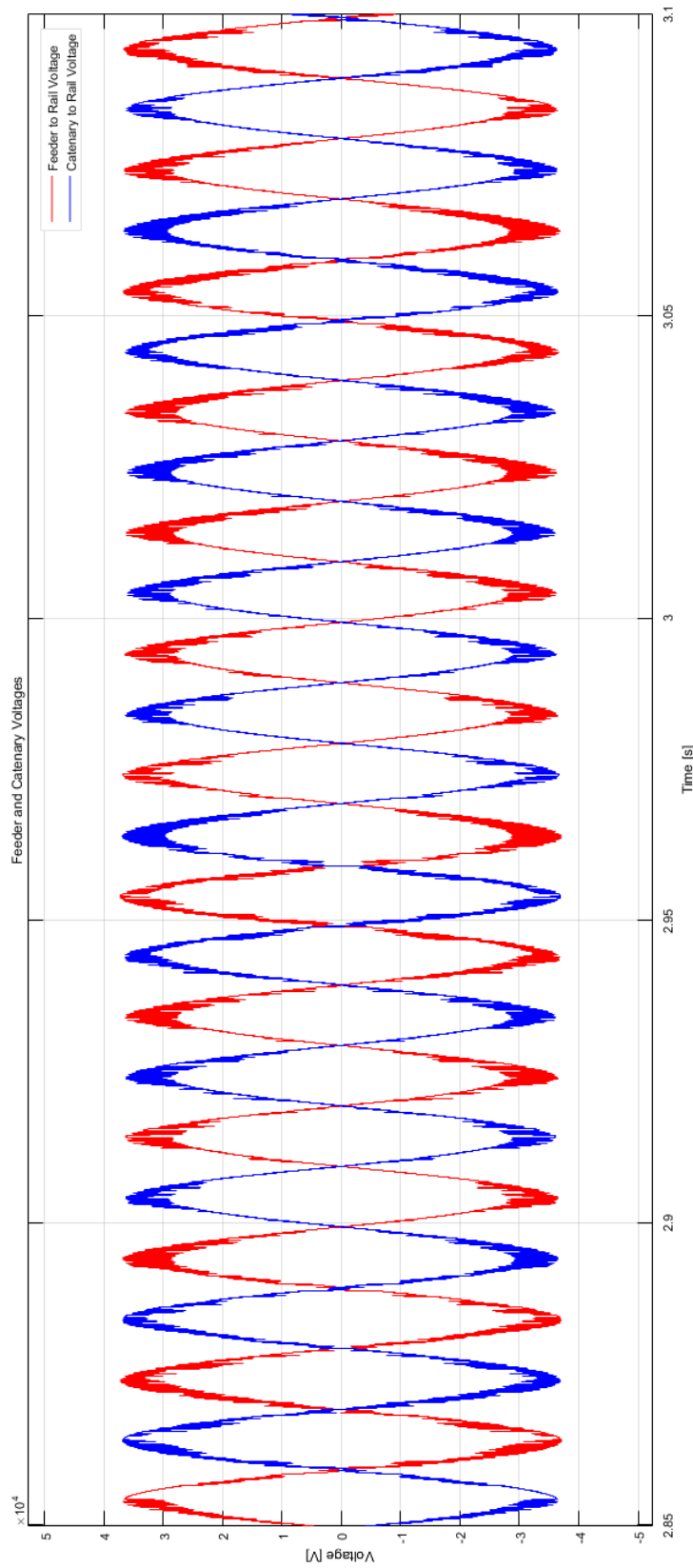
Figure 5.15: Catenary and feeder voltages on the charging facility connection point
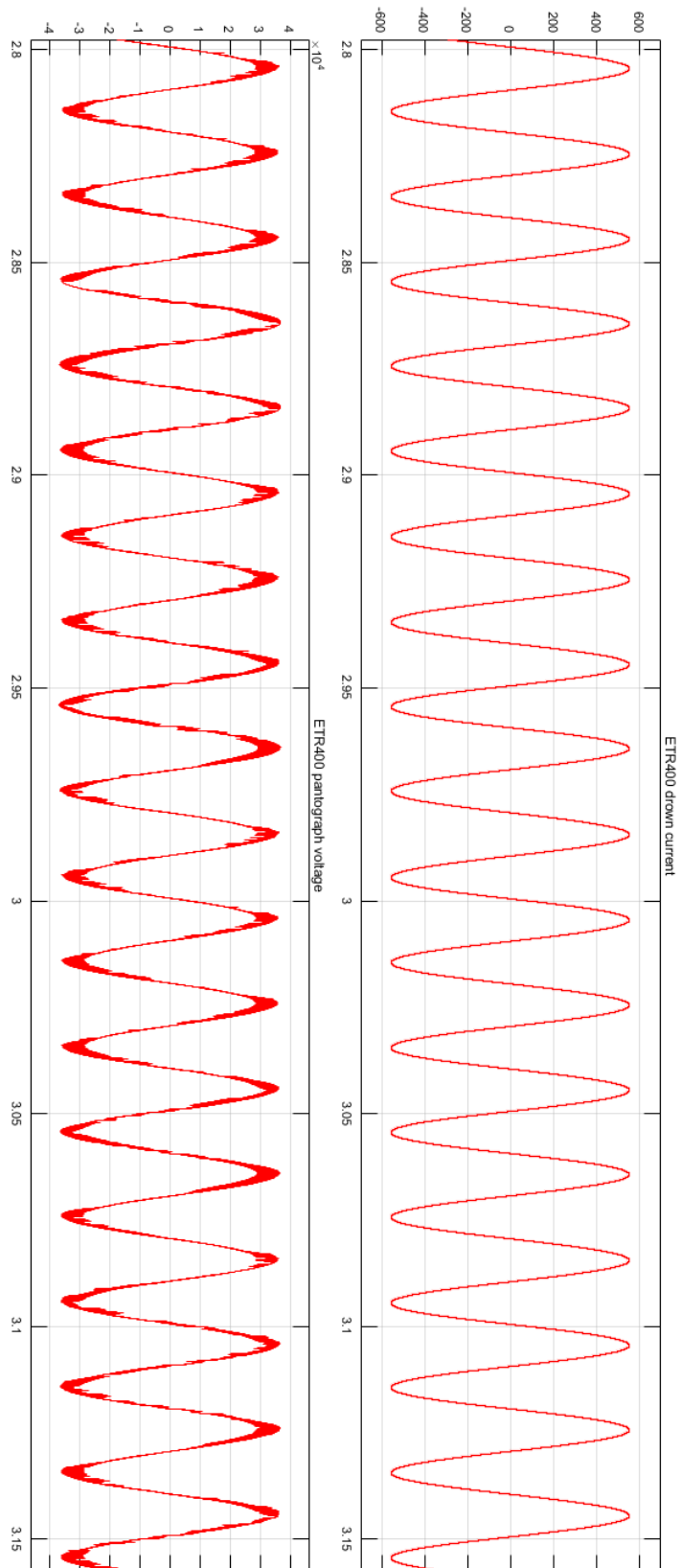
Figure 5.16: Voltage on the train position and current drown by the train
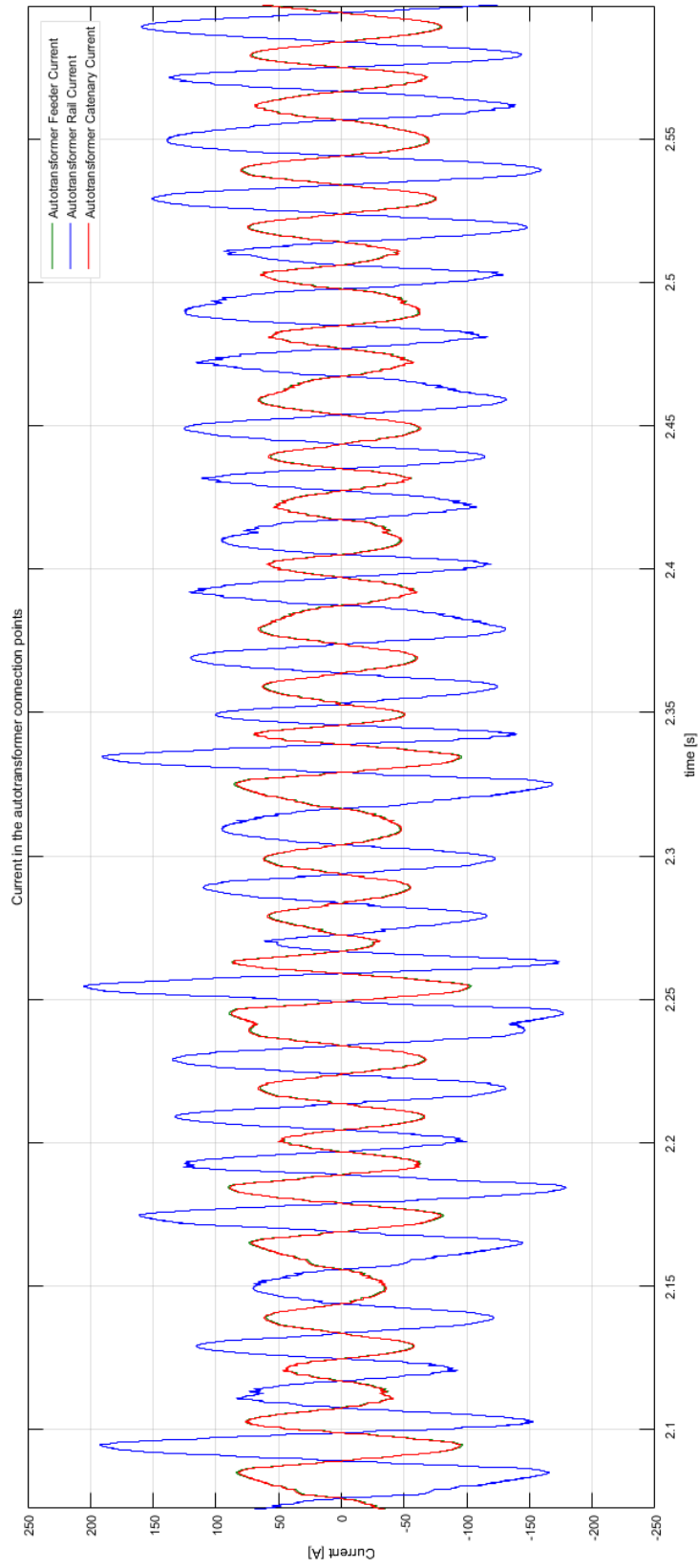
Figure 5.17: Current drawn by the balancing autotransformer with the charging stations and a train on the tracks
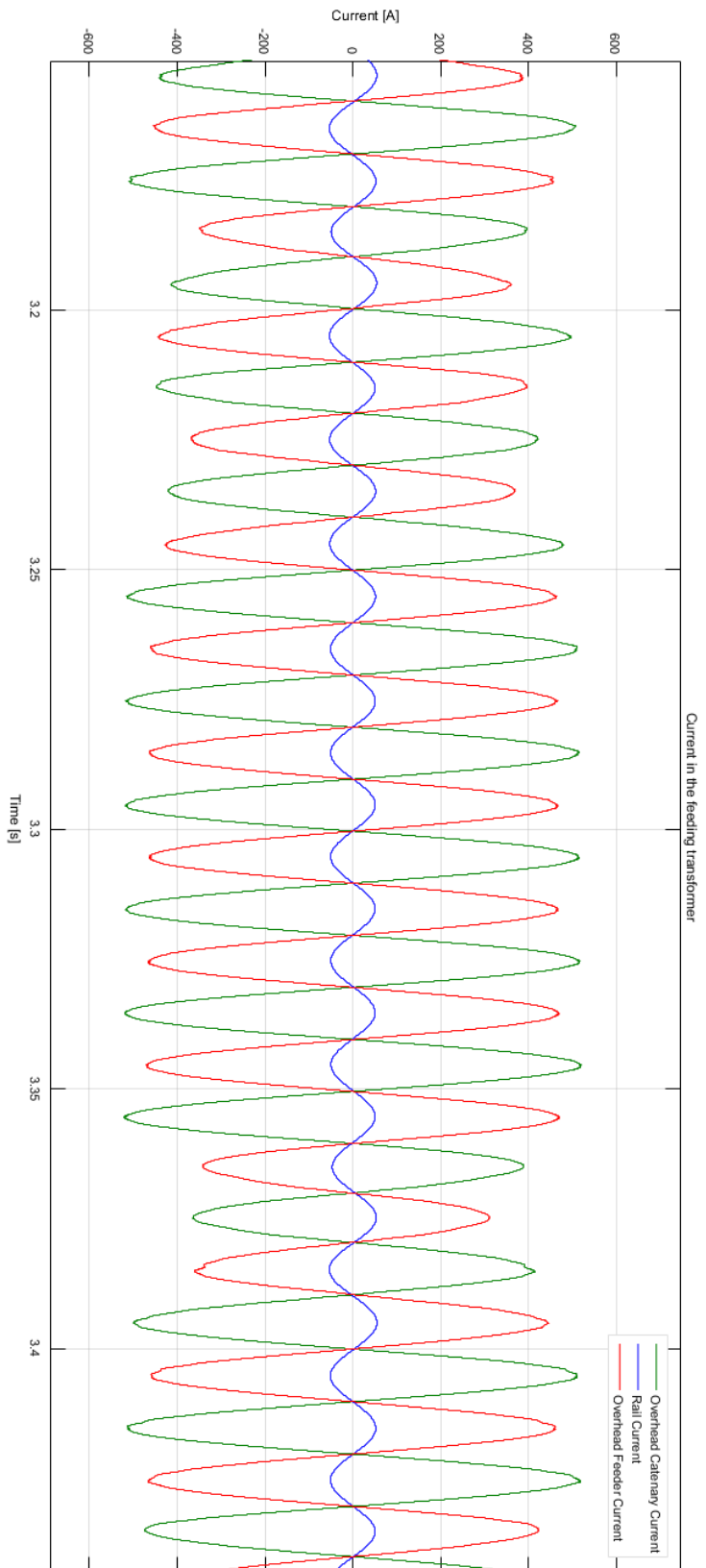
Figure 5.18: current measured on the feeding transformer low voltage winding with the charging stations and a train on the tracks

The last scenario evaluates the ability of the system to power two ETR 400 at 9.8 MW each travelling in opposite direction and the same 40 charging bays. This is very demanding and the system struggles to power the load: this is shown by the voltage value which dropped to about 19 kV as shown in figures 5.19 and 5.20

The main similarity with the preceding scenario is that the currents in the feeding transformer and in the autotransformer are very influenced by the train rather than the relatively small load given by the charging bays. Figures 5.21 and 5.22 show the current drawn by the autotransformers and the feeding transformer respectively

The cause of this problem can be traced down to two thing: the power converter of battery charging facility or the connection of such a big load between feeder and catenary.I think the cause of this kind of problem is the connection of such a big load between feeder and earth. The system can cope with the load due to the line technical systems, such as signalling, switches and line diagnostics, but these loads have a maximum rating of 250 kV A each and each substation powers only a few of them.
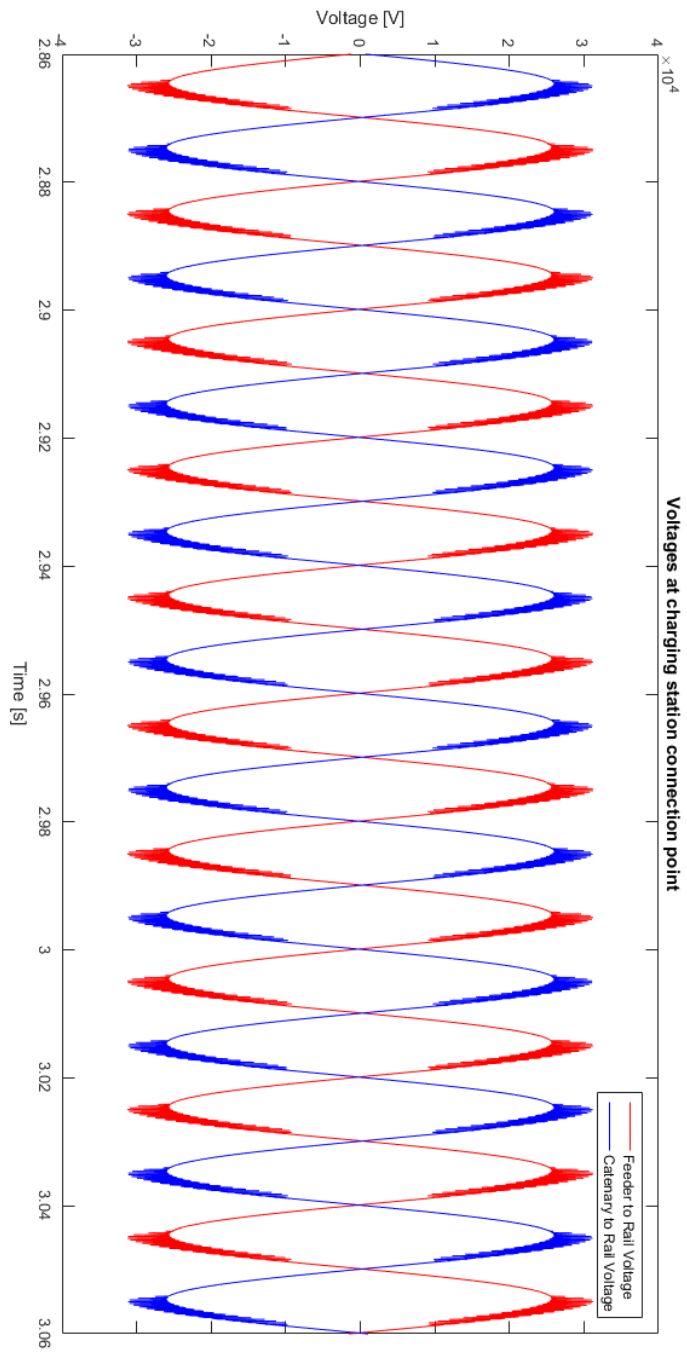
Figure 5.19: Voltages at the charging facility connection point with two trains on the track
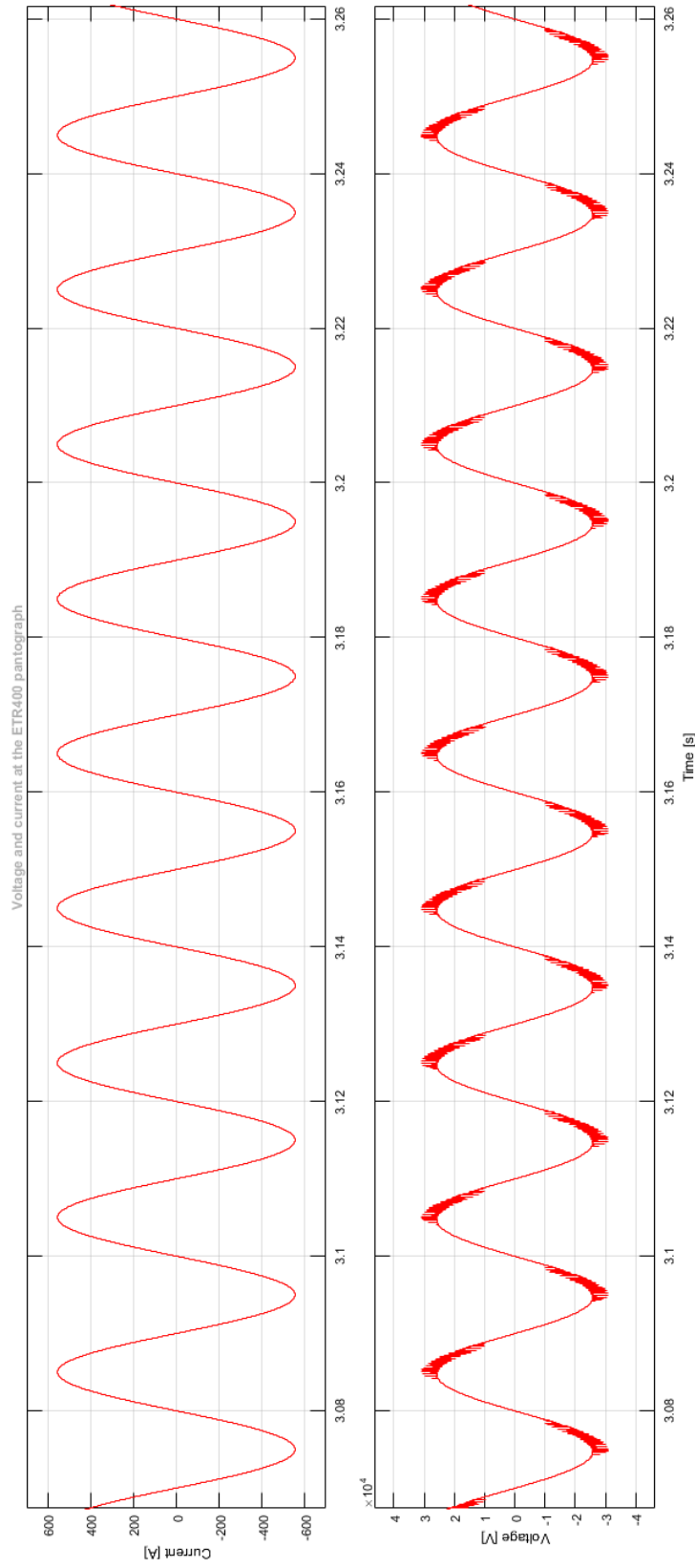
Figure 5.20: Voltage at the train pantograph and current drawn
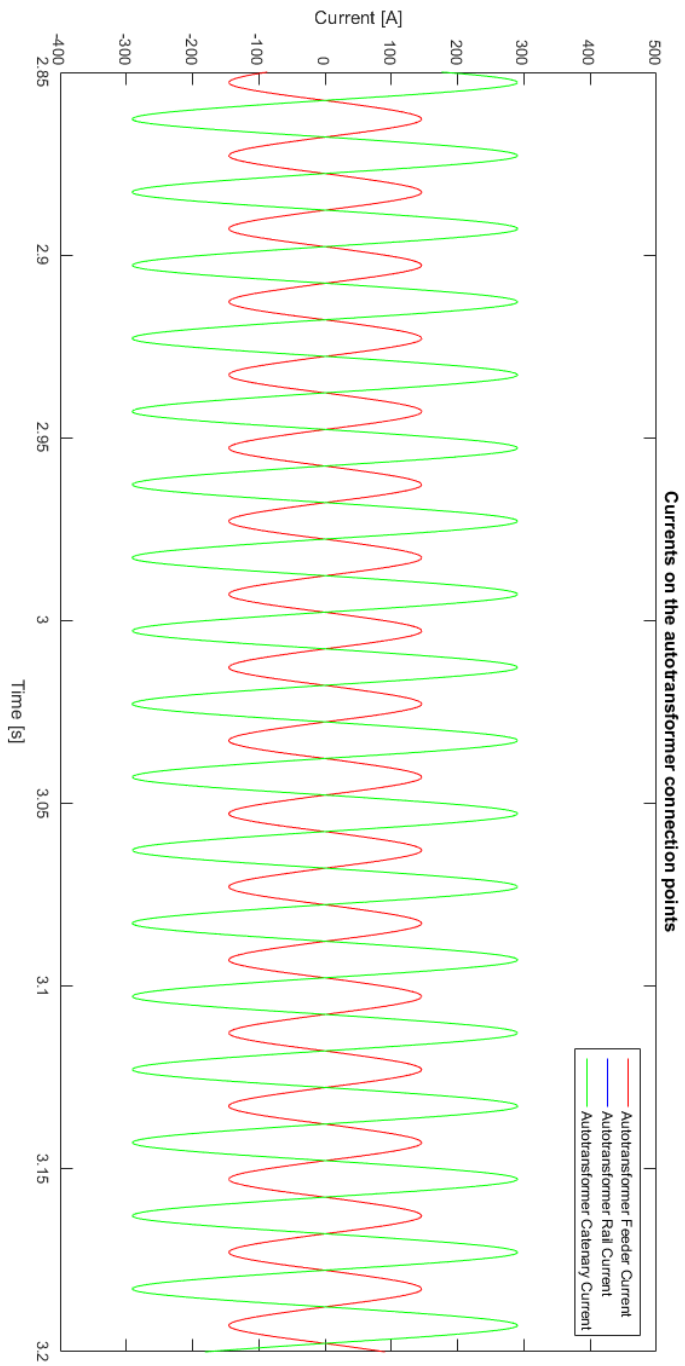
Figure 5.21: Current drawn by the autotransformer in the two trains scenario
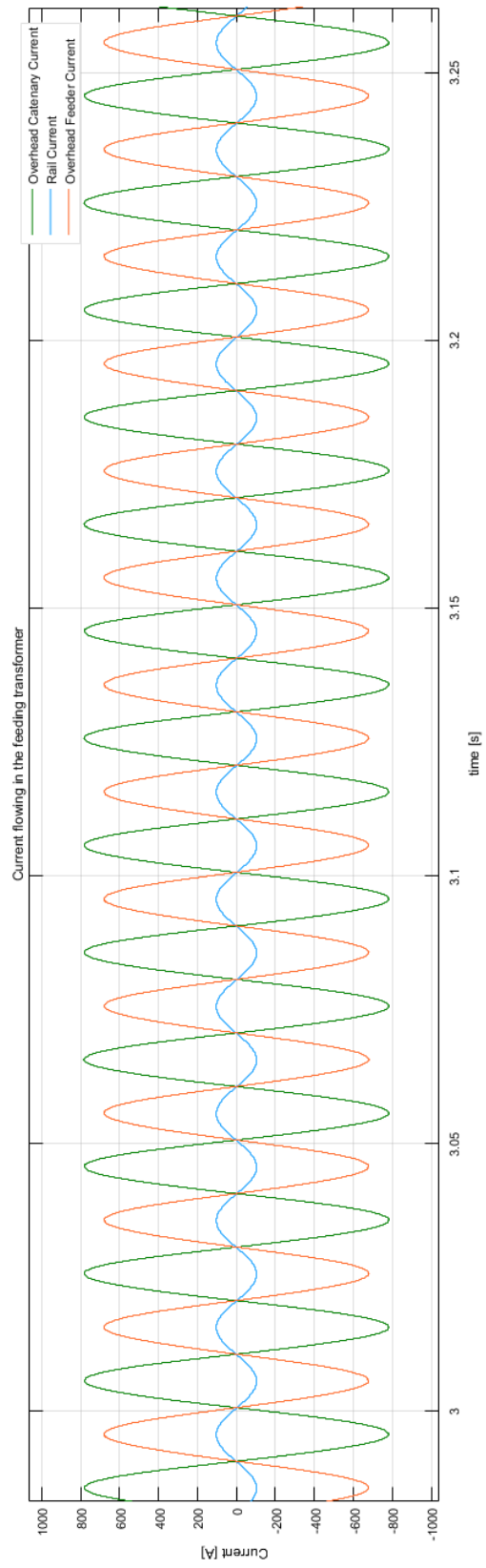
Figure 5.22: Current drawn by the feeding transformer in the two trains scenario

Chapter 6

Conclusions

The need to limit pollution leads to stricter emission standards which will increase the cost of producing traditional cars and the increase in oil prices will lead to more expensive fuel. In the meanwhile a reduction in battery costs and governments subsidies will lead to an increase in electric vehicle purchases. Another incentive to use electric vehicle come from both battery manufacturers and the car industry: as battery technology develops further, it is important to decrease the charging time for the battery pack while maintaining its performance for the entire life expectancy.

As Electric cars are going to become even more popular, it is necessary to built a fast charging infrastructure especially on the motorway network. One of the problems is finding a suitable power source to charge lots of cars quickly despite the increase in battery capacity and in number of vehicles in stock. As the high voltage grid is not always easily accessible, the best possible solution is connecting to high speed railway lines. This solution has to compromise the needs of the rail operators who want their trains adequately powered and the service areas who want to offer a service to car drivers. My research shows a compromise is possible but the charging station power has to be limited to allow trains to be properly powered. This means it is not possible to achieve the same refuelling rate of traditional cars because the charging time is much greater than a traditional car refuelling time and the high speed rail is not able to provide the extra power a larger charging facility needs. Nevertheless it can be a good solution to begin building the fast charging infrastructure where the high speed rail is easily accessible.

The main limitations of my study are two: the rectifier control and the line specifications. It may be possible to power a bigger load than expected by replacing the converter and its regulator with another with better performance in terms of power losses and higher switching frequency. The other issue is having based the study on the Italian high speed line specifications and may lead to different results if other infrastructure owner specifications are used instead. This study does not advocate the impossibility to use high speed lines powered with

the traditional over-head-line and rail scheme (i.e. with no autotransformers), but a separate study is needed.

Bibliography

[1] Maps indicating public charging points available at `http://www.plugshare.com/`.

[2] List of CHAdeMO association members available at `http://www.chademo.com/wp/members/`.

[3] Tesla's CHAdeMo adapter page on the Tesla store website: `http://shop.teslamotors.com/collections/model-s-charging-adapters/products/chademo-adapter`.

[4] CHAdeMO distribution maps. `http://www.chademo.com/`.

[5] CHAdeMO technological details. `http://www.chademo.com/wp/technology/details/`.

[6] CHAdeMO technological strengths. `http://www.chademo.com/wp/technology/strengths/`.

[7] CHAdeMO technological strengths: Optimal output power. `http://www.chademo.com/wp/technology/optimal/`.

[8] Technical details of the italian high speed lines. available in Italian only at `http://www.rfi.it/cms/v/index.jsp?vgnextoid=5dfe165f5f97b110VgnVCM1000003f16f90aRCRD`.

[9] Tesla's official maps for supercharger stations. `http://www.teslamotors.com/it_IT/supercharger`.

[10] Traction Power 2x25kV Autotransformer Feed Type Electrification System & System Voltages. Technical report, California High-Speed Rail Autority.

[11] Auto-transformer plan for reducing inductive interference in telegraph and telephone lines of the New York, New Haven & Hartford Railroad. *Electrical World*, 63(18):984–986, 1914. Available for download at `http://www.archive.org/details/electricalworld63newy`.

[12] Appendix 7 conceptual design of electrification system. Technical report, Metrolink, dec 2010. Available at `http://www.gotransit.com/electrification/en/current_study/Appendix%20Files/Appendix%207.pdf`.

[13] Focus group on european electro-mobility standardization for road vehicles and associated infrastructure. Technical report, CENELEC, oct 2011. Available at `http://www.cencenelec.eu/standards/Sectors/Transport/ElectricVehicles/Pages/default.aspx`.

[14] KAIST rolling out dynamic wireless charging in buses in South Korea. aug 2013. `http://www.greencarcongress.com/2013/08/kaist-20130808.html`.

[15] Directive 2014/94/EU of the European Parliament and of the Council on the deployment of alternative fuels infrastructure. available at `http://eur-lex.europa.eu/legal-content/EN/TXT/?uri=CELEX:32014L0094`, oct 2014.

[16] Amsterdam round-tables foundation and McKinsey and Company. Evolution electric vehicles in Europe, gearing up for a new phase? Technical report, April 2014. `http://www.mckinsey.com/~/media/McKinsey%20Offices/Netherlands/Latest%20thinking/PDFs/Electric-Vehicle-Report-EN_AS%20FINAL.ashx`.

[17] G. Astengo, C. Rossi, and G. Sciutto. In *Main Line Railway Electrification, 1989., International Conference on*.

[18] Hein-Willem Blokland. the rise of EVs and hybrid cars. Technical report, feb 2015.

[19] David Campione. Il frecciarossa 1000. April 2015.

[20] Tommy O. Jensen/Atkins Danmark. High performance railway power introduction to autotransformer system (AT). May 2012. `http://www.banekonference.dk/sites/default/files/AT-system%202012.pdf`.

[21] International energy agency. Global EV outlook. Technical report, apr 2013. `https://www.iea.org/publications/globalevoutlook_2013.pdf`.

[22] FIAT. FIAT Seicento Elettra press report. `http://www.fiatpress.com/press/detail/5017`.

[23] China National Institute for standardisation. China's standard proposal adopted into IEC standard. jul 2014. `http://en.cnis.gov.cn/xwdt/bzhdt/201407/t20140709_19405.shtml`.

[24] Zhengqing Han, Shuping Liu, Shibin Gao, and Zhiqian Bo. Protection scheme for china high-speed railway. In *Developments in Power System Protection (DPSP 2010). Managing the Change, 10th IET International Conference on*, pages 1–5, March 2010.

[25] IEC. IEC 61851-23 international standard.

[26] IEC. IEC 62196-3 international standard.

[27] Mark Kane. Tesla Model S charging inlet in Europe. `http://insideevs.com/tesla-model-s-charging-inlet-in-europe/`, 2013.

[28] Klaus Kersting. Standardisation needs and testing methods for multiple-outlet chargers. Technical report, jul 2014.

[29] Teruo Kobayashi. Breackthrough of Japanese Railway. *Japanese Railway & Transport Review*, (45).

[30] Sisi Li. Power flow in railway electrification power system, 2010.

[31] Salvatore Loiacono. L'auto elettrica, una storia infinita. `http://www.omniauto.it/magazine/13781/auto-elettrica-storia-infinita`.

[32] Mauro Di Mise. Fiat Panda Elettra: ecologia ante litteram. jan 2015. `http://www.cavallivapore.it/2015/fiat-panda-elettra-ecologia-ante-litteram/`.

[33] F. Musavi, M. Edington, and W. Eberle. Wireless power transfer: A survey of ev battery charging technologies. In *Energy Conversion Congress and Exposition (ECCE), 2012 IEEE*, pages 1804–1810, Sept 2012. found at `http://ieeexplore.ieee.org/Xplore/home.jsp`.

[34] Andrea Nardinocchi. Electrification and power supply. 2011. `http://www.apta.com/mc/hsr/previous/2011/presentations/Presentations/Electrification-and-Power-Supply.pdf`.

[35] Bloomberg News. China seen stepping up push for electric cars in five year plan. sep 2015. `http://www.bloomberg.com/news/articles/2015-09-29/china-seen-stepping-up-push-for-electric-cars-in-five-year-plan`.

[36] Allen McFarland Nicholas Case. California leads the Nation in adoption of electric vehicles. `http://www.eia.gov/todayinenergy/detail.cfm?id=19131`.

[37] State Grid Corporation of China. Ev infrastructure and standardization in china. oct 2013. published at `https://www2.unece.org/wiki/download/attachments/12058681/EVE-07-14e.pdf`.

[38] Nick Owe. Supercharger. `http://www.teslamotors.wiki/wiki/Supercharger`.

[39] Marco Peruzzotti. L'ora della rivincita. *Autotecnica*, (8):124–130, 2015.

[40] E. Pilo, R. Rouco, and A. Fernandez. A reduced representation of 2 times;25 kv electrical systems for high-speed railways. In *Rail Conference, 2003. Proceedings of the 2003 IEEE/ASME Joint*, pages 199–205, April 2003.

[41] Volkswagen Ralf Milke. Combined charging the universal charging system key features and major benefits. Technical report.

[42] H. Roussel. Power supply for the atlantic tgv high speed line. In *Main Line Railway Electrification, 1989., International Conference on*, pages 388–392, Set 1989.

[43] Markkus Rovito. OLEV technologies' dynamic wireless inductive system charges vehicles while in motion. May 2014. `https://chargedevs.com/features/olev-technologies-dynamic-wireless-inductive-system-charges-vehicles-while-i`

[44] Sharif Sakr. Tesla will open up its supercharger patents to boost electric car adoption. jun 2014. `http://www.engadget.com/2014/06/09/tesla-to-share-supercharger-patents/`.

[45] T. Sezi and F.E. Menter. Protection scheme for a new ac railway traction power system. In *Transmission and Distribution Conference, 1999 IEEE*, volume 1, pages 388–393 vol.1, Apr 1999.

[46] J.U. Shenoy, K.G. Sheshadri, K. Parthasarathy, H.P. Khincha, and D. Thukaram. Matlab/psb based modeling and simulation of 25 kv ac railway traction system - a particular reference to loading and fault conditions. In *TENCON 2004. 2004 IEEE Region 10 Conference*, volume C, pages 508–511 Vol. 3, Nov 2004.

[47] steven hedelstein. Electric cars aren't selling because makers can't, don't market them: Report. sep 2015. `http://www.greencarreports.com/news/1100135_electric-cars-arent-selling-because-makers-cant-dont-market-them-report`.

[48] CHAdeMO Technical WG Takeshi Haida. IEC / EN standardization. Technical report, 2014. Available at `http://www.chademo.com/wp/wp-content/uploads/2014/10/IEC_standarization_update.pdf`.

[49] Enrico Tironi. *Appunti alle lezioni di Impianti Elettrici*, chapter Calcolo dei parametri delle linee. CUSL, 2011.

[50] US Department of Energy. battery test results. available at `http://media3.ev-tv.me/DOEleaftest.pd`, 2011.

[51] John Voelcker. BMW, VW, and ChargePoint to build 100 CCS fast-charging sites for electric cars. jan 2015. `http://www.greencarreports.com/news/1096446_bmw-vw-and-chargepoint-to-build-100-ccs-fast-charging-sites-for-electric-cars.`

[52] R.D. White. Ac 25kv 50 hz electrification supply design. In *Railway Electrification Infrastructure and Systems, 2009. REIS 2009. 4th IET professional Development Course on*, pages 93–126, June 2009.

[53] Domenick Yoney. Tesla, european automaker may share supercharger network. sep 2015. `http://www.autoblog.com/2015/09/27/tesla-european-automaker-share-supercharger-network-video/`.

[54] Dario Zaninelli. *Sistemi elettrici per l'alta velocità ferroviaria*, chapter 1 Linee AV/AC a 2 x 25 kV - 50 Hz, pages 6 – 8. polipress, 2010.

[55] Dario Zaninelli. *Sistemi elettrici per l'alta velocità ferroviaria*, chapter Modello in ATP dell'intero sistema, page 202. polipress, 2010.

[56] Dario Zaninelli. *Sistemi elettrici per l'alta velocità ferroviaria*, chapter Appendice A, pages 255 – 263. Polipress, 2010.

List of Figures

List of Tables